An alternative secretory pathway in the malaria parasite *Plasmodium falciparum*

Dissertation
zur Erlangung des Doktorgrades der Naturwissenschaften
(Dr. rer. nat.)

dem Fachbereich Biologie
der Philipps-Universität Marburg
vorgelegt von

Thuvaraka Thavayogarajah
aus Detmold

Marburg/Lahn 2014

Vom Fachbereich Biologie der Philipps-Universität Marburg als Dissertation angenommen am: _____

Erstgutachter	Prof. Dr. Klaus Lingelbach
Zweitgutachter	Prof. Dr. Anthony Holder

Tag der Disputation am:

" Imagination is more important than knowledge.
Knowledge is limited.
Imagination encircles the world. "

- Albert Einstein-

Für meine Mutter

The major part of this thesis is prepared for submission:

Thavayogarajah, T., Gangopadhyay, P., Becker, K., Holder, A., Przyborski, J.M. and Lingelbach K. (2014) An alternative secretory pathway in the malaria parasite *P. falciparum* **(manuscript in preparation)**

Other publications (from undergraduate studies):

Jessica M. Vanslambrouck, Angelika Bröer, Thuvaraka Thavayogarajah, Jeff Holst, Charles G. Bailey, Stefan Bröer and John E. J. Rasko (2010) Renal imino acid and glycine transport system ontogeny and involvement in developmental iminoglycinuria. *Biochemical Journal* 428 (397-407)

Table of contents

Abbreviations

AcbA	acyl coenzyme A binding protein
ADP	adenosine diphosphate
AK1	adenylate kinase 1
AK2	adenylate kinase 2
AKLP1	adenylate kinase-like protein 1
AKLP2	adenylate kinase-like protein 2
AMP	adenosine monophosphate
ARF1	ADP-ribosylation factor 1
ATP	adenosine triphosphate
BFA	Brefeldin A
bp	base pairs
BSA	bovine serum albumin
BSD	Blasticidine S deaminase
cDNA	complementary DNA
CDPK1	calcium-dependent protein kinase 1
CDPK4	calcium-dependent protein kinase 4
CRT	chloroquine resistance transporter
DDT	dichlorodiphenyltrichloroethane
DHFR	dihydrofolate reductase
DNA	desoxyribonucleic acid
dNTP	desoxynucleotide triphosphate
DTT	Dithiothreitol
ECL	Enhanced chemiluminescence
E.coli	*Escherichia coli*
ER	endoplasmic reticulum
Exp1	Exported protein 1
FGF2	fibroblast growth factor 2
GAPs	GTPase-activating proteins
gDNA	genomic DNA

GDP	guanosine diphosphate
GEFs	guanine nucleotide exchange factors
GFP	green fluorescent protein
GRASP1	Golgi reassembly-stacking protein 1
GTP	guanosine triphosphate
HASPB	hydrophilic acylated protein B
hDHFR	human dihydrofolate reductase
HRP	horseradish peroxidase
HT	host targeting signal
IL1β	interleukin-1β
iRBC	infected red blood cell
KAHRP	knob-associated histidine-rich protein
kDa	kilodalton
LB	Luria-Bertani
MC	Maurer's clefts
mRNA	messenger RNA
MSA	multiple sequence alignment
MSP1	merozoite surface protein 1
MVB	multivesicular bodies
MW	molecular weight
NMT	*N*-myristoyltransferase
NPPs	new permeability pathways
OD	optical density
PAGE	polyacrylamide gel electrophoresis
PATs	palmitoyl acyltransferases
PBS	phosphate buffered saline
PCR	polymerase chain reaction
PEXEL	*Plasmodium* export element
Pf	*Plasmodium falciparum*
*Pf*EMP1	*P. falciparum* erythrocyte membrane protein-1
PIC	protease inhibitor cocktail

PIP3	phosphatidylinositol (3,4,5)-triphosphate
PI(4,5)P2	phosphatidylinositol 4,5-bisphosphate
PKC	protein kinase C
PMSF	phenylmethylsulphonyl fluoride
PPM	parasite plasma membrane
PV	parasitophorous vacuole
PVM	parasitophorous vacuole membrane
PTEX	*Plasmodium* translocon of exported proteins
RBC	red blood cell
RBCM	red blood cell membrane
REX 1 and 2	ring-exported protein 1 and 2
RNA	ribonucleic acid
RT	room temperature
SDS	sodium dodecyl sulfate
SDS-PAGE	sodium dodecyl sulfate polyacrylamide gel electrophoresis
SERP	serine-rich protein
SLO	Streptolysin O
SP	signal peptide
SRP	signal recognition particle
TVN	tubovesicular network
UV	ultraviolet
V	voltage

Summary

The malaria parasite *P. falciparum* invades human red blood cells (RBCs). During invasion a compartment surrounding the parasite, the so-called parasitophorous vacuole (PV), is formed. The parasite resides and develops within the PV, which protects the parasite from the host cell cytosol. During its intraerythrocytic growth the parasite exports a vast number of proteins to the host cell in order to maintain its survival within the RBC. Proteins, which are directed to the host cell cytosol and host cell membrane, respectively, therefore are challenged to cross the parasite plasma membrane, the PV and the parasitophorous vacuolar membrane (PVM). However, the secretion and export mechanisms of many parasite proteins are still not understood.

The current study focuses on the discovery of an alternative secretory pathway to the ER/Golgi route in the malaria parasite *P. falciparum* in infected RBCs. Two proteins appeared to be promising candidates of an alternative secretory pathway: the *Pf*ADP-ribosylation factor 1 (ARF1) and the *Pf*adenylate kinase 2 (AK2). Both proteins contained a *N*-myristoylation site at their N-terminus, which is indicative for *N*-myristoylation. *N*-myristoylation is a co-translational modification of a protein, whereby a fatty acid (myristate) is irreversibly attached to the glycine residue at the N-terminus of a protein via the *PfN*-myristoyltransferase (NMT). A preceding proteomic analysis of the parasitophorous vacuole and a reporter construct study proposed for both *Pf*ARF1 (determined by a proteomic study) and *Pf*AK2 (determined by a reporter construct study) PV localization although both proteins lacked a signal peptide. That's why it was hypothesized whether or not *N*-myristoylation would drive protein secretion across the parasite plasma membrane (PPM). The subcellular localization of the *Pf*ARF1/GFP parasites and the *Pf*AK2/GFP parasites, respectively, were analyzed via epifluorescence microscopy and biochemical methods. In parallel, another batch of reporter constructs were generated and analyzed, where the *N*-myristoylation site of *Pf*ARF1 (this study) and *Pf*AK2 (Ma et al., 2012), respectively, was removed (*Pf*ARF1^{G2A}/GFP and *Pf*AK2^{G2A}/GFP). Live cell imaging showed that the fusion protein ARF1/GFP was localized as dot-like structures in the parasite. In contrast, the phenotype of the fusion

protein of the *Pf*ARF1^{G2A}/GFP parasites showed an evenly distributed signal in the parasite cytosol. Further analysis of the subcellular localization of the *Pf*ARF1 strongly supports its localization to compartments of the early secretory pathway of the parasite, but no localization in the PV. In contrast, the fusion protein *Pf*AK2/GFP localized to a ring-like structure around the parasite indicating PV localization. The *Pf*AK2^{G2A}/GFP parasites showed a cytosolic localization of the fusion protein (Ma et al., 2012). Biochemical analyses revaled that the fusion protein *Pf*AK2/GFP was secreted into the PV when the *N*-myristoylation site was present. Furthermore, it could be shown that the N-terminus of the *Pf*AK2 protein is sufficient for parasite plasma membrane targeting, stable membrane anchoring and subsequent protein translocation across the PPM. A possible role of the early secretory pathway in *Pf*AK2 trafficking and the folding state of *Pf*AK2 prior to translocation across the PPM was also examined. However, the exact mechanism how *Pf*AK2 is translocated across the PPM still remains elusive.

Zusammenfassung

Der Malariaerreger *P. falciparum* befällt rote Blutkörperchen im Menschen. Bei der Invasion der Erythrozyten formt der Parasit eine sogenannte parasitophore Vakuole (PV), die ihn dann umgibt. Der Parasit verbleibt und entwickelt sich in dieser PV, die ihn vom Zytosol der Wirtszelle schützt. Während des intraerythrozytären Wachstums exportiert der Parasit eine hohe Anzahl seiner eigenen Proteine in die Wirtszelle um sein Überleben in der Wirtszelle zu sichern. Proteine, die entweder in das Zytosol oder der Membran der Wirtszelle exportiert werden, müssen zunächst die Plasmamembran des Parasiten (PPM), die PV und die anliegende parasitophore Vakuolenmembran (PVM) passieren. Der Sekretions- und Exportmechanismus vieler Parasitenproteine ist jedoch noch immer unbekannt.

Ziel dieser Arbeit ist es alternative Sekretionswege zum klassichen ER/Golgi Sekretionsweg im Malariaparasiten *P. falciparum* aufzudecken. Zwei Proteine schienen geeignete Kandidaten eines alternativen Sekretionsweges zu sein: der *Pf*ADP-Ribosylierungsfaktor 1 (ARF1) und die *Pf*Adenylat kinase 2 (AK2). Beide Proteine besitzen eine *N*-myristoylierungsstelle am N-terminus was auf eine *N*-myristoylierung des jeweiligen Proteins hindeutet. *N*-myristoylierung ist eine ko-translationale Modifizierung eines Proteins, wobei eine Fettsäure (Myristat) irreversibel am Glycinrest am N-terminus eines Proteins durch die *PfN*-myristoyltransferase (NMT) angehängt wird. Eine vorangegangene Proteomuntersuchung der parasitophoren Vakuole und eine Untersuchung mit Reporterkonstrukten ergab für *Pf*ARF1 (Proteomuntersuchung) und *Pf*AK2 (Analyse der Reporterkonstrukte) eine PV Lokalisation, obwohl beiden ein Signalpeptid fehlt. Deshalb wurde die Hypothese aufgestellt, dass *N*-myristoylierung womöglich an der Proteinsekretion über die Plasmamembran des Parasiten beteiligt sein könnte. Demnach wurde die subzelluläre Lokalisation der *Pf*ARF1/GFP Parasiten und der *Pf*AK2/GFP Parasiten mithilfe von Epifluoreszenzmikroskopie und biochemischen Methoden untersucht. Parallel dazu wurden Reporterkonstrukte generiert und analyisert, bei denen die *N*-myristoylierungsstelle von *Pf*ARF1 (diese Arbeit) und *Pf*AK2 (Ma et al., 2012) entfernt wurden (*Pf*ARF1^{G2A}/GFP und *Pf*AK2^{G2A}/GFP). Beim live cell imaging war das Fusionsprotein ARF1/GFP als punktförmige Struktur im Parasiten

erkennbar. Der Phänotyp des Fusionsproteins der *Pf*ARF1^{G2A}/GFP Parasiten dagegen zeigte ein zytosolisches Signal im Parasiten. Weitere Analysen im Hinblick auf die subzelluläre Lokalisation des *Pf*ARF1 deuten auf eine Lokalisation dieses Proteins mit Kompartimenten des frühen Sekretionsweges des Parasiten hin jedoch auf keine Lokalisation in der PV. Im Gegensatz dazu war das Fusionsprotein *Pf*AK2/GFP als ringförmige Struktur sichtbar was auf eine PV Lokalisation hindeutet. Die *Pf*AK2^{G2A}/GFP Parasiten zeigten hingegen eine zytosolische Lokalisation des Fusionsproteins (Ma et al., 2012). Biochemische Untersuchungen konnten zeigen, dass das Fusionsprotein *Pf*AK2/GFP in Anwesenheit der *N*-myristoylierungsstelle in die PV sekretiert wurde. Des Weiteren konnte gezeigt werden, dass der N-terminus von *Pf*AK2 das Protein zur Plasmamembran führt und eine stabile Membranverankerung hervorruft bevor die Translokation über die Plasmamembran des Parasiten erfolgt. Eine mögliche Rolle des frühen Sekretionsweges im Transport von *Pf*AK2 und der Faltungszustand von *Pf*AK2 vor der Translokation über die Parasitenplasmamembran wurden ebenfalls untersucht. Dennoch ist der genaue Mechanismus der Proteintranslokation über die Plasmamembran des Parasiten nicht bekannt.

1 Introduction

1.1 Malaria

Since ancient times a disease today referred to as malaria ('mal' 'aria' meaning 'bad air') has been noted to have a detrimental effect on people's life quality, impeding population growth and affecting settling patterns throughout human history (Carter and Mendis, 2002; Sallares et al., 2004). Today malaria is recognized as one of the largest, life-threatening, infectious diseases in the world, caused by a eukaryotic parasite of the genus *Plasmodium* and transmitted by a bite of an infected female *Anopheles* mosquito. Although the causative agent of this disease was identified in the late 19th century malaria continues to be a major health problem in tropical and subtropical parts of the world, where billions of people are still exposed to this deadly disease (Fig. 1) (WHO 2011; cdc). In 2010 approximately 216 million clinical cases were reported by the World Health Organisation with 80 % occurring in African regions alone. Also 90 % of the 655 000 cases of deaths by malaria were registered in Africa (WHO 2011). In malaria-endemic regions pregnant women and children under the age of five (86 % of malaria deaths) succumb to this lethal disease more frequently than other groups of people as stated by the WHO in 2011. Countries, in which malaria is prevalent are also the ones suffering from a high poverty rate and a low economic growth making malaria prevention control and treatment more difficult (Gallup and Sachs, 2001; Sachs and Malaney, 2002).

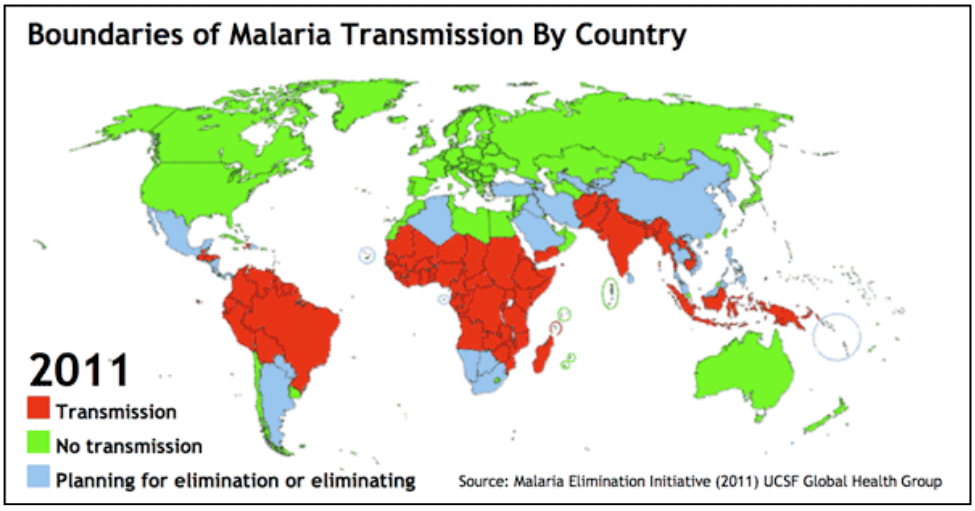

Figure 1.1 Malaria distribution

To date five different species of the genus *Plasmodium – P. vivax, P. ovale, P. malariae, P. falciparum* and *P. knowlesi* - are known to cause malaria in humans. While *P. vivax* and *P. ovale*, the causative agents of tertian malaria, and *P. malariae*, the causative agent of quartian malaria, are less likely to lead to severe forms of malaria outbreaks in humans, *P. falciparum* infections are mostly responsible for the high morbidity and mortality rates in endemic regions of Africa (cdc). Only recently *P. knowlesi*, a *Plasmodium* species known to infect macaque monkeys with malaria, was discovered to cause malaria in humans as well. (Singh et al., 2004; Cox-Singh et al., 2008).

Since the early 20th century many projects emerged to fight this deadly disease involving the use of the synthetic insecticide **d**ichloro**d**iphenyl-**t**richloroethane (DDT) to prevent transmission by mosquitoes and the chemical compound chloroquine, known to inhibit the development of the blood-stage parasite. However, the increasing resistance in the mosquitoes and the *Plasmodium*-species, respectively, and the adverse effect of DDT on the environment made these attempts over the period of time unfruitful (cdc). Nevertheless, many malaria eradication programmes, especially in the early 21st century, are determined to reduce the high malaria casualties by the use of bed-nets treated with insecticide, artemisin-based combination therapies, etc. In fact the combination of these various methods has reduced the number of malaria cases of deaths by around 33 % since 2000 as registered in African regions, which are monitored by the WHO (WHO 2011). However, the number of malaria infections is still high and strains resistant to the available current anti-malarial drugs are already occurring. That is why continuous study on the biology of the parasite, to eventually develop an efficient vaccine and developments of new drugs against malaria, still needs to be continued.

1.2 The complex life-cycle of *Plasmodium falciparum*

Plasmodium falciparum has a very complex life-cycle involving mosquitoes as vectors and humans as hosts for its survival. The transmission of *P. falciparum* into a human occurs when an infected female *Anopheles* mosquito bites a human for a blood-meal

thereby injecting saliva into the human. The saliva of an infected mosquito contains asexual forms of the parasite, the so-called sporozoites, which after entering the circulatory blood system travel to and invade liver cells for invasion (exo-erythrocytic stage). After entering liver cells the sporozoites multiply asexually and re-differentiate into thousands of merozoites in a process referred to as schizogony (Shortt, 1951). These thousands of merozoites are initially released in so-called merosomes (detached membrane-bound structures from the host cell) into the blood stream to escape the immune system (Sturm et al., 2006). Once the merozoites are completely released into the blood stream they target and invade red blood cells (erythrocytic stage). Following invasion a single merozoite multiplies into 20-30 daughter cells in an asexual process which takes about 48 hours: Initially the merozoite (now called the ring-stage) increases in size (0-12 hours post invasion) resulting into the more mature trophozoite form (12-30 hpi) before the nucleus of the trophozoite form divides into many nuclei forming the so-called multinucleated schizont (30-48 hpi). After division of the multinucleated schizont into many individual merozoite forms the red blood cell ruptures releasing the newly formed parasites into the circulatory system to invade new erythrocytes (Wenk and Renz, 2003; Cowman and Crabb, 2006). However, a late trophozoite-stage occasionally also differentiates into a sexual form of the parasite, the gametocytes, which remain in the erythrocyte. Only when the erythrocytes containing these gametocytes are taken up via a blood-meal by a mosquito do they transform into gametes - male and female - in the gut of the mosquito. Fusion of the male and female gametes leads to a diploid zygote, the motile ookinete, which forms eventually an oocyst in the midgut of the mosquito. There the haploid sporozoite-forms are produced after many rounds of mitotic division (Wenk and Renz, 2003; Beier et al., 1998; Matuschewski, 2006). Eventually, these asexual sporozoites travel through the mosquito body to the salivary glands of the mosquito, where they can enter the host, once the infested mosquito bites a human re-starting the cycle (Fig. 1.2) (Matuschewski, 2006).

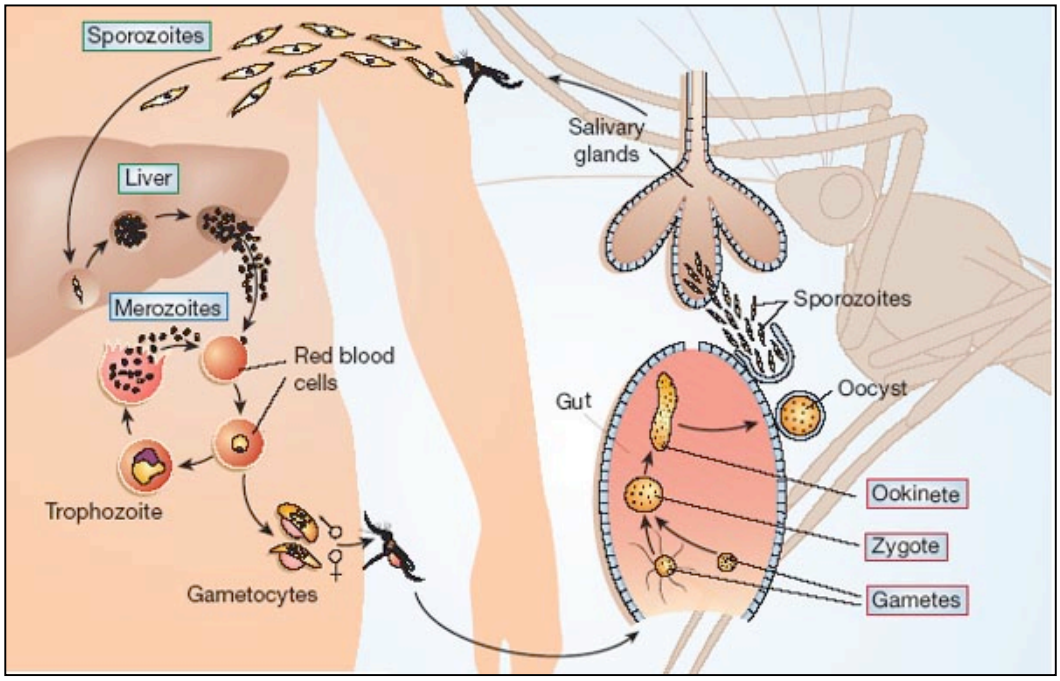

Figure 1.2 Life-cycle of *P. falciparum*

A bite of a female *Anopheles* mosquito leads to the transmission of the malaria parasite into the human. Initial asexual multiplication takes place within the liver cells, before the infective merozoite form invades and multiplies within the red blood cells. The gametocytes, the sexual forms of the parasite, are produced in the human; however, the sexual development of *P. falciparum* occurs in the midgut of the mosquito (according to Ménard, 2005).

The first symptoms caused by *P. falciparum* infection emerge after a week or even longer, when the infected individual suffers from headache, fever or chills. This is usually a result of the intraerythrocytic growth of the parasite, which is followed by rupture of the erythrocyte and the release of new merozoites. If the *P. falciparum* infection is not treated within the next 24 hours, it can lead to severe illness due to rapid spreading of infected red blood cells in the circulatory system. This affects several organs, for example the nervous system (cerebral malaria) and can lead to metabolic acidosis and anemia as a consequence of hemolysis, resulting in coma and death of the infected person (Miller et al., 2002; reviewed in WHO 2013).

1.3 The intraerythrocytic stage

1.3.1 *P. falciparum*-infection leads to extensive modification of the red blood cell

Plasmodium belongs to the phylum Apicomplexa - a large and diverse group of obligate intracelluar parasitic protists – which has one feature in all of their invasive stages in common: the apical complex. The apical complex, containing three secretory organelles – the micronemes, the rhoptries and the dense granules – enables parasites like *Plasmodium* to actively invade their host cells distinguishing this group from other pathogens regarding their mode of invasion (Aikawa, 1971; Cowman and Crabb, 2006). Interestingly, the merozoites - the invasive forms of *P. falciparum* produced during infection in humans - choose to invade erythrocytes, terminally differentiated cells, which lack a nucleus, subcellular organelles and do not perform any lipid- and protein synthesis (Mohandas and Gallagher, 2008). To reside and asexually multiply within this kind of a host cell therefore demands extensive modifications of the erythrocyte by the parasite. Already the invasion process, which comprises 1) the initial binding of the parasite to the host cell, 2) its repositioning and 3) the formation of a tight junction with the host cell (Dvorak et al., 1975; Bannister and Dluzewski, 1990) accompanied by the discharge of various proteins from the secretory organelles (Kats et al., 2008; Dowse et al., 2008; Cowman and Crabb, 2006) leads to a disruption of the red blood cell membrane and also affecting its cytoskeletal protein composition (McPherson et al., 1993; Roggwiller et al., 1996). However, the major alterations of the host cell takes place once the parasite has gained entry into the red blood cell and starts exporting a large number of its own proteins into the host cell cytosol and membrane (Maier et al., 2009; Marti et al., 2005). One of the prominent protein, which is exported to the red blood cell membrane, is the so-called ***P. f**alciparum* **e**rythrocyte **m**embrane **p**rotein **1** (PfEMP1). PfEMP1 is a large protein of the size of 200-350 kDa and is responsible for antigenic variation. These proteins are the major cause of the pathogenicity of *P. falciparum*-infection due to their characteristics to adhere to receptors of the endothelium preventing destruction of infected **r**ed **b**lood **c**ell**s** (RBCs) by the immune system (Su et al., 1995; Baruch et al., 1995). Their presentation on the surface of the RBC is supported by another kind of protein, the **k**nob-**a**ssociated **h**istidine **r**ich **p**rotein (KAHRP), which causes knob-like protrusions in the erythrocyte membrane (Culvenor

et al., 1987; Pologe et al., 1987; Trager et al., 1966; Crabb et al., 1997). The interaction between PfEMP1 proteins and KAHRP not only increases the chances of receptor binding and sequestration of infected cells under the flow conditions of the circulatory system (Crabb et al., 1997), but also leads to increased rigidity of the erythrocyte membrane (Glenister et al., 2002). Another key aspect in the survival of the parasite is the nutrient acquisition throughout its intraerythrocytic development. Therefore *P. falciparum* not only modifies host cell transporters for constitutive nutrient uptake, but was also found to create **n**ew **p**ermeability **p**athway**s** (NPPs) in the membrane of the host cell (Kutner et al., 1985; Kirk, 2001).

1.3.2 Novel structures and compartments in *P. falciparum*-infected red blood cell

Apart from the already mentioned secretory organelles at the apical complex harbouring different lipids and proteins, which mainly play a role in the invasion process of the merozoite, other structures and compartments formed by *P. falciparum* during its intraerythrocytic development are also only found in the phylum Apicomplexa and in particular in *Plasmodium* (Fig. 1.3).

An ultrastructural analysis of the infected RBC supported the long-standing notion of the existence of parasite produced membranous structures in the erythrocyte cytosol: the Maurer's clefts. These thin structures are composed of an electron-dense coat with a translucent lumen most likely located in close proximity to the erythrocyte membrane, possibly supporting the trafficking of parasite proteins to the host cell membrane (Aikawa et al., 1986; Wickert and Krohne, 2007; Lanzer et al., 2006). Another set of membranous network also located in the red blood cytosol and found to play a role in nutrient acquisition is the so-called **t**ubo**v**esicular **n**etwork (TVN) (Atkinson and Aikawa, 1990; Lauer et al., 1997). These tubular and vesicular membranous structures seem to be connected with the membrane of the **p**arasitophorous **v**acuole (PV) (van Ooij et al., 2008), a compartment which is formed by the parasite during host cell invasion and which surrounds the parasite throughout its entire development inside the RBC (Lingelbach and Joiner, 1998). The PV is a compartment existing in some of the Apicomplexan parasites like *Toxoplasma* and *Plasmodium* and acts as a barrier between parasite and host cell cytosol. Although the PV itself is topologically different from the

parasite and the host cell, the **p**arasitophorous **v**acuolar **m**embrane (PVM) seems to consist of proteins and lipids of the host cell (Lauer et al., 2000; Murphy et al., 2004), but is also proposed to be of parasite origin (Bannister and Dluzewski, 1990), this still being a matter of debate. The cellular function of the PV is not fully understood, however, it is suggested to play a role in the protection of the parasite from detrimental substances of the host cell cytosol and enables nutrient uptake for parasite growth (Lingelbach and Joiner, 1998). According to two independent screening studies of parasite exported proteins to the host cell by Marti and colleagues and Hiller and colleagues more than 250 proteins were discovered to be secreted through the PVM (Marti et al., 2004; Hiller et al., 2004), many of them being responsible for the virulence of *P. falciparum* infection. However, a proteomic approach to study the PV content revealed not only a large number of proteases and chaperones possibly playing a role in the lysis process during parasite release, but also revealed many proteins of unknown function. In general, the role of the PV can be attributed to a sorting compartment for distinguishing between resident PV proteins and proteins *en route* to the host cell, leaving the latter ones to pass through the PVM (Nyalwidhe and Lingelbach, 2006).

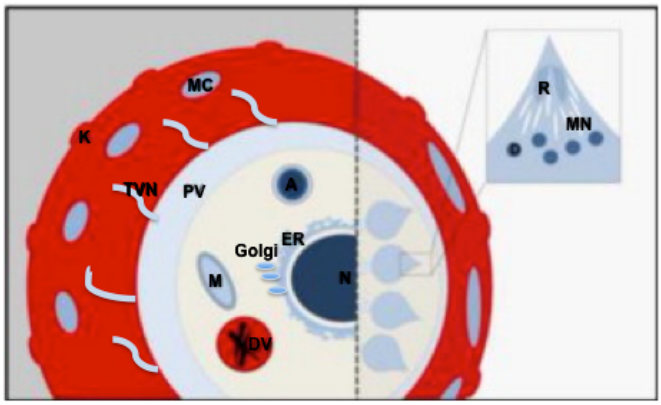

Figure 1.3 Compartments of *P. falciparum*-infected red blood cell

Left side: Trophozoite stage of *P. falciparum*-infected red blood cell displaying the nucleus, the ER, the Golgi-complex, the mitochondrion (M), the food (digestive) vacuole (DV) and the apicoplast (A) within the parasite cytosol. The parasite is surrounded by the PV, from which the TVN is formed and found located inside the erythrocyte cytosol similar to the Maurer's clefts (MCs). At the erythrocyte membrane knob-like protrusions are shown (K). Right side: Schizont-infected RBC with the apical organelles: rhoptries (R), micronemes (MN) and dense granules (D) (modified according to Deponte et al., 2012).

Apart from the PV two other compartments are also present in the parasite: the food vacuole and the apicoplast (**apico**mplexan **plast**id). The food vacuole is formed by a cytosomal system, membrane-enclosed structures of parasite origin, which take up hemoglobin in portion – hemoglobin makes up 95 % of the red blood cell cytosol- during parasite growth. Inside the food-vacuole hemoglobin is degraded, and heme is crystallized to the dark-pigment hemozoin (Francis et al., 1997). The apicoplast is a non-photosynthetic four-membrane-bound plastid located in the cytosol of the parasite and found to be crucial for the parasite's survival. Its function is not fully understood but it seems to play a role in fatty acid, isoprenoid and heme synthesis (Waller and McFadden, 2005). Although *Plasmodium* contains some compartments characteristic only of Apicomplexan parasites, the following common eukaryotic compartments are also found in the parasite: *Plasmodium falciparum* has a nucleus harbouring a haploid genome (Gardner et al., 2002), a single mitochondrion containing its own, but highly reduced genome (Bender et al., 2003) and the common compartments of the secretory system found in all eukaryotic cells. These are the **e**ndoplasmic **r**eticulum (ER) and an unstacked Golgi-complex. Both compartments, however, show some differences in their morphology to their counterparts in higher eukaryotes (Couffin et al., 1998; Van Wye et al., 1996).

1.3.3 Protein secretion mechanisms in the *P. falciparum*-infected red blood cell

Being a eukaryotic organism, protein secretion in *P. falciparum* via the early secretory pathway is most likely to resemble that of other eukaryotes. However, there are many exceptions to the rule since *Plasmodium* harbours compartments, which are missing in other eukaryotic cells and to which proteins are directed to. Before focusing on the protein secretion mechanism during the intraerythrocytic stage of *P. falciparum* the general model for the early secretory pathway - keeping in mind that there are many variations to the rule across eukaryotes - in eukaryotes is described:

The early secretory pathway in eukaryotes: Early studies on intracellular protein trafficking in eukaryotes included morphological, genetic and biochemical analyses mainly on yeast in order to identify the components of the secretory membrane system and to understand the underlying molecular mechanisms of its regulation (Palade, 1975; Rothman, 1994). In brief: secretory protein synthesis begins in the cytosol at ribosomes,

which are associated with the endoplasmic reticulum (rough ER) - a large intracellular compartment spread throughout the cytoplasm, consisting of many membranous layers interconnected with each other and mainly specialized in protein- and lipid biosynthesis. The pre-proteins contain a N-terminal **s**ignal **p**eptide (SP) of mostly 15-30 hydrophobic amino acids, which is produced during translation and is recognized and bound to a so-called **s**ignal **r**ecognition **p**article (SRP). The SRP stops protein translation, then binds to the SRP-receptor in the ER membrane that directs the entire SRP-ribosome complex to a translocator residing in the ER membrane – the Sec61 complex, which is known to be highly conserved in bacteria and eukaryotic cells – where protein translation proceeds once the SRP/SRP-receptor is released. The proteins are co-translationally transferred across the ER membrane, where soluble proteins are fully released into the lumen of the ER after translation, whereas integral membrane proteins become embedded in the ER membrane. The signal peptide is cleaved off by a signal peptidase. Many of the soluble and integral membrane proteins either become resident ER proteins or are further trafficked to the plasma membrane or other compartments. The forward trafficking of these proteins is dependent on another compartment, the Golgi-complex, which consists of tubular membranous structures, divided into functionally distinct *cis*-, *medial* and *trans*-Golgi stacks. The proteins leave the ER once they are packaged into vesicles termed COPII-coated-vesicles. These vesicles then fuse with the *cis*-Golgi and progressively move through the *medial*- and *trans*-Golgi (anterograde transport) in a budding and fusion process, before they are released from the Golgi-complex to the cell surface or to other compartments inside the cell. During the vesicular transport through the Golgi-complex proteins are post-translationally modified by resident Golgi-enzymes specialized in performing different kinds of glycosylation reactions. Retrograde transport from the *cis*-Golgi towards the ER via COPI-coated vesicles occurs when ER resident proteins accidentally enter the anterograde secretion pathway. They are recognized via their XDEL ER-retrieval sequence by specialized receptors located at the *cis*-Golgi and are trafficked back to the ER (Fig. 1.4) (Blobel and Dobberstein, 1975a; Blobel and Dobberstein, 1975b; Palade, 1975; Rothman, 1994; Alberts et al., 2008).

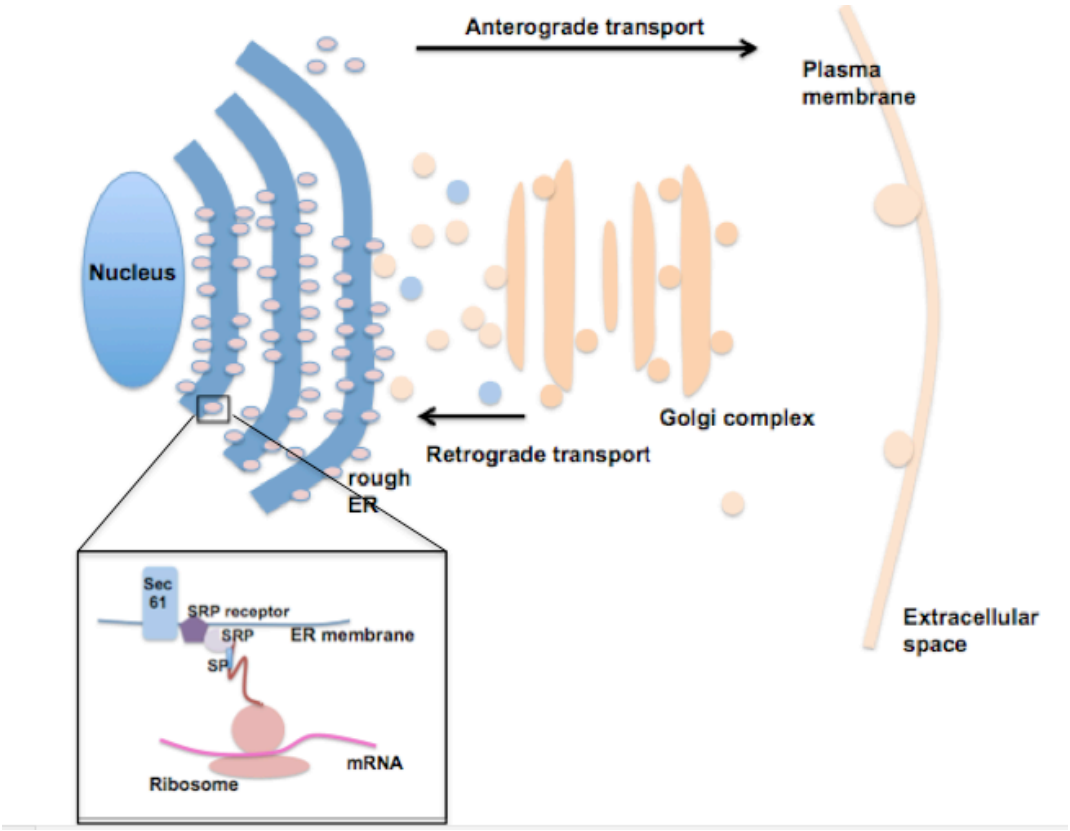

Figure 1.4 Simplified model of the classical secretory pathway of the eukaryotic cell

Protein translation begins in the cytosol at ribosomes associated with the ER. Proteins destined to be secreted to the extracellular space contain a signal peptide (SP) at their N-terminus, which is recognized and bound to a signal recognition particle (SRP). Translation stops until the SRP-ribosome complex is bound to a SRP-receptor, which then trafficks the entire SRP-ribosome complex to a translocon in the ER-membrane (Sec 61 complex), where the protein is co-translationally translocated across the ER membrane. This protein is then trafficked via vesicles generated from the ER to the Golgi-complex and is released from the Golgi-complex via vesicles into the extracellular space. The trafficking of proteins from the ER towards the plasma membrane is referred to as anterograde trafficking. However, ER-proteins, which accidentally escape the ER, are transferred back from the Golgi to the ER, in a process called retrograde transport.

Early secretory pathway in *P. falciparum*: Many different *in vitro* and *in silico* studies on the intraerythrocytic stage of *P. falciparum* revealed the existence of some components playing a role in the early secretory pathway. These are for example the gene homologue of the mammalian α-subunit of the Sec61 translocon *PfSec61* (Couffin et al., 1998) and the lumenal proteins of the ER *PfERC2* and *PfBIP* (Kumar et al., 1991; La Greca et al., 1997) supporting the existence of an ER in the parasite cytosol. The existence of a Golgi apparatus was initially doubted since typical Golgi stacks could not

be found by electron microscopy (Aikawa, 1988) and parasite proteins were not subjected to any kind of N-linked glycosylation (Dieckmann-Schuppert et al., 1992). However, other studies revealed the existence of typical Golgi proteins like the ERD2-receptor, which binds to proteins with a KDEL-retrievel sequence (Elmendorf and Haldar, 1993), the GTPase Rab 6 (van Wye et al., 1996) and the Golgi re-assembly stacking proteins 1 and 2 (Struck et al., 2005; Struck et al., 2008a; Struck et al., 2008b) indicating the existence of a possible rudimentary Golgi-complex. Furthermore, the gene of the ADP-ribosylation factor 1, a small GTPase important for vesicular trafficking in the early secretory pathway, was isolated, expressed and characterized from *P. falciparum* and more recently its crystal structure was also determined (Stafford et al., 1996; Cook et al., 2010). These findings are in accordance with an *in silico* analysis by Gardner and colleagues in 2002. They identified potential homologue gene candidates of proteins involved in the early secretory pathway like for example the SRP, a signal peptidase and proteins involved in the budding and fusion of secretory vesicles (Gardner et al., 2002). Furthermore, studies with the fungal metabolite Brefeldin A (BFA), a known inhibitor of the secretory pathway, was shown to inhibit the secretion of a number of parasite proteins (Benting et al., 1994; Hinterberg et al., 1994; Baumgartner et al., 2001; Lippincott-Schwartz, 1989).

Many of the proteins secreted from *P. falciparum* not only contain the 'classical' signal sequence found in other eukaryotic organisms, but also revealed a modified version of the SP: a prolonged stretch of hydrophobic amino acids of up to 80 amino acids and recessed from the N-terminus of the protein (Lingelbach, 1993; Cooke et al., 2004). In addition, it could be shown that proteins containing the classical signal sequence are directed towards the **p**arasite **p**lasma **m**embrane (PPM), the PV and the PVM, respectively, while those containing the recessed signal are found transported beyond the PVM *en route* to the host cell (Albano et al., 1999; Lingelbach, 1993). Here, too, many exceptions to the rules exist, like in the case of STEVOR (Przyborski et al., 2005) and the **h**istidine-**r**ich **p**rotein **2** (HRP2) (Howard et al., 1986), both containing a classical signal sequence, but are found exported to the host cell. Further trafficking of exported proteins, after entering the classical secretory pathway, is postulated to occur in a vesicle-mediated process (two-step model): vesicles containing the exported proteins fuse with the PPM and release the content into the lumen of the PV, before the

protein is trafficked to the host cell across the PVM (Ansorge et al., 1996; Charpian and Przyborski, 2008).

Protein secretion beyond the PVM: Compared to protein secretion in higher eukaryotes, in which many secretory proteins are subsequently secreted to the extracellular milieu via exocytosis by just crossing one membrane - the plasma membrane of the respective cell - many malarial proteins are found and predicted to be exported beyond the PVM (Marti et al., 2004; Hiller et al., 2004). This calls for additional targeting signals in the amino acid sequence of these proteins. Indeed a conserved motif consisting of five amino acids (RxLxE/Q/D), referred to as ***P****lasmodium* **ex**port **el**ement (PEXEL) or **h**ost **t**argeting signal (HT), was found in two independent *in silico* and reporter construct studies. They are present at the N-terminus of the exported proteins in close proximity to the recessed signal peptide (~ 20 amino acids downstream). These studies enabled the identification of a large number of proteins – soluble and transmembrane proteins - coded in the parasite genome and containing the PEXEL motif (~ 8 % of proteins), which are ever since collectively called the 'exportome' of *P. falciparum* (Marti et al., 2004; Hiller et al., 2004). Furthermore, the predicted genes of the malarial 'exportome', containing the PEXEL motif are found to be localized at subtelomeric regions of the parasite genome, where proteins responsible for host cell modifications are normally found (Maier et al., 2008). Interestingly, more recent studies revealed that the first three residues of the PEXEL motif (RxL) are actually cleaved during the early secretory pathway in the ER by an aspartic protease, which has been identified as Plasmepsin V, followed by N-acetylation of the cleaved protein (Chang et al., 2008; Boddey et al., 2010; Russo et al., 2010). Although different models for further trafficking towards the PV involving the remaining PEXEL residues and Plasmepsin V dependent export, respectively, have been proposed, none of it has been verified (Boddey et al., 2010; Crabb et al., 2010). Another model, although heavily debated, suggests the role of **P**hosphatidyl**i**nositol(3,4,5)-tri**p**hosphate (PIP3) in PEXEL-protein delivery to the PV (Bhattacharjee et al., 2012). Whatever the mode of protein secretion in the late secretory pathway (Golgi ➔ PPM ➔ PVM) might be, it seems like that exported proteins are first secreted into the PV before being directly translocated across the PVM in an ATP-dependent process as shown in two independent localization studies with exported

proteins (Ansorge et al., 1996; Wickham et al., 2001). This corresponds with the earlier mentioned two-step model in protein secretion (Charpian and Przyborski, 2008) assigning the PV as a transit compartment. This finding coincides with experiments using the dihydrofolate reductase system (DHFR) showing that exported proteins need to be unfolded before passing the PVM (Gehde et al., 2009). This observation strongly suggest the existence of a translocation system in the PVM. In fact, an ATP-driven translocon, composed of five different *Plasmodium* proteins, was found in the membrane of the PV and appears to be a possible candidate responsible for protein translocation of exported proteins across the PVM. Since PEXEL proteins seem to be unique to the Apicomplexan *Plasmodium* the translocon termed ***P**lasmodium* **t**ranslocon of **ex**ported proteins (PTEX) also consists of parasite proteins restricted to the *Plasmodium* genome (de Koning-Ward et al., 2009; Bullen et al., 2012). However, this transport model system only seems to fit for the export of soluble parasite protein, since proteins containing a 'transmembrane domain' would rather end up in the parasite plasma membrane, when secreted via the secretory pathway. One solution to this dilemma would be the way these proteins are synthesized meaning that they are initially synthesized as 'soluble' proteins, which take up their membrane topology only after entering their destination in the host cell. This hypothetical model actually coincides with solubility studies of different transmembrane containing exported proteins (Papakrivos et al., 2005; Przyborski et al., 2005; Saridaki et al., 2009).

However, some well-known exported proteins of *P. falciparum* lack the typical PEXEL motif and they are generally termed **P**EXEL-**n**egative **e**xported **p**roteins (PNEPs). These are for example the **s**keletal-**b**inding **p**rotein **1** (SBP1), the **m**embrane-**a**ssociated **h**istidine-**r**ich **p**rotein **1** (MAHRP1) and the **r**ing **ex**ported proteins 1 and 2 (REX 1 and 2). These proteins are resident proteins of the Maurer's clefts, which not only lack a distinguishable PEXEL motif, but also a typical signal sequence for ER entry. However, localization and solubility studies revealed the existence of a single transmembrane region in each of these proteins - except for REX 1, which contains a recessed signal peptide – which appears to be responsible for entering the secretory pathway. This is furthermore supported by studies revealing their sensitivity to BFA (Saridaki et al., 2009; Spycher et al., 2008; Dixon et al., 2008; Haase et al., 2009). However, the further transport of these proteins, which pass the PV and PVM until reaching their final

destination in the host cell cytosol, still remains enigmatic. The transport process possibly involves other, not yet identified atypical signals/regions in the amino acid sequence of these proteins and possibly also other kind of translocons in the PVM. Since the number of exported PNEPs in the malaria genome might be greater than known to date, the chance to discover alternative secretory pathways in *P. falciparum* is quite high.

1.4 Unconventional protein secretion

As described in the previous chapter, secretory proteins are released into the extracellular milieu via the conserved secretory pathway universal to almost all eukaryotic organisms: the 'classical secretory pathway' involving the ER/Golgi-complex. In contrast, many studies in the past years have revealed the secretion of a small number of proteins, which lack a signal peptide to enter the classical secretory pathway and were not affected in their secretion to the cell surface in the presence of BFA (Rabouille et al., 2012). Thus, these proteins were found to be secreted in a mostly ER-to-Golgi independent manner into the extracellular space (Fig. 1.5). That is why this mode of secretion is referred to as 'unconventional protein secretion' and is used by a small number of proteins involved in cell survival, angiogenesis and in inflammatory responses (Nickel, 2005).

In general, two mechanisms for unconventional protein secretion were discovered: vesicular pathways versus non-vesicular pathways. A well-studied candidate of the non-vesicular pathway is the **F**ibroblast **g**rowth **f**actor **2** (FGF2) – a protein involved in angiogenesis – which was found to be directly translocated across the plasma membrane (Schäfer et al., 2004). The translocation process requires the interaction with **p**hospho**i**nositide phosphatidylinositol(**4,5**)-bis**p**hosphate ($PI(4,5)P_2$) - a component located at the inner leaflet of the plasma membrane - and heparan sulfates found at the outer leaflet of the plasma membrane (Temmerman et al., 2008; Zehe et al., 2006). Another candidate secreted in a non-vesicular mechanism is for example the yeast mating factor α, which is translocated via the membranous ABC transporter Step6 (McGrath and Varshavsky, 1989). Other unconventional secretion pathways involve vesicle-mediated secretion, as in the case of **i**nter**l**eukin **1β** (IL1β) (Rubartelli et al.,

1990). Although the mechanism of the processing pattern of IL1β and the components involved are mostly understood (Franchi et al., 2009), the nature of the vesicles responsible for trafficking IL1β to the plasma membrane is still not clear. One model proposes the secretion of IL1β via secretory lysosmes, a compartment assigned to have a dual function: degradation of proteins, but also storage of secretory proteins before regulated release to the extracellular space upon external stimuli (Andrei et al., 1999; Griffiths, 1996). However, two further mechanisms were also suggested to be involved in the secretion of IL1β: microvesicle shedding at the external side of the plasma membrane (MacKenzie et al., 2001) and the formation of **m**ulti**v**esicular **b**odies (MVB), respectively, which are vesicles formed inside endosomes and are afterwards released as vesicles into the extracellular space, then referred to as 'exosomes' (Stoorvogel et al., 2002). Just recently, other studies discovered an unusual vesicle-mediated secretion pattern of the **ac**yl-CoA-**b**inding protein **A** (AcbA) from *Dictyostelium discoideum* involving proteins responsible for the formation of autophagosomes. The autophagosomes then fuse with the plasma membrane to release AcbA (Cabral et al., 2010; Duran et al., 2010; Manjithaya et al., 2010). In addition, some studies imply the role of endosomes, which form multivesicular bodies to fuse with the plasma membrane. This hypothesis is supported by the findings of proteins, which are characteristic of this pathway (Duran et al., 2010; Manjithaya et al., 2010). Furthermore, the yeast ortholog to the mammalian GRASP1 is proposed to play a role in secretion of AcbA as well (Kinseth et al., 2007). Last but not least, a pathway termed the 'Golgi bypass' is used by transmembrane proteins. These proteins initially enter the classical secretory pathway and are eventually released at the plasma membrane, but on their way avoid the Golgi-complex. This for instance is characterized by their insensitivity to BFA (Grieve and Rabouille, 2011).

The appearance of the increasing number of unconventionally secreted proteins and the different mechanisms involved raises the question, why some proteins are differently secreted from the cell, compared to the huge majority of secretory proteins, which uses the classical ER-to-Golgi pathway. So far, two hypotheses to address this question exist: First, it is assumed that in the case of FGF2, this protein, while trafficked through the classical secretory pathway, would bind at a very early stage to glycoproteins, leading to aggregation of the protein and non-secretion of FGF2. The second model, however,

proposes the secretion of a non-functional protein due to posttranslational modification, caused while trafficking via the ER/Golgi pathway. Indeed, the latter model was supported by experiments with FGF2. A signal peptide was fused to FGF2 directing this protein into the classical secretory pathway, however, the protein was not secreted into the extracellular space in its functional form (Nickel, 2010; Wegehingel et al., 2008). Since many of the proteins involved in unconventional protein secretion seem to be biomedically relevant, they appear to be suitable drug targets, if their mode of secretion and the components involved would be totally independent of the ER-to-Golgi route.

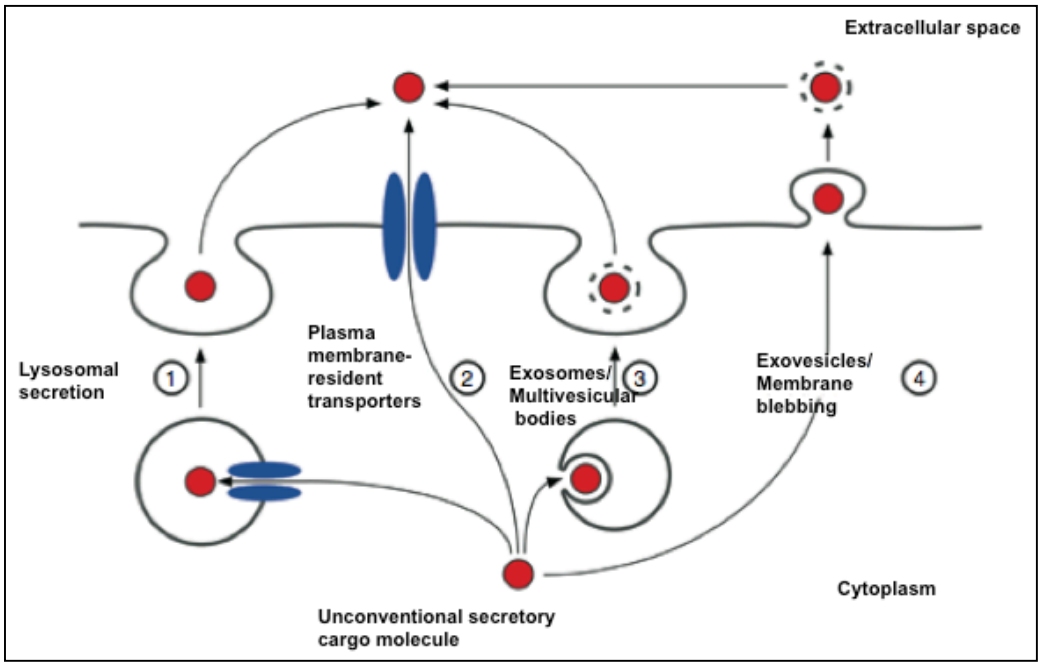

Figure 1.5 Unconventional protein secretion mechanisms

Four different types of unconventional protein secretion mechanisms are illustrated. Type1: Vesicular trafficking via lysosomal secretion. Type 2: Non-vesicular trafficking via plasma membrane resident transporters. Type 3: Vesicular trafficking via formation of multivesicular bodies. Type 4: Membrane blebbing is the microvesicle shedding at the external side of the plasma membrane. Missing in this illustration: Golgi-bypass pathway (according to Nickel, 2005).

Interestingly, mechanisms of unconventional protein secretion also appear in protozoan parasites as described for the *Leishmania* **h**ydrophilic **a**cylated **s**urface **p**rotein **B** (HASPB) (Denny et al., 2000) and the **C**alcium-**d**ependent **p**rotein **k**inase **1** (CDPK1) of *P. falciparum* (Möskes et al., 2004). Both proteins show the same mode of unconventional protein secretion: dual acylation of the N-terminus of the respective

proteins, which mediates export to the extracellular surface and the parasitophorous vacuole, respectively. The role of acylation-dependent export is discussed in the next chapter.

1.5 Role of fatty acid acylation of proteins in plasma membrane binding

1.5.1 Protein *N*-myristoylation

N-myristoylation is a co- and post-translational modification of proteins found in all eukaryotic cells. Proteins are characterized as *N*-myristoylated, when a 14-carbon saturated fatty acid (myristate) is irreversibly attached to the N-terminal glycine residue of the target protein. The glycine residue at the N-terminus of a protein sequence is a prerequisite for *N*-Myristoylation to take place. At first, methionine - the initiating amino acid in the protein sequence 'Met-Gly-...' - is removed by a methionine aminopeptidase during translation, leaving the glycine residue at the 2nd position of the N-terminus exposed. The myristate from Myristoyl-CoA is then linked to the glycine residue via an amide bond by the ***N*-myristoyltransferase** (NMT) (Fig. 1.6). NMT is an enzyme present in all eukaryotic cells and was discovered to be essential for the viability of different eukaryotic organisms (Resh, 1999; Wright et al., 2010). Importantly, NMT protein substrates require in addition to the glycine residue at the N-terminus specific amino acids downstream of the protein sequence – serine or threonine are usually found at position 6 and lysine and arginine, respectively, are found at position 7/8 - to be recognized by the NMT (Resh, 1999). However, more recent studies showed that *N*-myristoylation also posttranslationally takes place in cells undergoing apoptosis involving caspase cleavage (Zha et al., 2000).

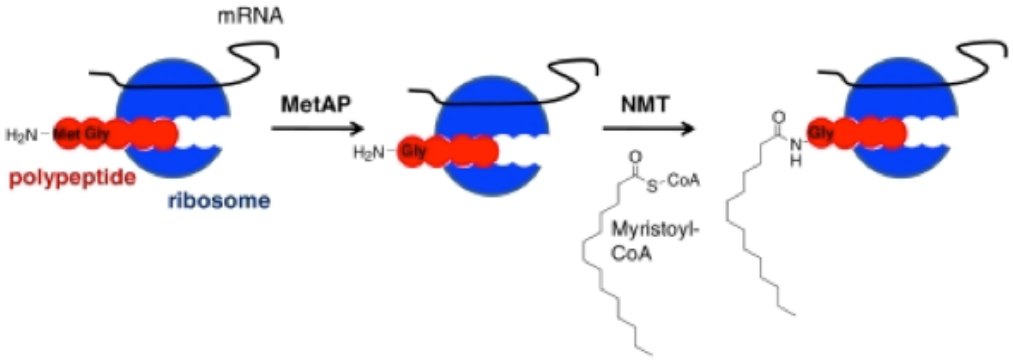

Figure 1.6 Co-translational *N*-myristoylation

During translation the initiating methionine is removed by a methionine aminopeptidase (MetAP). Then the 14-carbon saturated fatty acid (myristate) is irreversibly attached to the glycine residue at the second position of the protein sequence via the Myristoyl-CoA by the *N*-myristoyltransferase (NMT) (according to Wright et al., 2010).

N-myristoylation is commonly found in proteins involved in signal transduction (protein kinases and phosphatases), G_{α} proteins, calcium-binding proteins, **A**DP-**r**ibosylation **f**actors (ARF) and also MARCKS (membrane and cytoskeletal-bound proteins) as known for mostly animal and fungal cells. Most of these proteins play a role in signalling processes and in the case of the ARFs in vesicular shuttling revealing their functional importance in these organisms (Resh, 2006). Furthermore, bioinformatic studies, using prediction models, revealed that about 0.5 % of the proteome in eukaryotes appear to be substrates of the NMT (Maurer-Stroh et al., 2002). It appears that apart from viral proteins, bacterial proteins can also be subjected to *N*-myristoylation by the *N*-myristoyltransferase of their respective eukaryotic host cell (Maurer-Stroh and Eisenhaber, 2004). The myristoyl moiety enables a reversible binding of the protein to the plasma membrane and to other intracellular membranes in a eukaryotic cell, respectively. However, due to the low binding energy of myristate to the phospholipids of a membrane (approximately 10^{-4} M K_d) a myristoylated protein cannot efficiently anchor to the plasma membrane (Peitzsch and McLaughlin, 1993). In order to achieve a sufficient binding to the phospholipid bilayer, a second signal within the amino acid sequence of the myristoylated protein is required. This hypothesis is referrred to as the 'two-step model'. The second signal can either be another fatty acid group like palmitate (16-carbon saturated fatty acid) or a polybasic cluster of amino acids, located in proximity to the *N*-myristoylation site. The binding of the respective protein to the membrane occurs when ten of the fourteen carbon atoms of the myristate insert into the phospholipid bilayer and the polybasic cluster of amino acids interacts with the acidic phospholipids of the cellular membrane (electrostatic interaction). The dual binding property induced by the myristate and the polybasic domain synergize leading to a stable anchoring of the protein to the membrane (Murray et al., 1997; Murray et al., 1998; Sigal et al., 1994; Buser et al., 1994). A similar mechanism to establish a strong membrane attachment is achieved by dual acylation of a protein with a myristate and a palmitate moiety (Resh, 1999), which will be discussed in more detail

in the next section. Interestingly, the attachment of a myristate to a respective protein also plays a role in membrane targeting to the right target membrane (Murray et al., 1998), although the mechanisms involved here are not yet understood. Further, the membrane anchoring of *N*-myristoylated proteins can be characterized as a dynamic process, since the myristate moiety on the respective protein switches between two different conformations: it is either exposed on the outside of the protein enabling membrane attachment, or it is segregated into a hydrophobic groove of the protein leading to detachment from the membrane. This mechanism known as the 'myristoyl switch' can be induced by e.g. a ligand or electrostatic interaction (Fig. 1.7) (McLaughlin and Aderem, 1995). A ligand induced myristoyl switch has been characterized for the **A**DP-**r**ibosylation **f**actor (ARF) proteins, which are regulated by the binding of GTP, which induces the exposure of the myristoyl moiety - initially located in a hydrophobic pocket in its GDP-bound form - and subsequent binding to the membrane (Amor et al., 1994). MARCKS proteins, on the other hand, are regulated by **p**rotein **k**inase **C** (PKC), which phosphorylates the stretch of the N-terminal polybasic serine residues - the second motif required for membrane binding in the two-step model – leading to an increased negative charge at the polybasic domain. This diminishes the electrostatic interaction with acidic phospholipids leading to the dissociation of the respective protein from the plasma membrane (Thelen et al., 1991).

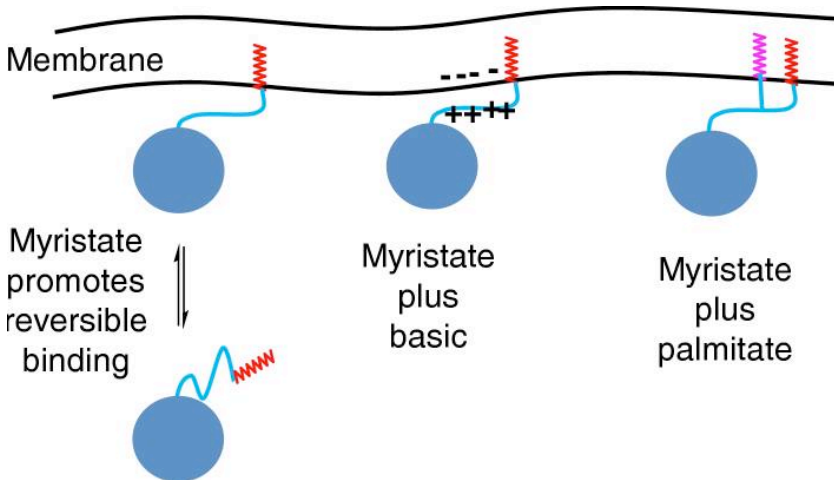

Figure 1.7 Two-signal model of myristate-mediated protein binding to the membrane

The low binding energy of the myristoyl-group on the protein promotes reversible binding to the membrane. A second signal is required for stable membrane anchoring: either a polybasic cluster of amino acids to interact with the negatively charged phospholipid groups of the membrane via electrostatic interaction or a second saturated fatty acid like palmitate. Blue circle (protein), red (myristate), pink (palmitate) (according to Wright et al., 2010).

1.5.2 Protein-Palmitoylation

Similar to *N*-myristoylation protein palmitoylation is a lipid modification, whereby usually a 16-carbon saturated fatty acid is attached to a cysteine residue via a thioester bond. Compared to the irreversible attachment of myristate to a protein, palmitoylation was found to be a reversible modification (Linder and Deschenes, 2003). This is due to the labile thioester linkage between protein and palmitate. The dynamic feature of protein palmitoylation is regulated by palmitoylation and depalmitoylation in regard to the function and localization of the respective protein (Zacharias et al., 2002; Wedegaertner and Bourne, 1994). So far, two different classes of enzymes responsible for palmitoylation and de-palmitoylation have been discovered: Protein acyltransferases (PATs) catalyze palmitate transfer to the respective protein, while the protein acylthioesterases are in charge of removing palmitate from the protein (Resh et al., 2006; Mitchell et al., 2006). Interestingly, no consensus sequence for palmitoylation exists except for the presence of the cysteine residue and in addition *in vitro* studies revealed a non-enzymatic addition of palmitate from palmitoyl-CoA to proteins (Bañó et al., 1998). However, proteins which are subjected to palmitoylation are usually peripherally attached membrane proteins or proteins containing a transmembrane domain. Proteins containing a transmembrane domain are usually palmitoylated at the junction between cytoplasm and membrane or at the C-terminus located in the cytoplasm. In contrast, the peripherally associated membrane proteins can be dually acylated or are just palmitoylated by adjacent cysteine residues. A cysteine residue at the N-terminus often exists in close proximity to a lipidation site like a preceding *N*-myristoylation site. Upon palmitoylation a protein becomes more hydrophobic, which leads to a strong protein-membrane anchoring (two-step model). Dually acylated proteins with palmitoylation and preceding *N*-myristoylation are found among G_{α} proteins and tyrosine kinases and frequently exhibit the motif 'Met-Gly-Cys' at their N-terminus (Smotrys and Linder, 2004; Nadolski and Linder, 2007). Mutational analyses revealed that substitution of either of the amino acids responsible for lipid modification leads to a decrease or even loss of the protein binding capacity to the plasma membrane (Resh, 1999). More intriguingly, some studies claim that these dually fatty acid acylated proteins are targeted to specific membrane regions of the plasma membrane, the so-called rafts. Rafts are microdomains in the plasma membrane, which

are enriched in cholesterol and sphingolipids. However, the mechanism responsible for this observation has not been verified to date (Smotrys and Linder, 2004). In summary, palmitoylation is an important feature of proteins in regard to protein-membrane attachment, trafficking of transmembrane proteins and regulation of intracellular signalling processes of many proteins (Linder and Deschenes, 2003).

1.6 Acylated proteins as candidates of an alternative secretory pathway in *P. falciparum*?

1.6.1 *P. falciparum* ADP-ribosylation factor 1

Like other eukaroytic organisms, the malaria parasite *Plasmodium falciparum* also contains genes encoding the **A**DP-**r**ibosylation **f**actor (ARF), a small GTP binding protein, which plays a crucial role in vesicular trafficking (Stafford et al., 1996; Boman and Kahn, 1995). ARF proteins belong to the superfamily of Ras proteins – a small group of GTPases – and are involved in a number of cellular processes, like for example in vesicular biogenesis and trafficking processes of the secretory pathway (Boman and Kahn, 1995). To date six highly conserved members of the ARF protein family are known for mammalian cells (Kahn et al., 1991). However, so far, only one of the two genes encoding ARF proteins, the gene *arf1*, in *P. falciparum*, is isolated, expressed and characterized (Stafford et al., 1996) and structurally determined (Cook et al., 2010). One of the functions attributed to ARF proteins is their role in the COPI pathway (retrograde transport from *cis*-Golgi to the ER), where they recruit other coat proteins and initiate vesicle formation upon activation. Activation of the soluble GDP-bound ARF to the GTP-bound form, which is able to bind to the membrane is catalyzed by the **g**uanine nucleotide **e**xchange **f**actor**s** (GEFs). The attachment to the membrane occurs, when the *N*-myristoylation site at the N-terminus of the protein is exposed in the GTP bound conformation of ARF. However, once the GTP on the ARF protein is hydrolyzed to GDP by **G**TPase **a**ctivating **p**roteins (GAPs) ARF is released from the membrane and the myristoyl moiety is covered in a hydrophobic groove of the protein. The release of ARF from the vesicle also leads to the detachment of other coat proteins from the vesicle, whereby ARF functions as a trigger. The vesicle formation and cargo

trafficking in e.g. the anterograde pathway depends on the cycling of ARF between its soluble GDP-bound state and the membrane-associated GTP-bound state (Boman and Kahn, 1995; Kirchhausen, 2000).

Although some components of the classical secretory pathway are gradually being identified within the parasite cytosol, some studies also report the export of these components and the presence of secretory vesicles in the host cell. These findings implicate the existence of a vesicle-mediated secretion pathway for some parasite proteins from the parasite cytosol to their host cell and host cell membrane, respectively (Trelka et al., 2000; Taraschi et al., 2001). Further studies, apart from electronmicroscopical evidence, supporting the model of a dual operating system in the parasite cytoplasm and the host cell cytosplasm, are missing. On the contrary, a new study with GFP reporter constructs proposed the localization of the components involved in the secretory pathway exclusively to the parasite cytosol (Adisa et al., 2007). Another interesting aspect observed by Stafford and colleagues is that a high mRNA level of *Pf*ARF1 is reached during merozoite formation, shortly before a high level of *msp1* mRNA – **m**erozoite **s**urface **p**rotein **1** (MSP1) is located on the merozoite surface - is expressed. They hypothesize a role of *Pf*ARF1 in MSP1 shuttling to the merozoite surface via the ER-to-Golgi pathway (Stafford et al., 1996). A different observation regarding the localization of ARF was made by a recent proteome analysis of the PV, where *Pf*ARF1 was found to be located in the PV of the parasite (Nyalwidhe et al., manuscript in preparation), this hypothesis, however, still needs to be reviewed.

1.6.2 *P. falciparum* adenylate kinase (2)

Adenylate kinases are ubiquitous enzymes, which play an important role in energy-dependent and nucleotide signalling processes. This enzyme catalyzes the following magnesium dependent reversible reaction: ATP + AMP ⇔2 ADP maintaining the ratio between AMP and ATP in response to the cellular energy need. To date eight different isoforms of adenylate kinases have been discovered in mammalian cells showing distinct intracellular compartmentalization, a localization in different tissues and a developmentally regulated gene expression (Dzeja and Terzic, 2009). In contrast, two adenylate kinases (*Pf*AK1 and *Pf*AK2), a GTP:AMP phosphotransferase (*Pf*GAK) and two adenylate kinase-like proteins (*Pf*AKLP1 and *Pf*AKLP2) have been characterized

in the malaria parasite *P. falciparum* to date (Ulschmid et al., 2004; Rahlfs et al., 2009; Ma et al., 2012). These findings reveal the need of the parasite for a high level of adenylate kinase activity to deal with the increased ATP-turnover rate due to the high energy consumption for example during invasion, but also for the biosynthesis of macromolecules. Indeed, infected erythrocytes compared to non-infected cells reveal an increased glucose uptake, a substrate of the glycolytic pathway, responsible for producing high amounts of ATP (Roth, 1990). Differences in the kinetic properties of adenylate kinases might be a result of the distinct subcellular localization and in case of the mammalian adenylate kinase isoenzymes also might be due to tissue-specificity. The mammalian AK1, for example, is mostly found in brain and muscle cells revealing its high activity in these cells and also in erythrocytes, whereas mammalian AK2 is predominantly found in the intramembrane space of the mitochondria in liver, kidney, heart and spleen. Mammalian AK3, however, is largely found in the mitochondrial matrix of the liver and the heart and is actually a GTP:AMP phosphotransferase showing a high substrate specificity to GTP rather than ATP (Khoo and Russell, 1972; Wilson et al., 1976; Tomasselli et al., 1979; Dzeja and Terzic, 2009). *P. falciparum* AK1 exhibits a higher substrate specificity (75 U/mg) compared to AK2 (10 U/mg), which might be a result of the distinct subcellular localization (Ulschmid et al., 2004). In fact, immunofluorescence analyses with reporter constructs revealed the localization of *Pf*AK1, *Pf*AKLP1 and *Pf*AKLP2 in the parasite cytosol. The *Pf*GAK, however, was assigned to the mitochondrion of the parasite being a possible homologue to the mammalian GAK. More intriguingly, the phenotype of *Pf*AK2 was different, insofar, that the observed signal of the chimera was a ring-like structure around the parasite with a knob-like protrusion formed towards the PV and the host cell (Ma et al., 2012). The amino acid sequence of *Pf*AK2 has a *N*-myristoylation site and studies on expressed recombinant *Pf*AK2 and *Pf*NMT revealed *Pf*AK2 to be a substrate of *Pf*NMT (Rahlfs et al., 2009). Further, the group of Becker could also show that substitution of the glycine residue by alanine at the N-terminus of *Pf*AK2 changes the localization of adenylate kinase 2 to a rather cytosolic signal as observed for *Pf*AK1 (Ma et al., 2012). These results, taken together, identify *Pf*AK2 as a *N*-myristoylated membrane-bound protein.

1.7 Objective

Over the years many studies on the intraerythrocytic stage of the malaria parasite *P. falciparum* have already revealed a great amount of information on protein secretory pathways different from the ER/Golgi route as a result of the parasite's development within the red blood cell. However, the secretory pathway of many parasite proteins, especially those involved in the pathogenesis, still remain obscure.

This study focuses on the existence of alternative secretory pathways to the classical secretory pathway during the intraerythrocytic stage of *P. falciparum.* A preceding proteomic analysis of the parasitophorous vacuole revealed the secretion of parasite proteins into the PV, which lack any known signal sequence (Nyalwidhe et al, manuscript in preparation). A small percentage of the proteins identified in the PV contained a putative myristoylation site, including the *P. falciparum* ADP-ribosylation factor 1 (ARF1) – a protein known to be myristoylated in eukaryotic cells. Since it is known that the myristoylation site of ARF1 can anchor this protein to membranes, it was hypothesized that this protein might bind to the inner leaflet of the parasite plasma membrane and is subsequently flipped over into the PV. In order to validate these results on the subcellular localization of *Pf*ARF1 reporter construct studies, co-localization studies, fluorescence analyses and biochemical analyses were performed. In parallel to *Pf*ARF1, a different study revealed the secretion of another protein into the PV, the so-called *Pf*adenylate kinase 2. Similar to *Pf*ARF1, this protein also lacks a signal sequence, but contains a *N*-myristoylation site and was found to be a substrate of *Pf*NMT (Ma et al., 2012; Rahlfs et al., 2009). To further validate and investigate the subcellular localization of *Pf*AK2 mutagenesis analyses, fluorescence analyses, biochemical analyses and a translocation study with the mDHFR fusion system were carried out. Finally, the sequences of the N-terminus of *Pf*ARF1 and *Pf*AK2 were compared to each other to identify possible key differences in their amino acid sequences. Potential motifs in the sequence of *Pf*AK2, which might play a role in the translocation process of this protein across the parasite plasma membrane, which were missing in the sequence of *Pf*ARF1, were sought. Subsequently, a chimeric reporter construct of the N-terminus of both proteins was designed and analyzed via fluorescence and biochemical methods.

2 Materials and Methods

The appliances, materials and chemicals used are listed below, including the reference to the companies and the company headquarters they were purchased from.

2.1 Materials and Chemicals

2.1.1 Appliances

Appliances	Company	Company headquarters
Agarose gel chambers	Gibco BRL	Neu Isenburg
Analytical balance 2412	Sartorius	Göttingen
Autoclave	Thermo Scientific	USA
Blotting apparatus	Phase	Lübeck
Centrifuge (5804R)	Eppendorf	Hamburg
Flow Herasafe	Thermo Scientific	USA
Gel documentation system	INTAS	Göttingen
Electroporator (gene PulserII)	Bio-Rad	USA
Incubator B5060-EC/CO2	Heraeus	Hanau
Incubator Shaker (G25)	New Brunswick Scientific Co	USA
Magnetic columns	Miltenyi Biotech	Bergisch Gladbach
Magnetic stirrer	IKA	Staufen
Mikro 22 R Centrifuge	Hettich	Tuttlingen
PCR cycler	Biometra	Göttingen
pH meter	Bio-Rad	München
Powersupply	Bio-Rad	München
Precision balance 1205 MP	Sartorius	Göttingen
Thermoblock	Heidolph	Schwabach
Thermomixer 5436	Eppendorf	Hamburg
VARIO Mac Separator	Miltenyi Biotech	Bergisch Gladbach

Vortexer (Reax 2000)	Heidolph	Schwabach
Waterbath	Köttermann	Uetze/Hänigsen

2.1.2 Materials

Materials	Company	Company headquarters
Centrifuge tubes	Eppendorf	Hamburg
Cryotubes	Sarstedt	Nümbrecht
Culture flasks (25 cm^2 and 75 cm^2)	Greiner	Frickenhausen
Erlenmeyer flasks	Kobe	Marburg
Electroporation cuvettes	Bio-Rad	USA
Exposure cassettes	Rego	Augsburg
Falcon tubes	Greiner	Frickenhausen
Gel loader tips	VWR	Darmstadt
Medical X-ray films RX NIF	Fuji	Japan
Microscope slides	VWR	Darmstadt
Nitrocellulose membrane	Schleicher & Schuell	Dassel
Petri dishes	VWR/Greiner	Darmstadt
Pipette tips	Sarstedt/Greiner	Nümbrecht/Frickenhausen
Plastic material	Sarstedt//Greiner	Nümbrecht/Frickenhausen
Whatman paper	Schleicher & Schuell	Dassel

2.1.3 Chemicals

Chemicals	Company	Company headquarters
Agar	Roth	Karlsruhe
Agarose	Roth	Karlsruhe
Ammonium peroxodisulfate (APS)	Roth	Karlsruhe
Ammonium sulfate ($(NH_4)_2SO_4$)	Roth	Karlsruhe
Ampicillin	Roth	Karlsruhe
Bovine serum albumin	PAA	Cölbe
Calcium chloride ($CaCl_2$)	Roth	Karlsruhe

Chloroform	Merck	Darmstadt
Cresol red	Sigma Aldrich	Taufkirchen
Diethyl pyrocarbonate (DEPC)	Roth	Karlsruhe
Dimethylsulfoxide (DMSO)	Fluka	Neu-Ulm
1,4-dithio-DL-threitol (DTT)	Fluka	Neu-Ulm
Dipotassium phosphate (K_2HPO_4)	Roth	Karlsruhe
Disodium phosphate (Na_2HPO_4)	Roth	Karlsruhe
Ethanol p.a. (EtOH)	Roth	Karlsruhe
Ethidium bromide (EtBr)	Sigma	Taufkirchen
Ethylendiamintetra-acetic acid (EDTA)	Roth	Karlsruhe
EGTA	Roth	Karlsruhe
Glutaraldehyde	Roth	Karlsruhe
Glycine	Roth	Karlsruhe
Glycerol anhydrous	AppliChem	Darmstadt
Hoechst 33258	Molecular Probes	USA
Hydrochloric acid 37 %	Roth	Karlsruhe
Hydrogen peroxide (H_2O_2)	Merck	Darmstadt
Isopropanol	Merck	Darmstadt
Luminol	AppliChem	Darmstadt
LB-agar (Lennox)	Roth	Karlsruhe
Magnesium chloride ($MgCl_2$)	Roth	Karlsruhe
Magnesium sulfate ($MgSO_4$)	Roth	Karlsruhe
Methanol	Roth	Karlsruhe
Milk powder	Roth	Karlsruhe
NNN'N-tetra methylene ethylene diamine (TEMED)	Roth	Karlsruhe
o-Cresolsulfonephtalein (Cresol red)	Sigma Aldrich	Taufkirchen
p-coumaric acid	Roth	Karlsruhe
PageRuler Prestained Protein Ladder	Fermentas	USA
Pepton	Roth	Karlsruhe
Phenylmethylsulfonyl fluoride (PMSF)	Serva	Heidelberg

Potassium acetate (CH_2CO_2K)	AppliChem	Darmstadt
Potassium chloride (KCl)	Roth	Karlsruhe
Potassium dihydrogen phosphate (KH_2PO_4)	Roth	Karlsruhe
Protease Inhibitor Cocktail Set III	Calbiochem	USA
Proteinase K	AppliChem	Darmstadt
RNaseOUT	Invitrogen	USA
RostisolV®HPLC Gradient Grade Water	Roth	Karlsruhe
Rotiphorese Gel 30	Roth	Karlsruhe
Saponin	Roth	Karlsruhe
SOB-Medium	Roth	Karlsruhe
Sodium carbonate (Na_2CO_3)	Roth	Karlsruhe
Sodium chloride (NaCl)	Roth	Karlsruhe
Sodium sulfite (Na_2SO_3)	Roth	Karlsruhe
Sodium dodecyl-phosphate (SDS)	AppliChem	Darmstadt
Sodium hydroxide (NaOH)	Merck	Darmstadt
Streptolysin O	S.Bhakdi	University Mainz
Sucrose	Roth	Karlsruhe
Trichloroacetic acid	Roth	Karlsruhe
Tris	AppliChem	Darmstadt
Triton X-100	Roth	Karlsruhe
TRIzol® Reagent	Invitrogen	Groningen
Urea	Roth	Karlsruhe
Yeast extract	Roth	Karlsruhe

2.1.4 Cell Culture Materials

Cell culture materials	Company	Company headquarters
AlbuMaxII	Invitrogen	Groningen
Blasticidin S	InvivoGen	USA
D-Sorbitol	Roth	Karlsruhe
Gelafundin	B. Braun AG	Melsungen
Giemsa	Merck	Darmstadt

Human erythrocyte concentrate (A/rh$^+$ and O/rh$^+$)	University medical centre Marburg, Bloodbank	Marburg
Human Plasma (A/rh$^+$)	University medical centre Marburg/Giessen, Bloodbank	Marburg
Hypoxanthine	PAA	Cölbe
RPMI 1640	Gibco	Karlsruhe
RPMI 1640	PAA	Cölbe
WR99210	Jacobus Pharmaceuticals	USA

2.1.5 Molecular Biological Kits

Molecular Kits	Company	Company headquarters
Gel Extraction Kit	Seqlab	Göttingen
PCR Purification Kit	Seqlab	Göttingen
Minipreparation Kit	Seqlab	Göttingen
Plasmid Maxi Kit	Qiagen	Hilden

2.2 Enzymes

Enzymes	Company	Company Headquarter
DNase	AppliChem	Darmstadt
KOD DNA polymerase	Novagen	Darmstadt
RNase	AppliChem	Darmstadt
SuperScript^{TM} III one-step RT-PCR system	Invitrogen	Groningen
T4 DNA Ligase	Invitrogen	Groningen
Taq DNA polymerase	New England Biolabs	Schwalbach
Restriction enzymes (AvrII, BsshII, KpnI, XhoI, XmaI,)	New England Biolabs	Schwalbach

2.3 Antibodies

In the following table the primary and secondary antibodies used are listed, with a reference to the source of supply.

Primary antibody	Dilution factor (IFA)	Dilution factor (Western blotting)	Obtained from
Chicken anti-GFP (polyclonal)	1:500	---	abcam
Mouse anti-GFP (monoclonal)	---	1:1000	abcam
Mouse anti-Band3 (monoclonal)	---	1:1000	Sigma aldrich
Rabbit anti-aldolase (polyclonal)	---	1:5000	Group Lingelbach
Rabbit anti-ARF (polyclonal)	1:2000	1:1000	Group Holder
Rabbit anti-Exp1 (polyclonal)	---	1:500	Group Lingelbach
Rabbit anti-SERP (polyclonal)	---	1:1000	Group Lingelbach

Secondary antibody	Company	Company Headquarter
Goat anti-chicken Cy2	JacksonImmunso Research Laboratories	USA
Goat anti-mouse HRP	DAKO	Glostrup
Goat anti-rabbit HRP	DAKO	Glostrup
Swine anti-rabbit HRP	DAKO	Glostrup

2.4 Solutions and buffers

In this section the solutions and buffers used for molecular biological and proteinbiochemical work are listed.

Solutions and buffers	Individual components
Ammonium peroxodisulfate (APS)	10 % in ddH_20
Ampicillin	stock: 50 mg/ml working concentration: 50 µg/ml
Blocking solution for IFA	3 % BSA in PBS (pH 7.4)
Blocking solution for western blotting	5 % milk powder in PBS (pH 7.4)
Colony mix	1 ml Cresol red solution 600 µl Taq buffer (10 x) 120 µl dNTPs 10 mM

	4.28 ml water, sterile
Cresol red solution	0.1 g o-Cresolsulfonephtalein 60 % sucrose
Developer (X-ray)	6.4 mM Metol 80 mM Hydroquinone 571 mM sodium sulfite (Na_2SO_4) 452 mM sodium carbonate (Na_2CO_3) 34 mM potassium bromide (KBr)
DNA extraction buffer A	100 mM sodium chloride (NaCl) 50 mM sodium acetate (NaOAc), pH 5.2 1 mM EDTA
DNA loading dye (6x)	1 % bromophenol blue 30 % glycerol 50 mM Tris/HCl, pH 8 5 mM EDTA
ECL solution	5 mM Luminol 0.8 mM p-coumaric acid 200 mM Tris/HCl pH 8.5
Electrophoresis running buffer	124 mM Tris 960 mM glycine 0.05 % SDS
Fixation buffer	4 % paraformaldehyde 0.00075 % glutaraldehyde in PBS (pH 7.4)
Permeabilization buffer	0.1 % Triton X-100 in PBS (pH 7.4)
Phosphate buffered saline (PBS)	140 mM sodium chloride (NaCl) 2.7 mM potassium chloride (KCl) 1.4 mM monopotassium phosphate 0.8 mM disodium phosphate
Ponceau S staining solution	0.2 % Ponceau S 3 % trichloroacetic acid
Quenching buffer	125 mM glycine in PBS (pH 7.4)
Sample buffer (2x) for proteins	100 mM Tris/HCl pH 6.8 5 mM EDTA 20 % glycerol 4 % SDS 0.2 % bromphenolblue 100 mM dithiothreitol
Separating buffer (4x)	1.5 M Tris/HCl pH 8.8
Stacking buffer (4x)	500 mM Tris/HCl pH 6.8 0.4 % SDS

Taq buffer (10x)	200 mM Tris/HCl pH 8.8 100 mM potassium chloride (KCl) 100 mM ammonium sulfate 20 mM magnesium sulfate ($MgSO_4$) 1 % Trion X-100
TE-buffer (10 x)	890 mM Tris 890 mM acetate 20 mM EDTA
Western blot transfer buffer	48 mM Tris/HCl pH 9.5 39 mM glycine 0.04 % SDS 20 % methanol

The media used for culturing and growing bacteria are listed in the following:

Media	**Individual components**
LB (Luria-Bertani)-agar	35 g/l LB agar
SOC-medium	SOB medium (autoclaved) 20 mM glucose (sterile filtered)
Super broth medium, pH 7.0	35g/l tryptone 20 g/l yeast extract 5 g/l sodium chloride 5 ml/l sodium hydroxide

The solutions used for culturing *P. falciparum* are listed in the following:

Solutions	**Individual components**
Blasticidin S hydrochloride	Stock solution: 10 mg/ml working concentration: 4 µg/ml
Cytomix	120 mM KCl 0.15 mM $CaCl_2$ 2 mM EGTA 10 mM K_2HPO_4/KH_2PO_4, pH 7.6 25 mM HEPES, pH 7.6
Freezing solution	28 % glycerol 3 % d-sorbitol 0.65 % sodium chloride
RPMI medium	500 ml RPMI medium supplemented with - 50 ml of heat-activated human plasma - 20 µg/ml neomycin - 200 µM hypoxanthine
Thawing solution	I. 12 % sodium choride (NaCl)

	II. 1.6 % sodium chloride (NaCl) III. 0.9 % sodium chloride, 0.2 % glucose
WR99210	20 mM stock (8.6 mg in 1ml DMSO) working concentration: 5 nM

2.5 Vectors and oligonucleotides

2.5.1 Vectors

The following table displays the basic vectors used for this study.

Basic vectors	Selectable marker	Resistance	Tag	Reference
pARL2_GFP	β-Lactamase, DHFR	Ampicillin, WR99210	GFP	J. Przyborski, N. Gehde
pARL2_mCherry_BSD	β-Lactamase, Blasticidin S deaminase	Ampicillin, Blasticidin	mCherry	J. Przyborski, S. Külzer

2.5.2 Oligonucleotides

The following oligonucleotides were designed for this study and purchased from Eurofin MWG Operon. The restriction sites are underlined and the mutations introduced by *site-directed* mutagenesis in the following nucleotide sequences are highlighted.

Denotation	Primer sequence 5'→3'
Oligonucleotides used for the vectors	
pARL_F	CGTTAATAATAAATACACGCAG
pARL_R	GGCGGATAACAATTTCACACAGG
GFP+54_R	GTGCCCATTAACATCACCATC
Prefoldin subunit, putative (PF3D7_0904500)	
Pref_XhoI_F	GGCTCGAGATGGGTGATATAAAACAAAACAAATATG
Pref_XhoI_F_G2A	GGCTCGAGATG**GCT**GATATAAAACAAAACAAATATG
Pref_AvrII_R	GGCCTAGGATTAAGATCTATCCTATTTCCAAACTTC
Calcium dependent protein kinase 4 (PF3D7_0717500)	
CDPK4_XhoI_F	GGCTCGAGATGGGACAAGAGGTATCGAG
CDPK4_XhoI_F_G2A	GGCTCGAGATG**GCA**CAAGAGGTATCGAG

CDPK4_AvrII_R	GGCCTAGGATAATTACAAAGTTTGACTAGCATATCC
ADP-ribosylation factor 1 (PF3D7_1020900)	
ARF1_XhoI_F	GGCTCGAGATGGGTTTATATGTAAGTAGGTTATTTAATCG
ARF1^{G2A}_XhoI_F	GGCTCGAGATG**GCT**TTATATGTAAGTAGGTTATTTAATCG
ARF1_AvrII_R	GGCCTAGGTTTGGCATTATTTAAGTGTGTGGTTAGC
ARF1$^{1-17/+ C4/-V5/}$AK2^{+18-37}_XhoI (F) _ KpnI (R) *(produced by GeneArt® Gene Synthesis)*	**GG**CTCGAGATG**GGT**TTA**TGC**TATAGTAGGTTATTTAATCGTTTATTTCAAAAGAAA**GATGAAGAGGAAAAAAAGAAGAGAAAAAAAAGAAAAAGAAAATATATATTTTAAATGGAGCA**GGTACC**GC
Adenylate kinase 2 (PF3D7_0816900)	
AK2_XhoI_F	GGCTCGAGATGGGATCATGTTATAGTAGAAAAAATAAA
AK2^{G2A}_XhoI_F	GGCTCGAGATG**GCA**TCATGTTATAGTAGAAAAAATAAA
AK2^{C4A}_XhoI_F	GGCTCGAGATGGGATCA**GCT**TATAGTAGAAAAAATAAA
AK2^{G2AC4A}_XhoI_F	GGCTCGAGATG**GCA**TCA**GCT**TATAGTAGAAAAAATAAA
AK2_AvrII_R	GGCCTAGGATTGGGGTTATCATCTATAATGGAG
AK2$^{(\Delta 21-30)}$_F_oe-PCR*	CATTAGATGAAGAGGAAATATATATTTTAAATGGAGCATCTGGG
AK2$^{(\Delta 21-30)}$_R_oe-PCR*	GATGCTCCATTTAAAATATATATTTCCTCTTCATCTAATGATATTGTTG
AK2$^{1-37}$_KpnI_R	GGGGTACCTGCTCCATTTAAAATATATATTTTTTTTTTCTTCTT
Exported-protein1 (PF3D7_1121600)	
Exp1_XhoI_F	CGCTCGAGATGAAAATCTTATCAGTATTTTTTC
Exp1_AvrII_R	GCCTAGGGTGTTCAGTGCCAGTTACGAGG

* primers for overlapping-extension PCR (oe-PCR)

2.5.3 Plasmids designed for this work

The following table comprises the plasmids generated for this work. The basic vectors were used as backbone and the nucleotide sequences were introduced into these vectors.

Vector	Proteins selected/mutated/ detection system	Origin
pARL2_Pref_GFP	Chaperone	this work
pARL2_mPref_GFP	*G2A mutation	this work

pARL2_CDPK4_GFP	Kinase	this work
pARL2_mCDPK4_GFP	*G2A mutation	this work
pARL2_ARF1_GFP	GTPase, wildtype	this work
pARL2_ARF1^{G2A}_GFP	*G2A mutation	this work
pARL_AK2_GFP	Kinase, wildtype	Group Becker, Giessen
pARL_AK2^{G2A}_GFP	*G2A mutation	Group Becker, Giessen
pARL2_AK2^{C4A}_GFP	ǂC4A mutation	this work
pARL2_AK2^{G2AC4A}_GFP	*G2AǂC4A mutation	this work
pARL2_AK2$^{(\Delta 21-30)}$_GFP	Deletion of polybasic amino acids (Δ 21-30)	this work
pARL2_AK2$^{1-37}$_GFP	1-37 amino acids of N-terminus of AK2	this work
pARL2_ARF1$^{1-17/+C4/-V5}$AK2^{+18-37}_GFP	GTPase, ǂC4 addition, removal of V5, addition of polybasic cluster of AK2	this work
pARL2_AK2_mDHFR	Kinase, wildtype	this work
pARL2_Exp1_mCherry_BSD	PVM-marker	this work
pARL2_Grasp1_mCherry_BSD	cis-Golgi-marker	J. Riedel, bachelor thesis
pARL2_Rab6_mCherry_BSD	trans-Golgi-marker	J. Riedel, bachelor thesis
pARL2_Sec12_mCherry_BSD	ER-marker	J. Riedel, bachelor thesis

***G2A = glycine replaced with alanine at 2nd position at the N-terminus**
ǂC4A = cysteine replaced with alanine at 4th position at the N-terminus

2.6 Cells and Organisms

Strain	Genotpye	Reference
E. coli TOP 10	---	Invitrogen
P. falciparum 3D7	Clone derived from NF54 (isolated in the Netherlands)	The Walter and Eliza Insitute of Medical Research, Melbourne, Australia

2.7 Bioinformatics

In silico analyses of the nucleotide sequences and the resulting proteins were performed using the following databases.

Genetic databases	websites
BLAST	http://blast.ncbi.nlm.nih.gov/Blast.cgi
ClustalW	http://www.ebi.ac.uk/Tools/msa/clustalw2
ExPASy	http://www.expasy.org/
GeneDB	http://www.genedb.org/Homepage
OrthoMCL DB	http://orthomcl.org/orthomcl/
PlasmoDB	http://plasmodb.org/plasmo/
SignalIP	http://www.cbs.dtu.dk/services/SignalP/

2.8 Cell culture techniques

2.8.1 *In-vitro* cultivation of *Plasmodium falciparum*

All of the work was performed with the *Plasmodium falciparum* strain 3D7. The genome sequence of this clone, which was isolated from a patient in Amsterdam was analyzed by Gardner and his colleagues in 2002 (Gardner et al., 2002).

Asexual stages of *P. falciparum* were cultivated in suspension culture flasks in A^+ human erythrocytes at a hematocrit of 4 % and in RPMI medium, which was supplemented with 0.2 % hypoxanthine, 10 % human plasma and 0.1 mg/ml neomycin (stock 10 mg/ml) according to Trager and Jensen (Trager and Jensen, 1976). The culture was maintained at 37 °C and gassed with 90 % N_2, 5 % O_2 and 5 % CO_2 in an incubator. The parasitemia was checked by Giemsa-stain every day. Therefore a blood-drop from the suspension culture was taken from the bottom of the flask and smeared onto the slide. The smear was air-dried, fixed in MetOH for 30 seconds and then stained with a diluted Giemsa-solution (1:10 in H_2O) for at least 10 minutes. The Giemsa-stain was washed off the slide and the parasitemia was checked with a light microscope using immersion oil for a 100 x magnification of the specimen. The ratio of infected to non-infected cells was calculated after looking at different optical sections of the slide and the parasitemia was determined. The culture was then further cultivated, accordingly.

Synchronized cultures at ring-stage were split only when they reached a parasitemia above 10 %, while cultures containing late-stage parasites, were split when reaching a parasitemia above 5 %. A high parasitemia was only maintained when the infected cells were harvested shortly after for experiments.

2.8.2 Synchronization of *Plasmodium falciparum* with Sorbitol

Sorbitol synchronization of parasites was performed on a mainly ring-infected culture to eliminate mature parasites based on the increased permeability of erythrocytes infected with late-stage parasites compared to ring-stage parasites. As a result, highly synchronized ring-stage parasites were obtained for further cultivation (Lambros and Vanderberg, 1979). The culture was centrifuged at 1,600 x g for 2 minutes before the cell pellet was resuspended in 5 % Sorbitol-solution and incubated for 8 minutes at room temperature. Once the incubation was over, the entire mixture of Sorbitol and cells was spun at 1,600 x g for 2 minutes, and washed 2-3 times with RPMI before being further cultured.

2.8.3 Enrichment of trophozoite-stage parasites via Gelafundin flotation

Trophozoite-stage parasites were required and used for most of the experiments. That is why Gelafundin-based synchronization of trophozoite-infected cells was performed (Pasvol et al., 1978). Therefore a culture containing initially about 5 % late-stage parasites was sedimented in a centrifugation step, and the pellet was resuspended in 8 ml of the Gelafundin-solution and incubated for 10 minutes at 37 °C in a water bath. During the incubation time knob-associated cells float into the upper phase of the Gelafundin cell mixture, while non-infected and ring-stage parasites are found at the bottom. The upper-phase, containing enriched trophozoite-infected cells, was transferred to a new tube and spun at 1,600 x g for 2 minutes. The pellet obtained was resuspended in RPMI and the parasitemia was determined. The volume of RPMI added to the pellet equalled 10 x the volume of the pellet. Usually a 50 – 60 % enrichment of trophozoites after Gelafundin treatment was achieved.

2.8.4 High enrichment of late-stage parasites using a high gradient magnetic field

A different method to obtain highly enriched parasites at late-stage was the application of a high gradient magnetic field. This method enables a high synchronization and

enrichment of late-stage parasites based on the property of the malaria parasite to digest hemoglobin (Fe(II) diamagnetic complex) to hemozoin (Fe(III) paramagnetic complex). The paramagnetic properties of hemozoin are used to isolate *Plasmodium*-infected red blood cells at late-stage in the presence of a high magnetic field (Paul et al., 1981).

For the magnetic isolation of parasitized red blood cells a VarioMACS Separator (Miltenyi Biotec) and the appropriate magnetic columns (MACS; CS columns, Miltenyi Biotec), were used. Prior to magnetic isolation, the column was washed with 3 % BSA (dissolved in PBS, pH 7.4) and was fitted into the VarioMACS separator. The culture should contain initially a parasitemia of around 3-5 % infected cells at late stage. The culture was transferred from the flask into a 50 ml tube and then poured on the top of the CS column. The CS columns are composed of ferromagnetic fibers and when fitted to the VarioMACS Separator, the magnetic field is amplified, evoking a high gradient within the column. This allows an increased magnetic isolation of parasitized red blood cells. Once the entire culture was passed through the column, the column was washed with pre-warmed PBS (pH 7.4) until the eluent was free from red blood cells. The column was removed from the VarioMACS Separator and fitted into a bracket fixed to a stand and eluted with 2 x 15 ml PBS (7.4) in a 2 x 15 ml falcon tube. The eluent was centrifuged at 1,600 x g for 3 minutes, and the pellet from both tubes were pooled together, washed twice with pre-warmed RPMI medium before a blood-smear of 5 µl was prepared. The parasitemia, when using magnet-based isolation of infected cells, was always around 80 %.

2.8.5 Transfection and Co-transfection of *Plasmodium falciparum*

Transfection was performed with *Plasmodium*-infected erythrocytes at ring-stage with a parasitemia of 5 – 10 % (Wu et al., 1995). Plasmid-DNA (100 µg) was prepared by ethanol precipitation, air-dried and subsequently resuspended in 30 µl TE buffer. The DNA was properly mixed and dissolved at 50 °C before 370 µl of cytomix and 200 µl of ring-stage infected cells were added. The whole mixture was transferred to a 0.2 cm gap electroporation cuvette and pulsed at 0.310 kV at 950 µF (high capacitance). The time constant was always between 8 – 12 msec. Once electroporation was carried out, the cells were transferred to a 25 cm^2 cell culture flask containing 12 ml of pre-warmed RPS (Gibco) media and 400 µl O^+ erythrocytes. The media used for transfection was supplemented with 5 % human plasma, 0.25 % AlbuMax, hypoxanthine and neomycin.

The culture was maintained at 37 °C in an incubator. After 4-8 hours the appropriate drug, depending on the selection cassette integrated into the plasmid, was added to the culture. Either the parasites were selected with 5 nM WR99210, when the hDHFR was expressed or 4 µg/ml of BSD was added to the culture, when Blasticidin S deaminase was expressed from the selection cassette. In the first five days after transfection the medium was changed daily and the appropriate drug was added to the cells. Once no live parasites could be seen, the medium was only changed twice a week and the blood (O^+ erythrocytes) was changed every two weeks after transfection. The parasites were held under drug pressure. Once parasites were seen, which usually took 2-3 weeks, three to five aliquots with a parasitemia of 5 -10 % were frozen as stocks. When the parasitemia was about 5 %, the parasites were transferred from a 25 cm^2 to a 75 cm^2 culture flask and were cultured in RPMI medium and A^+ erythrocytes.

Co-transfection was performed as follows: *P. falciparum* ring-stage parasites were transfected successively with each of the constructs (construct 1 and construct 2, each containing a different selection cassette and a different gene of interest). Once one of the transfectants containing for example construct 1 started growing these parasites were synchronized with Sorbitol or Gelafundin. The synchronized ring-stage parasites can then be transfected with construct 2, containing a different gene of interest and another selection cassette. These newly co-transfected parasites were then kept under drug selection of WR99210 and BSD and after 2-3 weeks the co-transfected parasites started growing expressing both proteins from each constructs.

2.8.6 Cryopreservation of *Plasmodium falciparum*-infected erythrocytes

An *in-vitro* culture of *P. falciparum*-infected red blood cells was frozen at ring-stage when a parasitemia of 5 -10 % was reached. The whole culture was centrifuged at 1,600 x g for 2 minutes and the cell sediment was mixed in a ratio of 1:1 with a freezing solution, transferred to a cryotube and instantly snap-frozen in liquid nitrogen. The cryotube containing the frozen cells was incubated for about 10 minutes in liquid nitrogen before being put into long-term storage in a liquid nitrogen tank.

2.8.7 Thawing of cryopreserved *Plasmodium falciparum*-infected erythrocytes

The snap-frozen parasites in a cryotube were thawed at room temperature and transferred to a 15 ml tube. 200 µl of solution I containing 12 % sodium chloride

dissolved in ddH_2O (autoclaved) was added dropwise to the thawed parasites. After an incubation time of 3 minutes, 5 ml of solution II containing 1.6 % sodium chloride dissolved in ddH_2O (autoclaved), was added dropwise to the cells. The cells were incubated again for 3 minutes at room temperature before solution III containing 0.9 % sodium chloride dissolved in ddH_2O (autoclaved) mixed with 0.2 % glucose dissolved in ddH_2O (sterile filtered), was added to the thawed cells drop by drop. Once the incubation time of 3 minutes was over, the cells were sedimented at 1,600 x g for 2 minutes and washed twice with pre-warmed RPMI medium before being transferred to a new flask for culturing. Thawed transfectants were subjected to the appropriate drug 24 hours later after thawing.

2.9 Molecularbiological methods

2.9.1 Cultivation of *Escherichia coli*

E.coli strain Top10 was grown in the common bacterial growth medium Super Broth liquid, supplemented with the antibiotic ampicillin to a final concentration of 50 µg/ml for selection. LB-agar (Luria-Bertani) was used as a growth substrate for culturing bacteria on a solid medium.

Liquid cultures of *E. coli* were inoculated with the clone containing the desired plasmid and grown overnight at 37 °C with constant shaking. Plasmid DNA preparation was performed either in a small-scale (mini preparation) or large-scale (maxi preparation) isolation process.

2.9.2 Preparation of electrocompetent bacterial cells (*E. coli* strain TOP10)

A single colony of *E. coli* TOP10 was used to inoculate 10 ml of Super Broth at 37 °C to set up an overnight preculture. 600 ml of Super Broth were then inoculated with 6 ml of the preculture until the cells were grown to an OD of 0.6, which took about 3.5 hours with constant shaking at 37 °C. The cells were then harvested at 6,000 x g for 10 minutes at 4 °C. The supernatant was discarded and the pellet was resuspended in 600 ml ddH_2O and harvested again. This step was repeated three times before washing the pellet a final time with 600 ml of 10 % glycerol/ddH_2O. The cells were kept on ice during the whole procedure. Finally, the pellet was resuspended in 1.2 ml of ice-cold

10 % glycerol. Aliquots of 100 µl were made using sterile 1.5 ml reaction tubes, snap frozen with liquid nitrogen and stored at – 80 °C.

2.9.3 Mini- and Maxipreparation for isolation of plasmid DNA

Plasmid DNA from *E. coli* was isolated using Plasmid-preparation kits from Qiagen according to the manufacturer's protocols. The main steps in the isolation of plasmid DNA involve the disruption of the bacterial cells by alkaline lysis and neutralization of the lysate. A silica membrane column is used for the binding of the plasmid DNA from the cleared lysate, which is subsequently eluted in TE-buffer (Qiagen Protocol).
To obtain plasmid DNA, using the Maxipreparation procedure, the bacterial pellet was resuspended in twice the volume recommended by the manufacturer's protocol of the buffers P1, P2 and P3 (Przyborski et al., 2005).

2.9.4 Transformation of *E. coli* cells

E.coli TOP10 cells were transformed with plasmid DNA using electroporation. 50 µl of the electrocompetent cells were thawed on ice and then mixed with the ligation reaction. The ligation reaction contained the plasmid DNA, which was purified by precipitation with EtOH as described in section 2.9.13 and was then resuspended in 10 µl ddH_2O. The mixture of electrocompetent cells and DNA-solution was then transferred to a pre-cooled electroporation cuvette and pulsed by a voltage of 2 kV, with a capacitance of 25 µF and a resistance of 200 Ω. Immediately after electroporation the cells were resuspended in pre-warmed SOC medium and incubated in a shaker at 37 °C for 1 hour. 100 µl of the cell suspension was plated on a pre-warmed LB agar plate supplemented with ampicillin. The rest of the cell suspension was harvested by 1,000 x g for 2 minutes to reduce the volume before plating. The plates were incubated at 37 °C overnight.

2.9.5 Isolation of genomic DNA from *Plasmodium falciparum*

Isolation of genomic DNA was performed with trophozoite stages of *P. falciparum*. The parasitemia was about 5–10 %, before the parasites were isolated from infected erythrocytes by saponin lysis at a final concentration of 0.1 %. The pellet was washed a couple of times before it was resuspended in 200 µl PBS (pH 7.4). In the next step, 2 x DNA extraction buffer A and 100 µl of 20 % SDS were added to the sample, mixed by

inversion before being extracted with an equal amount of phenol-chloroform followed by centrifugation at 28,600 x g for 30 minutes. The phenol-chloroform extraction leads to a separation between DNA and proteins, by which the DNA can be found in the upper phase. The DNA in the upper phase was transferred to a new 1.5 ml tube, precipitated with ethanol, and dissolved in 500 µl TE-buffer (pH 8.0). The DNA-solution was then subjected two more times to phenol-chloroform extraction with a subsequent centrifugation step at 28,600 x g for 30 min to gain more purified DNA by removing all the other cell constituents. The top phase was collected and chloroform extraction was performed one more time to remove all the phenol left in the sample. In a final step the upper phase was collected once again and precipitated with ethanol before being dissolved in 50-100 µl TE-buffer (pH 8.0).

2.9.6 Isolation of mRNA from *Plasmodium falciparum*

Similar to the isolation of genomic DNA from *P. falciparum* RNA was obtained by saponin treatment of late-stage *Plasmodium*-infected cells. Therefore, a total of 2×10^8 cells were subjected to 0.1 % saponin and incubated on ice for 5 min followed by a centrifugation step at 2,500 x g for 5 minutes. The supernatant was discarded and the pellet was washed twice with PBS (pH 7.4) before resuspending the pellet in preheated Trizol reagent. The pellet dissolved in Trizol was then incubated on a Thermomixer at 37 °C for 5 minutes. 200 µl of chloroform was added to the pellet, mixed and spun at 28,600 x g for 30 min. The supernatant was removed and the pellet was washed with 70 % ethanol several times, before the pellet was air-dried. Finally, the pellet was dissolved in an appropriate amount of DEPC-treated water and 1 µl of RNaseOUT was added. RNaseOUT is a non-competetive inhibitor, which inhibits RNase A, RNase B and RNase C.

2.9.7 Quantification of nucleic acid

DNA and RNA, respectively, absorb UV light. That is why the concentration of nucleic acids can be determined using a spectrophotometer. The optical density (OD) is measured at 260 nm using a quartz cuvette. An absorbance unit of 1 at 260 nm correlates to 50 µg/ml of double-stranded DNA and 40 µg/ml of RNA, respectively.

If the DNA is not contaminated with proteins the OD at 260 nm/280 nm ratio will be 1.8. A lower ratio, however, indicates a low contamination of the DNA.

2.9.8 Reverse transcriptase PCR

Following isolation of total RNA from *P. falciparum* as described in 2.9.6 the mRNA was transcribed into cDNA by reverse transcriptase (RNA-dependent DNA polymerase). *In vitro* amplification of the coding sequences was performed in one-step using the SuperScript III one-step RT-PCR kit (Invitrogen), a system, which combines two enzymes, the SuperScript Reverse Transcriptase and the *Taq* High Fidelity enzyme. Initially the mRNA is converted into the single-stranded cDNA template at 45–60 °C degrees by the SuperScript Reverse Transcriptase, before the cDNA is used as a template for the *Taq* High Fidelity enzyme. The cycling conditions were set according to the primer annealing temperature and the size of the target sequences.

Table 2.1 Standard reaction mix for cDNA synthesis

Reagent	Volume
2 x reaction mix	25 µl
sense primer (50 pmol/µl)	1 µl
anti-sense primer (50 pmol/µl)	1 µl
template (approximately 1 µg/µl)	1 µl
SuperScript III RT / Platinum *Taq* Polymerase High fidelity enzyme mix	2 µl
autoclaved distilled water	**to 50 µl**

Table 2.2 Standard program for cDNA synthesis followed by PCR amplification

Reaction	Temperature	Time	Cycles
1. cDNA synthesis	50 °C	30 min	1
2. pre-denaturation	94 °C	2 min	
3. denaturation	94 °C	15 sec	39
4. annealing	55 °C	30 sec	
5. extension	68 °C	1 min/kb	
6. final extension	68 °C	5 min	1
7. end of program	4 °C	---	---

2.9.9 Polymerase chain reaction

The polymerase chain reaction was performed according to Mullis and colleagues (Mullis et al., 1986). The oligonucleotides for *in-vitro* amplification of DNA- and RNA-fragments were ordered from Eurofins MWG Operon and the list of primers can be found in section 2.5.2. The oligonucleotides were chosen according to a melting temperature between 50 °C – 65 °C, which was determined using the program Oligonucleotide Property Calculator. The stock-solution of the oligonucleotides was adjusted to 50 pmol/µl with DEPC-treated water and stored at -20 °C.

DNA-fragments, which were required for further cloning, were amplified using the KOD Hot Start DNA Polymerase. For colony PCR, however, the *Taq* polymerase was used, since a proofreading activity of the polymerase was not required (colony PCR: section 2.9.16). The cycling conditions were set according to the primer annealing temperature and the size of the target sequences.

Table 2.3 Standard reaction mix for PCR with KOD Hot Start DNA Polymerase

Reagent	Volumina
10 x PCR buffer for KOD Hot Start DNA Polymerase	5 µl
$MgSO_4$ (25 mM)	3 µl
dNTP (2 mM each)	5 µl
sense primer (50 pmol/µl)	1 µl
anti-sense primer (50 pmol/µl)	1 µl
template (approx. 1 -200 ng/µl)	1 µl
KOD Hot Start DNA Polymerase (1 U/ µl)	1 µl
ddH_2O (autoclaved)	to 50 µl
total amount	**50 µl**

Table 2.4 Standard PCR program with KOD Hot Start DNA Polymerase

Reaction	Temperature	Time	Cycles
1. activation	95 °C	2 min	
2. denaturation	95 °C	20 sec	35
3. annealing	50 °C	30 sec	

4. extension	72 °C	20 sec /1 kb	
5. final extension	68 °C	10 min	
6. end of program	4 °C	---	

Table 2.5 Colony PCR program with Taq polymerase

Reaction	Temperature	Time	Cycles
1. denaturation	94 °C	2 min	
2. denaturation	94 °C	15 sec	25
3. annealing	50 °C	30 sec	
4. extension	72 °C	60 sec /1 kb	
5. final extension	68 °C	10 min	
6. end of program	4 °C	---	

2.9.10 *In-vitro* site-directed mutagenesis

In-vitro site directed mutagenesis is a technique used to introduce mutations like point-mutations, deletions or insertions into the gene of interest. To obtain a deletion mutation via site-directed mutagenesis, two internal primers in addition to the flanked primers (forward and reverse primer), were required. As internal primers oligonucleotides were designed missing the bases to be deleted. These primers were designed to be complementary to the target sequence lacking the amino acids to be deleted and they were partially complementary to each other in order for them to hybridize in a final PCR reaction. In the first step, two PCR reactions were performed separately from each other according to the PCR standard program: the first PCR reaction mix contained the flanked forward primer and the internal reverse primer, while the second PCR reaction mix contained the internal forward primer and the flanked reverse primer. Initially, the 5'→3' part of the gene was amplified in each of the PCR reaction producing fragments with complementary overhangs, which then can hybridize in a final PCR reaction. Therefore the amplified products from each of the PCR reactions were mixed in a ratio of 1:1 being the template for the final PCR. The mutated DNA sequence was then amplified using both of the flanked primers (see Fig. 2.1) (Ho et al., 1989).

2.9.11 Agarose gel electrophoresis

Agarose gel electrophoresis was used to separate DNA fragments based on their size. This method relies on the migration of negatively charged DNA in an electrical field towards a positive pole using agarose gel as medium (Sambrook and Russell, 2001). The DNA samples were mixed with 6 x times loading buffer and depending on the expected size of the DNA the DNA fragments were separated in an agarose gel at concentrations ranging from 0.8 – 1.0 %. Agarose was made by mixing agarose powder with 1 x TAE buffer, which was also used as electrophoresis buffer and heated in a microwave until complete melting. Ethidium bromide was added to a final concentration of 0.5 µg/ml. Ethidium bromide is a fluorescent dye, which intercalates with DNA molecules and enables the visualization of DNA fragments in a gel when exposed to UV-light. To determine the size of the DNA fragments ranging from 100 bp to 12 kb 5 µl of a DNA ladder was added to the gel as well and the gel was run at 90 V for 20 – 40 minutes, depending on size of the DNA fragments to be analyzed. The gel was visualized with an ultraviolet transilluminator and pictures were taken with the Gel IX Imager.

2.9.12 Purification of DNA

DNA purification, after amplification by PCR or restriction digests, was performed using a PCR purification kit (Seqlab) according to the manufacturer's protocol; alternatively, the desired DNA fragment ('band') was excised from an agarose gel and then purified with a gel-extraction kit (Seqlab) following the manual of the supplier.

2.9.13 Ethanol precipitation of DNA

Precipitation of DNA with ethanol is required to concentrate DNA in aqueous solutions. Since ethanol is less polar than water nucleic acids are less soluble in ethanol. In the presence of ethanol and salt DNA tends to fall out of solution. Therefore 2 volumes of 100 % ethanol and 1/10 volume of sodium acetate (pH 5.2) was added to the DNA, mixed well and spun at 33,000 x g for 20 min at 4°C. The supernatant was removed and the pellet was washed with 70 % ethanol at 28,600 x g for 20 minutes at 4 °C before being air-dried and dissolved in either ddH_2O or TE-buffer.

2.9.14 Restriction of DNA

Restriction of DNA was performed using specific restriction endonucleases, which are able to recognize, bind and cut to specific recognition sites in the DNA. Digestion of plasmids and PCR products was performed in a total volume of 10 – 30 µl, respectively, with the appropriate restriction enzymes, a suitable buffer and if required 1 mg/ml of BSA. Incubation times and temperature varied depending on the restriction enzymes used. Subsequently, the digested DNA was purified using a PCR purification kit (Seqlab) and analyzed by agarose gel electrophoresis.

2.9.15 Ligation of DNA

Insert and vector, which were digested with the same restriction enzymes creating matching sticky ends, were ligated in the general molar ratio of 3:1 (insert:vector). The ligation reaction was performed overnight at 16 °C in a total volume of 20 µl using 1 U of the T4 DNA ligase (Invitrogen) and a 5 x suitable ligase buffer (Invitrogen). Usually 100 ng of the vector was used for the ligation reaction and the required amount of insert could be calculated according to the following formula:

$$\frac{\text{100 ng Vector} * \text{Insert (kb)} * 3}{\text{Vector (kb)}} = \text{Insert (ng)}$$

Subsequently, the DNA was ethanol-precipitated (section 2.9.13) and dissolved in 10 µl ddH_2O before transformation of electrocompetent *E. coli* cells was performed (section 2.9.4).

2.9.16 Screening for positive clones with colony PCR

Colony PCR enables the screening of *E. coli* colonies after transformation for identification of those clones containing the desired plasmid insert. Therefore a single bacterial clone on an agar plate was first transferred to a replica plate, before being added to the PCR reaction mix as the template. Cresol red was used as loading dye. The oligonucleotides selected were both the forward or reverse primer of the insert and the forward or reverse primer starting from a region inside the vector, respectively. The colony PCR was performed in a total volume of 25 µl containing the concentration of the dNTPs, the *Taq* polymerase, the *Taq* buffer and the primers in proportion to a

standard PCR (Table 2.4). The PCR program was similar to the standard PCR program, except for the reduction in the number of cycles to 25 (Table 2.5).

2.9.17 Sequencing of DNA

Plasmids sent for sequencing were isolated and purified with a purification kit from Seqlab according to the manufacturer's protocol. Samples were sequenced either at Seqlab Sequence Laboratories (Göttingen GmbH) or at GATC Biotech (Konstanz).

2.9.18 Generation of plasmid constructs for transfection

2.9.18.1 Overview of the vector used

The following vectors were designed by J. Przyborski, N. Gehde and Simone Külzer. The pARL2_GFP vector contains the coding region for the human dihydrofolate reductase, which confers resistance to WR99210. The pARL_mCherry vector contains the coding region for Blasticidin S deaminase, which confers resistance to Blasticidin. The genes of interest were not integrated into the genome. The CRT (chloroquine resistance transporter) promoter is a low-expression promoter and was used for episomal gene expression.

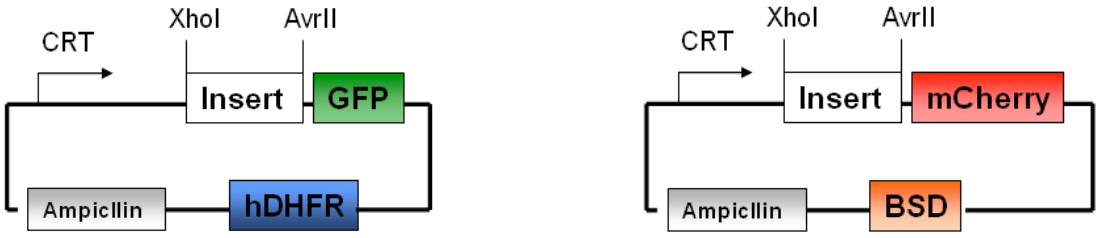

2.9.18.2 Constructs designed using the pARL2_GFP vector

In-vitro amplification of the cDNA from RNA from *P. falciparum* (strain 3D7) was performed for the following genes of *P. falciparum* using the one-step RT-PCR Kit (Invitrogen). The stop codon was omitted.

- PF3D7_0904500 (Prefoldin subunit, putative)
- PF3D7_0717500 (Calcium-dependent protein kinase 4)
- PF3D7_1020900 (ADP-ribosylation factor 1)

The primers used contained a XhoI (forward primer) and AvrII (reverse primer) restriction site for integration of the PCR product into the pARL2_GFP vector. Both the PCR product and the vector were digested with the same restriction enzymes XhoI and AvrII. The resulting construct was denoted with the Plasmodb ID, the restriction site and the orientation of the primer as exemplified for the coding sequence of ARF: PF3D7_1020900_XhoI_F. Another set of constructs was made with the above-mentioned coding sequences by *in-vitro* site directed mutagenesis. The genes selected (PF3D7_0904500, PF3D7_0717500, PF3D7_1020900 and PF3D7_0816900) for analysis contained a supposed myristoylation site, glycine, at the 2nd position of the N-terminus, which was changed to alanine (G2A) using a forward primer containing the respective mutated codon. The PCR products contained the respective point mutation and were integrated into the pARL2_GFP vector (e.g. PF3D7_1020900^{G2A}_XhoI_F). Genomic DNA of *P. falciparum* was extracted to obtain the coding sequence of PF3D7_0816900 (adenylate kinase 2). Five further constructs using PF3D7_0816900 as the gene of interest were generated via site-directed mutagenesis. When making the first construct a putative palmitoylation site with cysteine at the 4th position of the N-terminus was changed to alanine by designing a forward primer with the respective mutated codon. A second construct was generated by mutating both the myristoylation and the putative palmitoylation site of PF3D7_0816900 by using a forward primer with both of the mutations. The forward and reverse primer contained a XhoI and AvrII restriction site, respectively, to be integrated into the pARL2_GFP vector. Each of the PCR products comprising the respective mutated codon was amplified with the standard PCR program and was subsequently integrated into the pARL2_GFP vector following digestion of the PCR product and vector with the same restriction enzymes prior to ligation. Another construct with the coding sequence of PF3D7_0816900 was generated via site-directed mutagenesis by overlap extension PCR (Ho et al., 1989) deleting a stretch of polybasic amino acids at the N-terminus (Δ 21-30) of the gene. As internal primers oligonucleotides were designed missing the bases to be deleted [AAGAAAAAAAAAATATATATTTTAAATGGA corresponding to amino acids 21-30 of the N-terminus of PF3D7_0816900]. The PCR was performed in a two-step reaction as described in section 2.9.10. The final PCR product lacking the amino acids 21-30 at the N-terminus was integrated into pARL2_GFP after digestion with XhoI and

AvrII restriction enzymes. The following figure exemplifies the steps required in a site-directed mutagenesis PCR for the following gene: PF3D7_0816900 (Fig. 2.1).

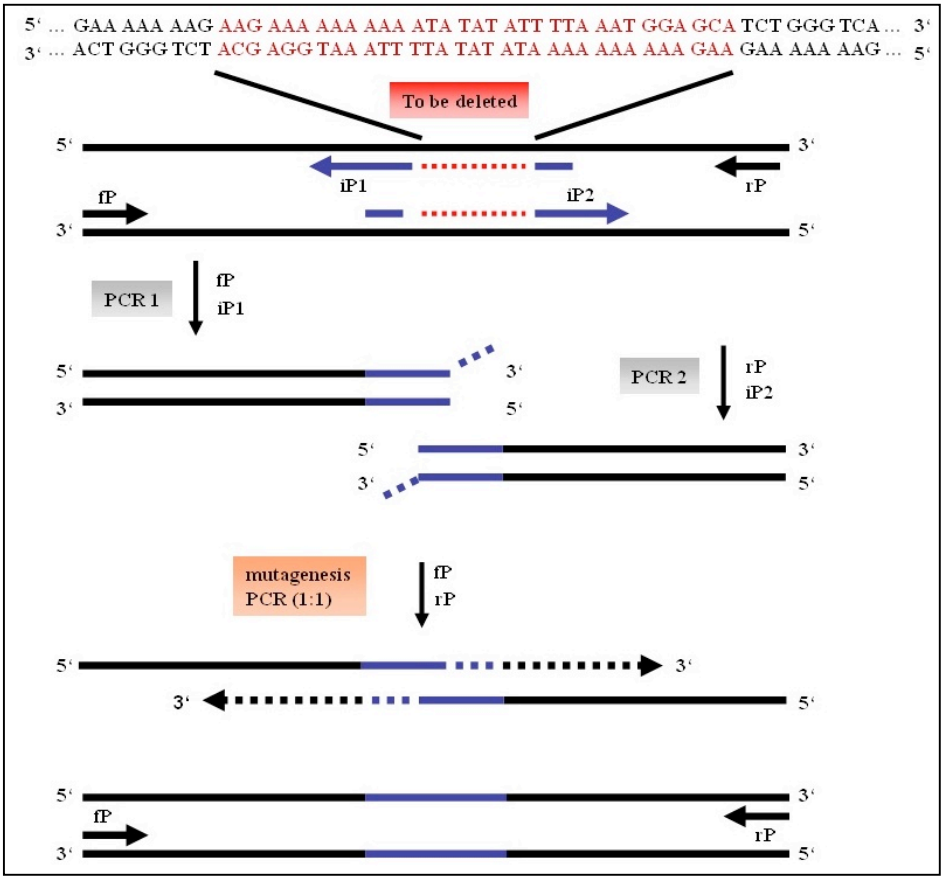

Figure 2.1 *In-vitro* site directed mutagenesis by overlap extension PCR (modified according to Ho et al., 1989)

Another construct was designed by amplifying the N-terminus of PF3D7_0816900 up to 37 amino acids with a forward primer containing a XhoI restriction site and a reverse primer containing KpnI as restriction site. The N-terminus of PF3D7_0816900 was fused upstream to GFP into the pARL2_GFP vector. The amplified PCR product and the vector were digested with the restriction enzymes XhoI and KpnI. Additionally, a chimeric construct of PF3D7_1020900 (ADP-ribosylation factor1) and PF3D7_0816900 (adenylate kinase 2) was created. Therefore, the N-terminus of PF3D7_1020900 with up to 17 amino acids was synthesized, introducing a putative palmitoylation site at position 4 and removing the valine residue at position 5. The

sequence was further extended with part of the N-terminus of PF3D7_0816900 ranging from the amino acid at position 18 to 37, which contains the polybasic stretch of amino acids of PF3D7_0816900. The synthesized sequence contained the restriction sites XhoI and KpnI and was cloned into the pARL2_GFP vector by fusing the insert upstream to GFP.

The list of the constructs made with the corresponding primer sequences can be found in section 2.5.

2.9.18.3 Constructs designed for co-localization studies inserted into the pARL_BSD vector

The sequences of the following genes from *P. falciparum* (3D7 strain) were amplified using cDNA, which was transcribed from the RNA and integrated into the pARL_BSD vector. The following three constructs were generated by Jan Riedel (BSc candidate / Group Lingelbach).

- PF3D7_1116400 (Sec 12)
- PF3D7_1017300.1 (Grasp 1)
- PF3D7_1144900 (Rab 6)

The sequence of PF3D7_1121600 was amplified from the genomic DNA of *P. falciparum* (3D7 strain) designed with the restriction sites XhoI (forward primer) and AvrII (reverse primer). The PCR product was cloned into pARL_BSD vector after digestion with the respective restriction enzymes.

2.10 Biochemical methods

2.10.1 Cell fractionation of *Plasmodium falciparum*-infected red blood cells

Trophozoite-infected cells were enriched using Gelafundin flotation or magnet based separation and subjected to hypotonic lysis. A total amount of 2 x 10^8 cells was resuspended in 1 mM Tris (stock: 10 mM) and lysed by repeated cycles of freezing and thawing in liquid nitrogen. Following centrifugation at 36,000 x g for 20 minutes at 4 °C, the lysate was separated into soluble and pellet fraction. The soluble fraction was spun again at the same speed to remove any remaining membrane contaminants before

being boiled in sample buffer at 100 °C for 10 minutes. The pellet fraction was washed 4-6 times in PBS (pH 7.4) containing 1 mM PMSF and PIC (1:200 dilution), boiled in sample buffer at 100 °C for 10 minutes and used for analysis by SDS-PAGE and immunoblotting.

2.10.2 Streptolysin O permeabilization of *Plasmodium falciparum*-infected erythrocytes

Streptolysin O (SLO) is known to be an important toxin produced by gram-positive bacteria of the genus *Streptococcus*. This toxin is able to bind to surface-exposed membrane cholesterol permeabilizing the membrane by causing holes up to 30 nm to the membrane (Bhakdi et al., 1985). SLO treatment of *Plasmodium*-infected cells leads to permeabilization of the erythrocyte membrane leaving the PVM and the parasite intact.

To identify and further analyze the subcellular localization of *P. falciparum* proteins in infected erythrocytes SLO treatment was performed. Immediately after enrichment of the trophozoite-stage infected erythrocytes with Gelafundin or magnet based separation a total of 2 x 10^8 cells were treated with 3 hemolytic units (HU) of SLO in 188 µl of PBS (pH 7.4). The cells were incubated at room temperature for 6 minutes and gently mixed every 2 minutes. Following incubation the cells were spun at 1,000 x g for 3 minutes. The supernatant was transferred to a new 1.5 ml eppendorf tube, washed two more times to remove any remaining contamination with the membrane fraction. The pellet was washed 4-6 times with PBS (pH 7.4) containing 1 mM PMSF and PIC (1:200 dilution). Subsequently, the pellet containing the intact parasite and intact PV was resuspended in an appropriate volume of PBS (pH 7.4) and was either directly used for experiments or was further separated into soluble and pellet fraction. Therefore the pellet fraction containing the intact parasite with the surrounding PV was dissolved in 1 mM Tris buffer (stock: 10 mM Tris in ddH_2O) and subjected to three repeated cycles of freeze and thaw. The lysed cells were spun at 28,600 x g for 20 minutes and the supernatant containing the soluble fraction was transferred to a new tube and washed two more times. The pellet fraction was washed 4 to 6 times with PBS (pH 7.4) containing protease inhibitors and was finally dissolved in an appropriate amount of PBS. All the samples obtained so far 1) supernatant fraction and 2) pellet fraction were

diluted in sample buffer and immediately boiled at 100 °C for 10 minutes in heating block before being stored at – 80 °C.

2.10.3 Saponin lysis of *Plasmodium falciparum*-infected erythrocytes

Saponin is a glycoside, which is commonly found in plants and is able to lyse erythrocytes by forming complexes with cell membrane cholesterol leading to the permeabilization of the membrane. Saponin is known to disintegrate the erythrocyte membrane and the parasitophorous vacuolar membrane of *P. falciparum* but leaves the parasite intact (Beaumelle et al., 1987).

Following Gelafundin or magnet based enrichment of trophozoite-stage infected erythrocytes a total of 2 x 10^8 cells were treated with 0.02 % saponin (stock 1mg/ml) dissolved in PBS (pH 7.4) containing 1 mM PMSF. The cells were incubated at room temperature for 3 minutes with only gently mixing. Once the incubation time was over, the cells were immediately centrifuged at 2,800 x g for 5 minutes at 4 °C. The supernatant was transferred to a new 1.5 ml eppendorf tube, while the pellet was washed 4-6 times with PBS (pH 7.4) containing 1 mM PMSF and PIC (1:200 dilution). To remove all the residual membrane in the supernatant fraction another centrifugation step was performed at 36,000 x g for 20 minutes at 4 °C. Sample buffer was added to the supernatant and the pellet, which was dissolved in PBS (pH 7.4) containing 1 mM PMSF and PIC (1:200 dilution). Both samples were boiled at 100 °C for 10 minutes in a heat block before further usage.

2.10.4 Protease protection assay

The protease protection assay was performed with trophozoite-stage parasites. Therefore the parasites were enriched using Gelafundin flotation or magnet based separation and treated with 0.02 % saponin (stock: 1 mg/ml) and SLO (3 HU), respectively. The supernatant was separated from the pellet fraction by centrifugation at 2,500 x g for 5 minutes followed by further centrifugation steps of the supernatant at 28,600 x g for 20 minutes at 4 °C removing all remaining cell debris. Subsequently, sample buffer was added to the supernatant fraction and the whole sample was boiled at 100 °C for 10 minutes. The saponin and SLO pellet, respectively, was washed 4-6 times with PBS (pH 7.4) and divided for the majority of the experiments into two samples each containing 1 x 10^8 cells. Sample 1) was just dissolved in PBS (pH 7.4) being the

negative control, while sample 2) was treated with 1 mg/ml Proteinase K being the test sample. The samples were then incubated on ice for 30 minutes. Once the incubation time was over, 1 mM PMSF and PIC were added to the samples to prevent further protease activity and incubated for 3 minutes at room temperature. Subsequently, sample buffer was added to the samples and they were boiled at 100 °C for 10 minutes in a heat block before storage at – 80 °C.

2.10.5 SDS-PAGE

Sodium **d**odecyl **s**ulfate **p**oly**a**crylamide **g**el **e**lectrophoresis (SDS-PAGE) is a widely used method to separate proteins on the basis of their molecular weight. SDS is a detergent known to disturb the 3-dimensional structure of the protein and applies an overall negative charge to the proteins forming SDS-polypeptide complexes. This enables the separation of proteins in a polyacrylamide gel, based only on their molecular weight, eliminating the differences in mass:charge ratio of the proteins. Protein samples were mixed and heated in 2 x loading buffer containing the reducing agent **di**thio**t**hreitol (DTT), which reduces the disulfide bonds within the proteins. The samples obtained after 1) saponin lysis, 2) SLO-lysis, 3) cell fractionation or after 4) treatment with Proteinase K were dissolved in an appropriate buffer before being mixed 1:1 with 2 x sample buffer and heated at 100 °C for 10 minutes in a heat block.
Electrophoresis was performed using a discontinuous buffer system and a 12 % polyacrylamide gel. The protein samples were run initially at 90 V leaving the proteins to migrate in the stacking gel, before the voltage was increased to 120 V once the proteins entered the separation gel. The protein ladder used to determine the molecular weight of the proteins was a Prestained Protein Ladder (Fermentas).

Table 2.6 Pipetting scheme for a 12 % gel

Reagent	Stacking gel	Separation gel (12 %)
Gel buffer (4x)	2.5 ml	7.5 ml
30 % acrylamide	1.3 ml	12 ml
ddH_2O	6.2 ml	10.25 ml
APS	250 µl	200 µl
TEMED*	15µl	25 µl

*N,N,N’,N’-Tetramethylethylenediamine

2.10.6 Semi-Dry-Immunoblotting

After separation of the proteins by gel electrophoresis they were electrophoretically transferred from the gel onto a nitrocellulose membrane for detection of the proteins by antibodies. The membrane was placed on the polyacrylamide gel and 'sandwiched' between 3 Whatman papers on each side, which were prior submerged in a western blot transfer buffer. Then the entire 'sandwich' was transferred to a blotting chamber. The transfer was carried out at 1 mA/cm^2 for approximately 1 hour. The electric field enables the proteins to move from the gel onto the membrane, displaying a copy of the protein pattern, which was originally in the polyacrylamide gel. After the electrophoretic transfer the membrane was stained with Ponceau red solution for five minutes and then rinsed in distilled water until protein bands were visible. The Ponceau staining was washed off with PBS (pH 7.4) for about 10 minutes before the membrane was blocked with 5 % milk powder (dissolved in PBS) for 1 hour at room temperature with constant shaking. This blocking step of the membrane is important to avoid unspecific binding of antibodies. The primary antibody was diluted in a 5 % milk solution to the desired working concentration (section 2.3) and incubated with the blot for 2 -3 hours at room temperature or overnight at 4 °C, depending on the antibody used. The membrane was then washed 3 times for 10 minutes with PBS (pH 7.4) to remove all unbound primary antibodies. The secondary antibody conjugated to Horseradish Peroxidase (HRP) was diluted 1:2000 in 5 % milk solution and added to the membrane for 1-2 hours at room temperature with constant shaking. Once the incubation time was over, the membrane was washed 3 x times with PBS (pH 7.4) to remove unbound antibodies. Antibody reactive-proteins were detected using the **E**nhanced **C**hemi**l**uminescence (ECL) detection system. Therefore the membrane was incubated with a substrate (luminol) that reacts with the conjugated secondary antibody in an enzyme-substrate reaction producing a fluorescent signal. The chemiluminescence was detected using a medical X-ray film.

2.11 Fluorescence microscopy

2.11.1 Live cell imaging

Plasmodium-infected cells were visualized using the Zeiss Axio Observer inverse epifluorescence microscope system. The cells were sedimented via a centrifugation step to obtain a cell pellet containing *Plasmodium*-infected and non-infected cells. The pellet was then washed 3 times with RPMI medium. For staining of nuclear DNA Hoechst dye was added (10 µg/ml) to the cells, which were resuspended in 1 ml RPMI, and incubated for 5 - 10 min at room temperature on a shaker. The cells were then ready to be visualized at room temperature using the inverse epifluorescence microscope with the appropriate filter sets and the Axiovision 4 software. Appropriate exposure times were chosen to prevent bleach out of the samples. All the data shown, represents at least 6-12 images taken for each sample.

2.11.2 Immunofluorescence assay

The immunofluorescence assay was performed according to Tonkin (Tonkin et al., 2004). *Plasmodium*-infected cells were fixed with 4 % paraformaldehyde/0.0075 % glutaraldehyde dissolved in PBS (pH 7.4) for 30 minutes at 37 °C. In a next step, glycine at a final concentration of 125 mM in 0.1 % TritonX-100/PBS (solubilization/permeabilization buffer) was added to the cells and incubated for 15 minutes on a roller at room temperature before the cells were sedimented at 1,000 x g for 2 minutes. The cells were then blocked in 3 % BSA/PBS for 1 hour. The primary antibody used was prepared in 3 % BSA/PBS and the cells were incubated with the primary antibody overnight at 4 °C. Once the primary antibody was removed, the cells were washed 3 times for 10 minutes with PBS (pH 7.4) before they were incubated with the appropriate secondary antibody for 2 hours at room temperature. The cells were washed again 3 times for 10 minutes with PBS (pH 7.4) before they were visualized by epifluorescence microscopy. The nuclear DNA of the fixed parasites was stained with Hoechst (50 ng/ml). Depending on the primary antibodies used (section 2.3) the appropriate Cy2- or Cy3-conjugated secondary antibody was employed in a 1:2000 dilution range.

2.11.3 Image processing with Image J

ImageJ is an open source Java-written program (http://rsbweb.nih.gov/ij/) used to process images. Images taken with the aforementioned epifluorescence microscope were imported into ImageJ64, converted to 8-bit grayscale and each image was subjected to background subtraction. Using the ImageJ plugin RGBmerge the RGB channels were split into red, green and blue before the individual images were overlaid. Before the images were saved as TIF files they were adjusted with the brightness/contrast tool. In order to make the figures, the figures were imported from ImageJ to PowerPoint (Microsoft). The figures were then compiled and saved as TIF files.

2.12 Experimental design

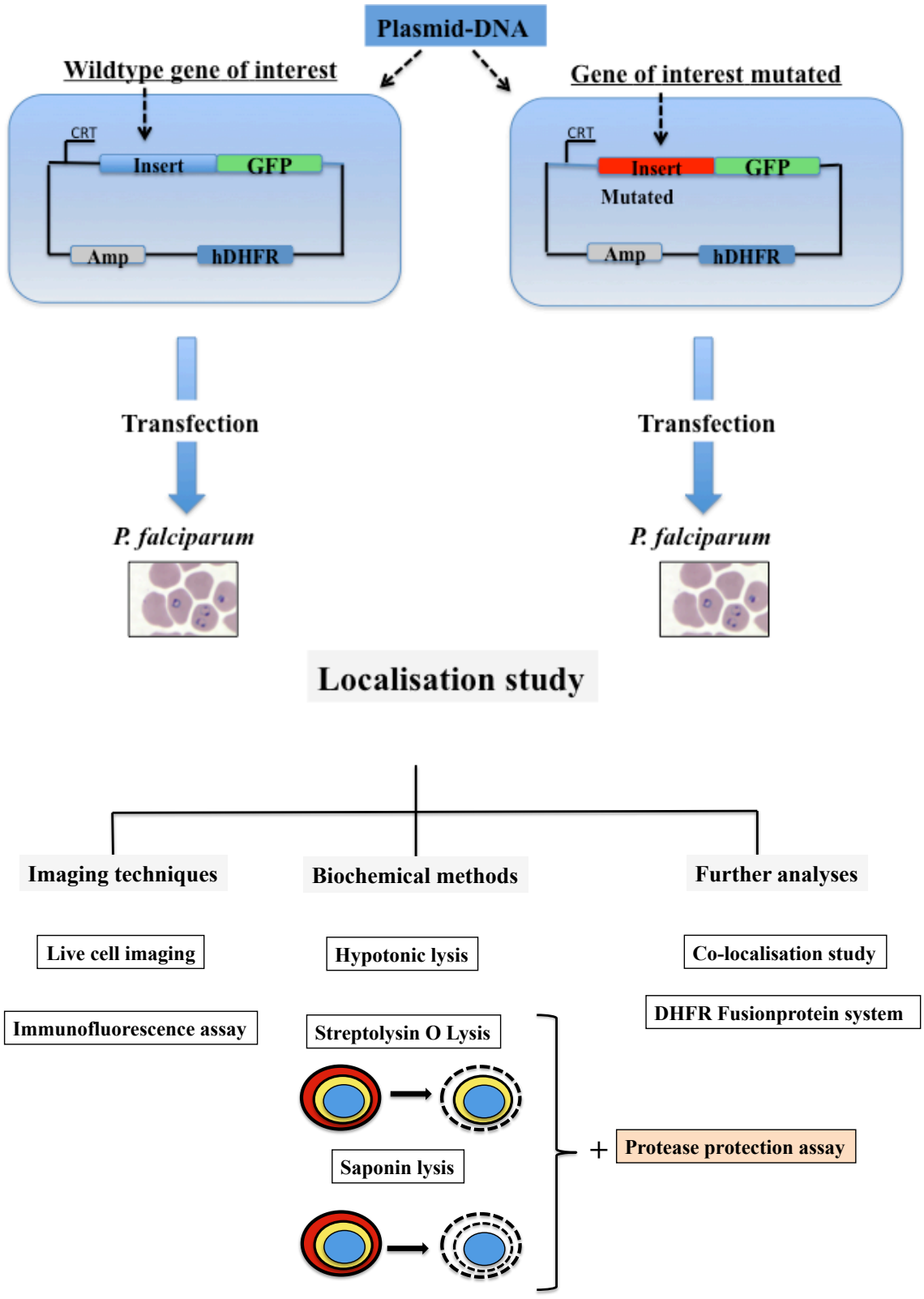

3 Results

A previous study of the parasitophorous vacuolar proteome of the intraerythrocytic stage of *P. falciparum* revealed the secretion of a number of proteins without a signal sequence. Approximately 50 % of the proteins lacked a signal sequence or any other known motifs responsible for the secretion of *P. falciparum* proteins into the PV. However, ~ 5 % of these proteins contained a glycine residue at the N-terminus, which is indicative for potential *N*-myristoylation (Nyalwidhe et al., manuscript in preparation). Proteins which lack a signal peptide but are *N*-myristoylated like the *Leishmania* HASPB and the *Plasmodium* CDPK1 have already been shown to be secreted into the extracellular space and the PV, respectively, suggesting that *N*-myristoylation can be seen as a mode of protein secretion among protists (Denny et al., 2000; Möskes et al., 2004). This hypothesis was further supported by a recent study of the *P. falciparum* adenylate kinase 2 (*Pf*AK2). This protein was proposed to be secreted into the PV, potentially involving *N*-myristoylation in the secretion process (Ma et al., 2012).

3.1 Selected candidate proteins

The selected candidate proteins for this study - Prefoldin (PF3D7_0904500), Calcium-dependent protein kinase 4 (CDPK4) (PF3D7_0717500) and the ADP-ribosylation factor 1 (ARF1) (PF3D7_1020900) - were first analyzed with the Myristoylator prediction program (www.expasy.com), from which the *Pf*CDPK4 (PF3D7_0717500) and the *Pf*ARF1 (PF3D7_1020900) were highly predicted to be myristoylated, compared with *Pf*Prefoldin (PF3D7_0904500). Another selected candidate protein of this study was the *Pf*AK2 (PF3D7_0816900), which has already been shown to be myristoylated by the *Pf*NMT (Rahlfs et al., 2009). In addition, all of these proteins were checked for the presence of a signal peptide using the prediction program SignalP 4.1. Server and none of them were predicted to contain a signal peptide.

Table 3.1 Prediction of *N*-myristoylation according to the Myristoylator prediction tool

	PF3D7__0904500 Prefoldin	**PF3D7__0717500 CDPK4**	**PF3D7__1020900 ARF1**
Myristoylator: Predicted as ...	non-myristoylated	myristoylated (High confidence)	myristoylated (High confidence)

In the following each of the proteins is described briefly:

Prefoldin is a molecular chaperone – a chaperone promotes correct protein folding – which interacts with other chaperones and was found in both eukaryotes and archaea (Vainberg et al., 1998). The function of Prefoldin fits with the identification of a great number of chaperones in the PV proteome analysis (Nyalwidhe and Lingelbach, 2006).

CDPK4 contains a putative myristoylation site similar to CDPK1, a parasite protein, which was found to be myristoylated and secreted beyond the parasite plasma membrane due to *N*-myristoylation (Möskes et al., 2004). Therefore it is reasonable to hypothesize that CDPK4 might also be targeted to the PV in an acylation-dependent manner.

ADP-ribosylation factor 1 is a highly conserved eukaryotic protein, which was found to be myristoylated at the N-terminus in various organisms including other protists. *Pf*ARF1 shows an overall structural and sequence similarity to the human ARF1 (Cook et al., 2010). Although ARFs are known to be mainly involved in vesicular trafficking of the secretory pathway (Boman and Kahn, 1995), the PV proteome approach assigned the localization of *Pf*ARF1 to the PV.

***Pf*adenylate kinase 2** was suggested to be located in the PV according to localization studies with GFP reporter constructs and fluorescence analyses of the respective protein (Ma et al., 2012). However, biochemical evidence and the mechanisms involved in the secretion of *Pf*AK2 into the PV are still missing.

To further analyze and investigate the localization of these candidate proteins and the potential secretion mechanism mutagenesis, fluorescence and thorough biochemical analyses were performed.

3.1.1 *Pf*ARF1 shows a different subcellular localization upon removal of the *N*-myristoylation site in *P. falciparum*-infected red blood cells

To figure out whether or not *Pf*Prefoldin, *Pf*CDPK4 and *Pf*ARF1 were indeed secreted into the PV and whether this is dependent on myristoylation, plasmids were constructed to express each of these proteins fused to GFP, creating chimeric fusion proteins. In parallel, a similar batch of these constructs was generated, where the glycine residue at the N-terminus of each of the proteins was changed to alanine (G2A) removing the putative *N*-myristoylation site. All of these constructs driven by the low-expression CRT promoter in the pARL2 plasmid were then transfected individually into the *P. falciparum* 3D7 strain for episomal expression. The resulting transgenic parasites were then analyzed via epifluorescence microscopy regarding the subcellular localization of the protein (wildtype versus G2A mutant). Both the *Pf*Prefoldin/GFP fusion protein and the variant *Pf*Prefoldin^{G2A}/GFP showed a strong cytosolic signal in the parasite indicating no difference in the subcellular localization between these two transgenic parasite lines (Fig. 3.1 A). The subcelluar localization of both *Pf*CDPK4/GFP and *Pf*CDPK4^{G2A}/GFP also showed a strong cytosolic signal in the parasite and no differences in their subcellular localization pattern (Fig. 3.1 B). These findings with *Pf*Prefoldin and *Pf*CDPK4 contradict the outcome of the PV proteome analysis, since a ring-like structure around the parasite would be expected for PV localization as was found with the *Pf*AK2/GFP (Fig. 3.4 A and Ma et al., 2012). Furthermore, the removal of the putative *N*-myristoylation site did not have any effect on the subcellular localization of the respective proteins.

The wildtype *Pf*ARF1/GFP also did not show the expected ring-like structure around the parasite indicative of PV localization. However, *Pf*ARF1/GFP was found to be localized to 1 to 2 dot-like structures in the parasite cytosol, while the variant of it, the *Pf*ARF1^{G2A}/GFP, showed a cytosolic localization (Fig. 3.1 C). This difference was further analyzed by subjecting the wildtype and variant parasite lines to hypotonic lysis and analyzing the samples via SDS-PAGE, western blotting and immunodetection. Hypotonic lysis was performed to distinguish between soluble and membrane-bound proteins. The full-length *Pf*ARF1 has a molecular weight of 21 kDa, while GFP has a molecular weight of 27 kDa. In the western blot analysis a band of approximately 48 kDa was detected in the supernatant fraction of the *Pf*ARF1/GFP and the

*Pf*ARF1^{G2A}/GFP parasite samples corresponding to the size of the fusion protein. As expected, a band of similar size could also be detected in the membrane-bound protein fraction of the *Pf*ARF1/GFP sample, but was missing in the *Pf*ARF1^{G2A}/GFP sample. These results indicate that the removal of the *N*-myristoylation site indeed affects the subcellular localization of the *Pf*ARF1 protein in the parasite. Band 3 was used as a marker protein for the membrane fraction, while the plasmodial aldolase was used as a marker protein for the soluble fraction and both proteins were detected in the expected fractions with the respective antibodies.

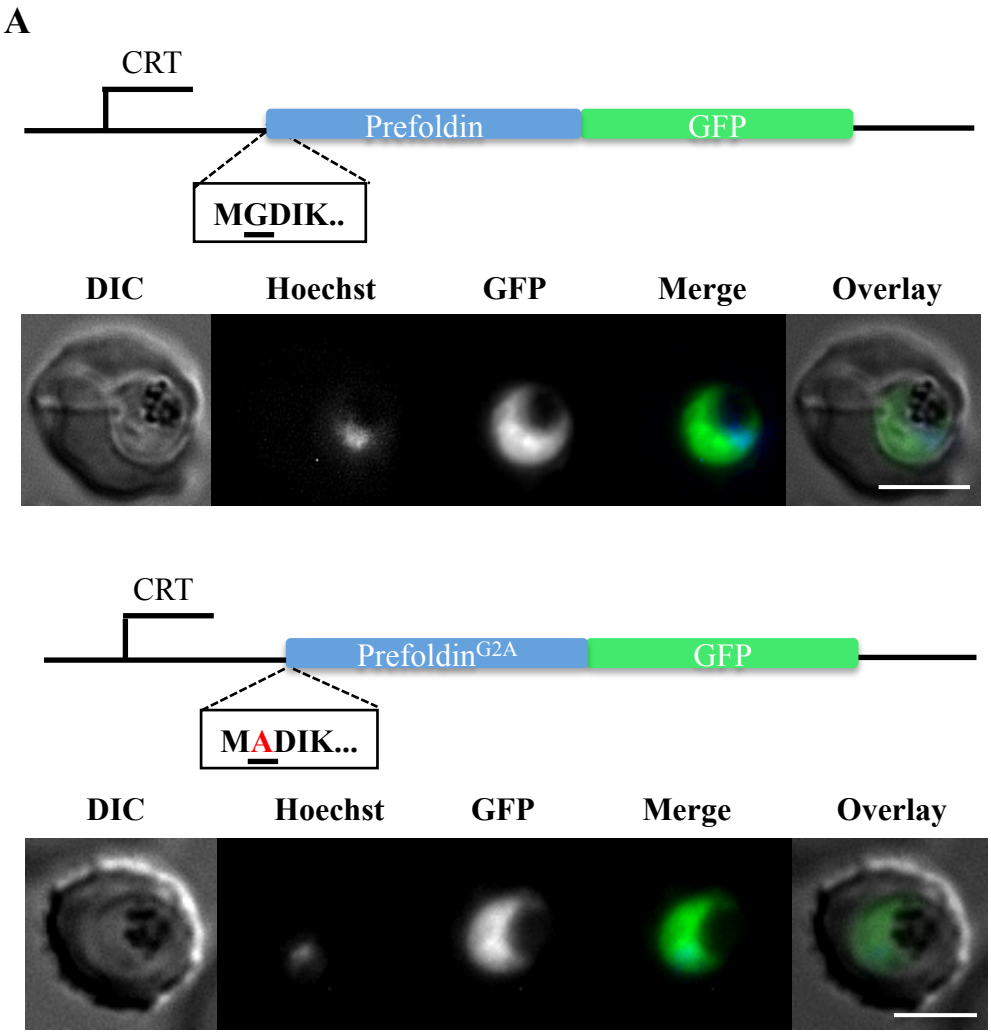

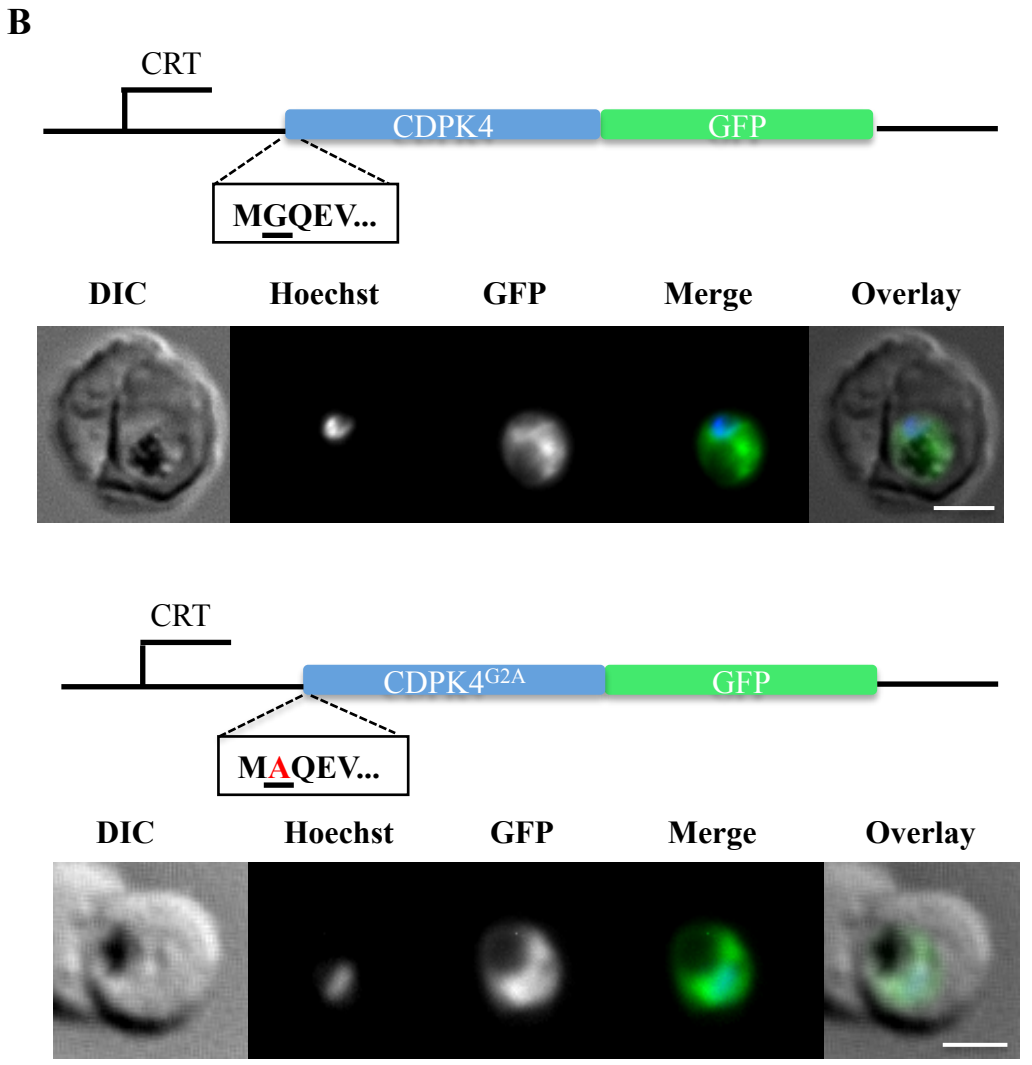
B
CRT
CDPK4
GFP
MGQEV...
DIC
Hoechst
GFP
Merge
Overlay
CRT
CDPK4G2A
GFP
MAQEV...
DIC
Hoechst
GFP
Merge
Overlay

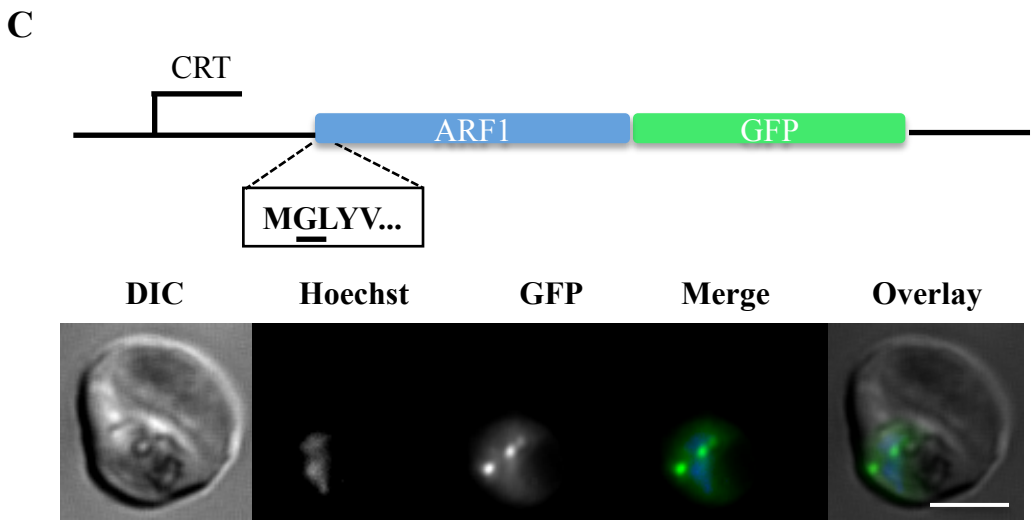
C
CRT
ARF1
GFP
MGLYV...
DIC
Hoechst
GFP
Merge
Overlay

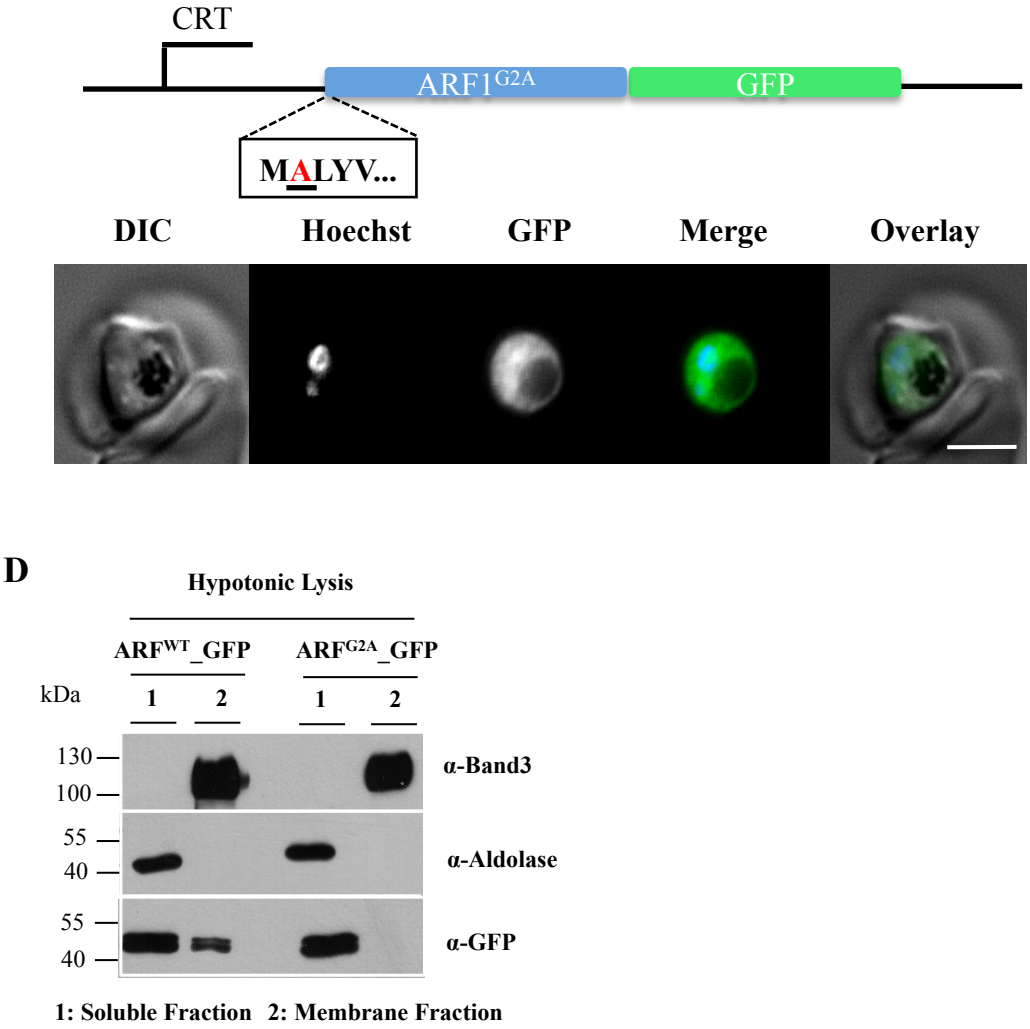

Figure 3.1 Live cell imaging of selected candidate proteins and biochemical analysis of *Pf*ARF1/GFP and *Pf*ARF1^{G2A}/GFP

(A, B) The fluorescence images of the *Pf*Prefoldin/GFP compared to the corresponding mutant transgenic parasite line and *Pf*CDPK4/GFP compared to *Pf*CDPK4^{G2A}/GFP parasites, respectively, show no differences between their phenotypes. The subcellular localization of the wildtype and the respective modified form of the protein appears to be similar. (C) The *Pf*ARF1/GFP fusion protein appears like dot-like structures in the parasite cytosol, while the phenotype of the ARF1^{G2A}/GFP variant shows an evenly distributed cytosolic signal. This indicates that the *N*-myristoylation site affects the subcellular localization of the protein. (D) Hypotonic lysis performed on the wildtype and the variant *Pf*ARF1/GFP parasite line, respectively, revealed a soluble protein pool in both samples. However, a membrane-bound protein pool could only be detected with an α-GFP antibody in the *Pf*ARF1/GFP parasite sample. As a control for proper hypotonic lysis Band 3 was used as a marker protein for the membrane fraction and aldolase was used as a marker protein for the soluble fraction and detected with the respective antibodies. DIC channel for high-contrast; in merge: green (GFP), blue (Hoechst = nucleus dye). Scale bar – 3 µm.

3.1.2 *Pf*ARF1 shows co-localization with marker proteins of the compartments of the secretory pathway

To further analyze the subcellular localization of *Pf*ARF1 a co-localization study with already verified marker proteins of the secretory pathway of *P. falciparum* was performed. Since ARF proteins are involved in the vesicle biogenesis of the secretory pathway *Pf*ARF1/GFP transgenic parasites were co-transfected with each of the following constructs individually: *Pf*Sec12 fused to mCherry in pARL2; *Pf*Grasp1 fused to mCherry in pARL2; *Pf*Rab6 fused to mCherry in pARL2. *Pf*Sec12 was identified as localized to the ER (Lee et al., 2008) and is a protein known to be involved in the vesicle formation of the anterograde transport (Barlowe and Schekman, 1993). *Pf*Grasp1 – Grasp proteins were found to play a role in the stacking of the Golgi-complex (Barr et al., 1997) – and was found to localize to the less elaborate Golgi-complex of *P. falciparum* (Struck et al., 2005). *Pf*Rab6 - the Rab6 protein of the Rab GTPase family was found to play a role in the intra-Golgi transport in eukaryotic cells (Martinez and Goud, 1998) – was found at the *P. falciparum* Golgi-complex (de Castro et al., 1996). Furthermore, a co-localization study with *Pf*Exp1 - an integral membrane protein localized to the PVM of the parasite during the blood-stage (Günther et al., 1991) - was performed as another attempt to investigate further the findings of the PV proteome analysis. Therefore *Pf*ARF1/GFP transgenic parasites were co-transfected with *Pf*Exp1 fused to mCherry in the pARL2 vector. As a control *Pf*ARF1^{G2A}/GFP transgenic parasites were transfected with each of the marker constructs individually.

During live cell imaging the signal of *Pf*Sec12/mCherry was observed in close proximity to the nucleus as a discrete structure that to a certain extent overlapped with the dot-like cytosolic signal of *Pf*ARF1/GFP indicating partial co-localization, which can be seen in the merge channel. *Pf*Grasp1/mCherry showed similar to *Pf*ARF1/GFP dot-like structures in the parasite cytosol near the parasite nucleus, which also resembles the fluorescence analyses of *Pf*Grasp/GFP transgenic parasites performed by Struck and colleagues (Struck et al., 2005). Merged images of *Pf*ARF1/GFP and *Pf*Grasp1/mCherry showed a strong co-localization of both proteins. *Pf*Rab6/mCherry also showed dot-like structures in the parasite. This observation coincides with the findings of de Castro and colleagues, where they claim that the maximal expression of this protein occurs at the trophozoite stage of *P. falciparum* during intraerythrocytic

development (de Castro et al., 1996). *Pf*Rab6/mCherry partially co-localizes with *Pf*ARF1/GFP, however, a complete co-localization like that seen for *Pf*Grasp1/mCherry and *Pf*ARF1/GFP could not be observed between the dot-like cytosolic signal of *Pf*ARF1/GFP and *Pf*Rab6/mCherry in the merged images. These findings, taken together, clearly reveal the localization of *Pf*ARF1 to compartments involved in the secretory pathway inside the parasite cytosol. In the co-localization study with the *Pf*ARF1/GFP protein co-expressed with *Pf*Exp1/mCherry a prominent ring-like structure around the parasite could be visualized during live cell imaging for *Pf*Exp1/mCherry. However, some signal could also be seen within the cytoplasm of the parasite. This finding corresponds to the results of a previous study where the fusion protein *Pf*Exp1/GFP was analyzed with respect to its localization during the blood-stage and was found to be partially localized to the food-vacuole of the parasite in addition to a PVM localization (Adisa et al., 2003). Merged images of *Pf*ARF1/GFP and *Pf*Exp1/mCherry showed no overlapping of the signals. This indicates that no co-localization between *Pf*ARF1 and the PVM marker of *Pf*Exp1 was detected, which is contradictory to the hypothesis of PV localization of *Pf*ARF1.

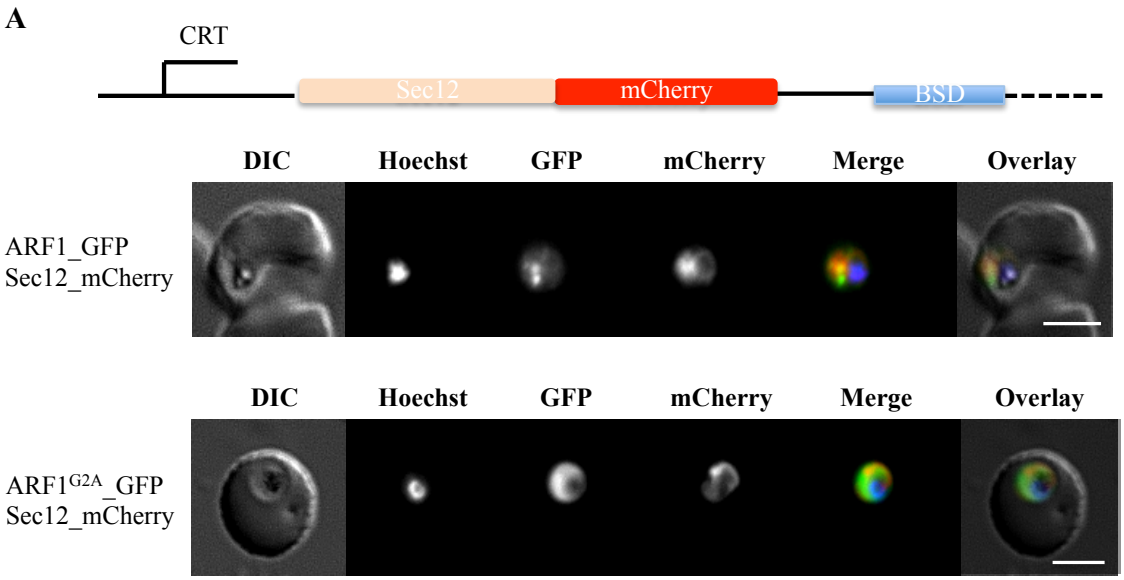

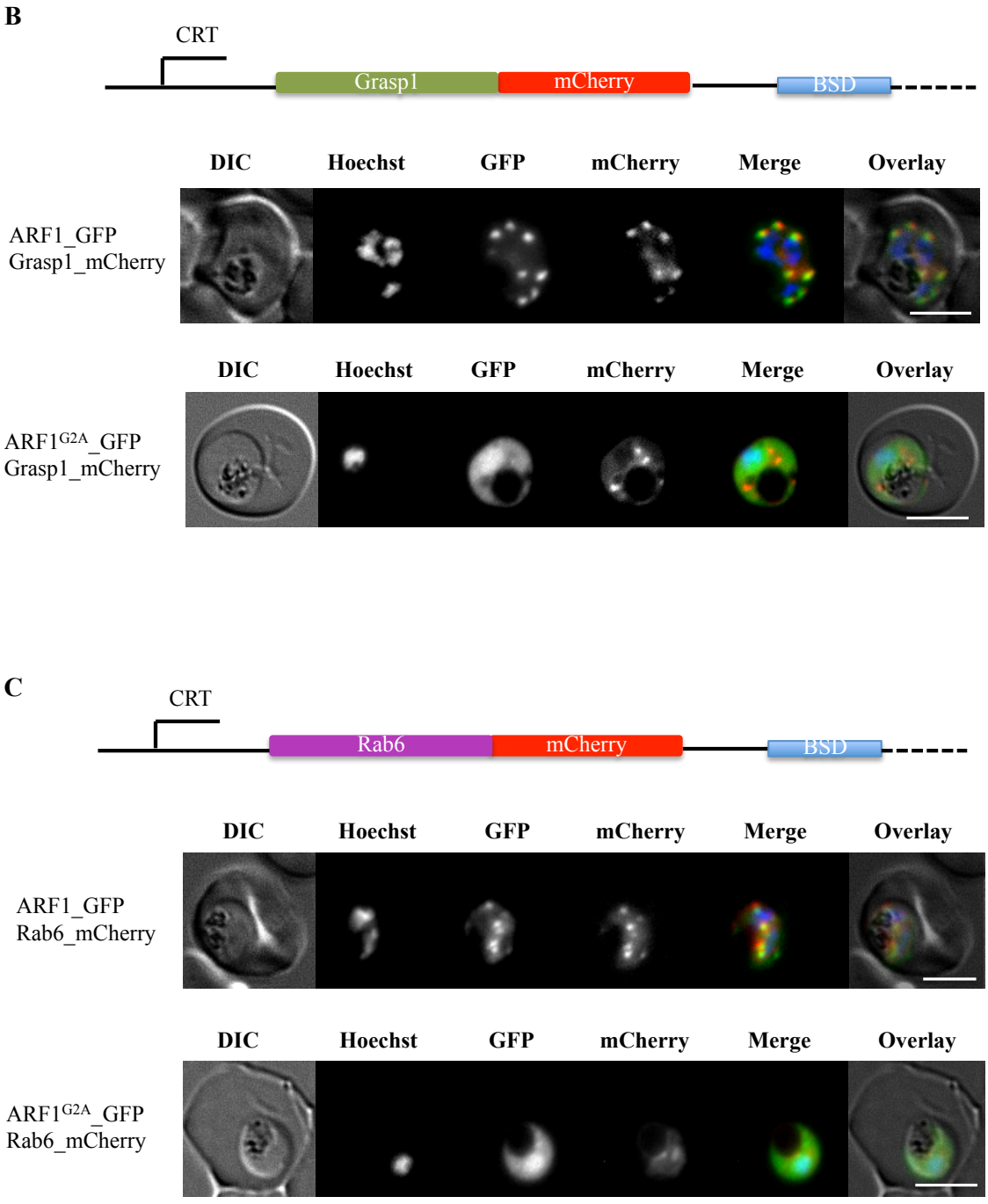
B
CRT
Grasp1
mCherry
BSD
DIC
Hoechst
GFP
mCherry
Merge
Overlay
ARF1_GFP
Grasp1_mCherry
DIC
Hoechst
GFP
mCherry
Merge
Overlay
ARF1G2A_GFP
Grasp1_mCherry
C
CRT
Rab6
mCherry
BSD
DIC
Hoechst
GFP
mCherry
Merge
Overlay
ARF1_GFP
Rab6_mCherry
DIC
Hoechst
GFP
mCherry
Merge
Overlay
ARF1G2A_GFP
Rab6_mCherry

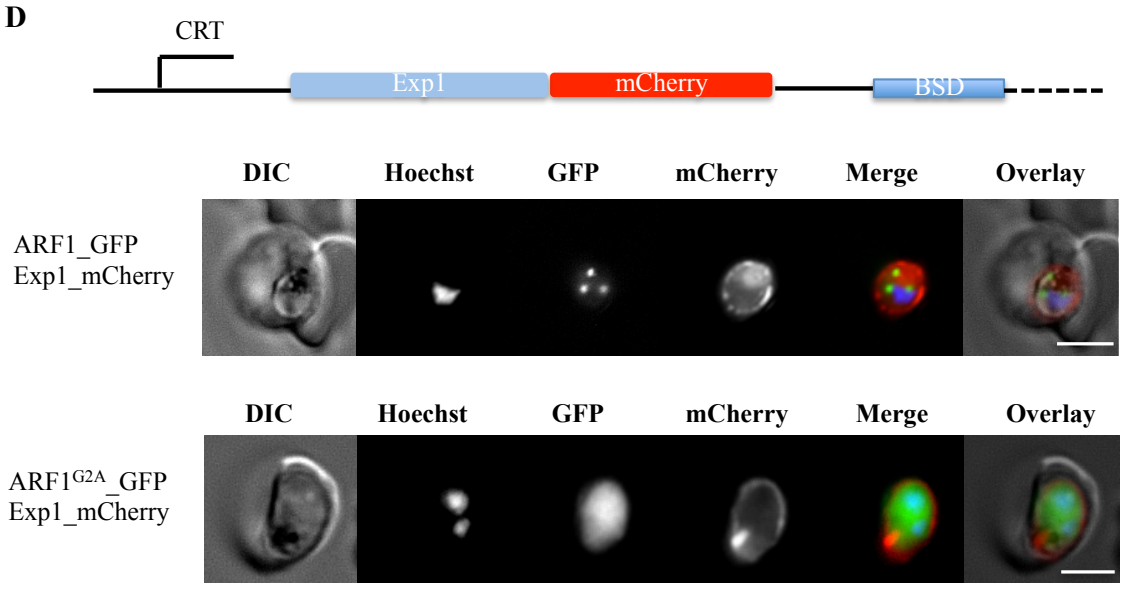

Figure 3.2 Co-localization of *Pf*ARF1/GFP with proteins localized to compartments of the secretory pathway

(A) *Pf*ARF1/GFP shows partial co-localizaton with the plasmodial ER marker protein *Pf*Sec12. (B) *Pf*Grasp1, a marker protein of the *cis*-Golgi-complex, shows dot-like structures within the parasite, which strongly overlap with the dot-like structures of *Pf*ARF1/GFP. (C) *Pf*Rab6, a marker protein of the *trans*-Golgi-complex, also show dot-like structures within the parasite, which partially overlap with the dot-like signals of the wildtype *Pf*ARF1. (D) *Pf*Exp1 is an integral PVM protein as can be seen from the prominent ring-like structure; however no overlap of the signal with *Pf*ARF1/GFP was visible. (A,B,C,D) The marker proteins of each compartment were also co-expressed with the *Pf*ARF1^{G2A}/GFP. DIC channel for high-contrast; in merge: green (GFP), red (mCherry), blue (Hoechst = nucleus dye). Scale bar – 3 µm.

3.1.3 *Pf*ARF1 is not secreted into the PV in the blood-stage according to biochemical analyses

Since the data from the PV proteome analysis and the fluorescence microscopy study are contradictory, a biochemical approach was performed. Therefore the *Pf*ARF1/GFP and *Pf*ARF1$^{G2A/}$GFP transgenic parasite lines were subjected to Streptolysin O and saponin treatment, respectively, and were then further analyzed by SDS-PAGE, western blot analysis and immunodetection. Streptolysin O is a bacterial-pore forming protein, which induces pores in the red blood cell membrane (RBCM) resulting in the release of the erythrocyte cytosol but leaving the PV and the parasite intact (Bhakdi et al., 1985). Saponin, however, is a detergent, which disintegrates the red blood cell membrane and

the parasitophorous vacuolar membrane resulting in the release of the erythrocyte cytosol and the vacuolar content and only leaving the PPM and the parasite intact (Beaumelle et al., 1987). The supernatant fraction after SLO lysis contains the red blood cell cytosol, while after saponin treatment the erythrocyte cytosol and the content of the PV is found in the supernatant fraction. The pellet fraction after SLO lysis contains the permeabilized RBCM, the intact PV and the intact parasite, while the pellet fraction after saponin lysis contains the parasite with an intact parasite plasma membrane and the permeabilized PVM and RBCM.

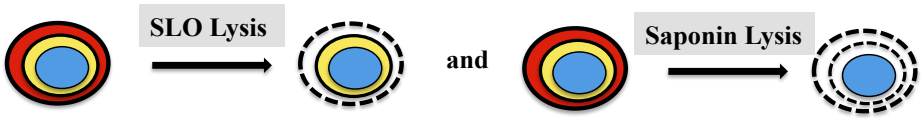

An analysis in which the respective transgenic parasite line is subjected to each of these methods and then the results are compared with each other enables the identification of the subcellular localization of the examined protein. In addition to the SLO and saponin treatment, a protease protection assay was performed. Therefore the pellet fraction after each of the two treatments was divided into two aliquots containing equal cell numbers, then one of the aliquots was treated with Proteinase K and leaving the other untreated (control). After SLO lysis and Proteinase K treatment those proteins which are located outside of the PV will be degraded by the presence of Proteinase K, while proteins protected by the PVM and the PPM remain unaffected. After saponin lysis followed by Proteinase K treatment those proteins which would be located beyond the parasite plasma membrane will be degraded, while the proteins protected by the PPM meaning inside the parasite, remain unaffected. The plasmodial soluble **se**rine **r**ich **p**rotein (SERP) located in the PV was used as a control to demonstrate that the PV remained intact after SLO lysis. *Pf*aldolase - a protein found in the cytosol of the parasite - was used as a control protein to show that the parasite remained intact after SLO and saponin treatment, respectively. A positive control for an efficient protease digestion in each of the experiment itself was not performed; however, the efficiency of protease digestion was shown for one of the variants of *Pf*AK2 (detailed in Fig. 3.7 C): the fusion protein analyzed (*Pf*AK2^{G2AC4A}) was protected by the PPM after saponin treatment. Proteinase K was given access to the fusion protein by permeabilizing the PPM of the saponin treated cells with a detergent (Triton X 100) and it was shown that Proteinase K was able to digest the fusion protein. This example indicates the efficiency

of Proteinase K for digestion of the fusion protein of one of the *Pf*AK2 variants. The protease protection assay was performed for each of the different variants with the same concentration and incubation time as performed for this particular variant (see Fig 3.7 C for further detail).

In the following experiment the GFP antibody detected *Pf*ARF1/GFP in the western blot analysis, while an antibody directed against *Pf*ARF1 detected both the endogenous *Pf*ARF1 and the fusion protein *Pf*ARF1/GFP. Fig 3.3 displays the results of the SLO and saponin lysis performed on the *Pf*ARF1/GFP and the *Pf*ARF1$^{G2A/}$GFP transgenic parasite lines, respectively. The PV marker protein *Pf*SERP and the parasite marker protein *Pf*aldolase are both found after SLO lysis and Proteinase K treatment predominantly in the pellet fraction. This indicates that the PV and the parasite almost remained intact and that both proteins were not accessible to Proteinase K. However, a faint band of approximately 40 kDa could also be detected with an α-aldolase antibody in the SLO supernatant fraction of the *Pf*ARF1/GFP transgenic parasite sample. The band size, however, is much weaker compared to the band size in the SLO pellet fractions. Although the majority of the control proteins were found in the SLO pellet fraction indicating an almost proper lysis, some lysis of parasites during the SLO and saponin treatment and during the incubation time did occur. This, however, is difficult to be avoided completely, which is a general issue of this treatment procedures as was also found in other studies using these lysis methods for investigation of protein localization in *P. falciparum* infected cells (Ansorge et al., 1997; Spielmann et al., 2006; Heiber et al., 2013). A band of approximately 50 kDa was detected with the α-GFP antibody which corresponds to the size of the fusion protein in both the SLO pellet fraction treated with Proteinase K and the untreated one of the ARF1/GFP and ARF1^{G2A}/GFP transgenic parasite samples, respectively. This indicates that the fusion proteins ARF1/GFP and ARF1^{G2A}/GFP, respectively, are not located beyond the PVM since the band in the SLO pellet fraction treated with Proteinase K was not digested. This indicates that both of the fusion proteins do not cross the PVM to be secreted into the host cell (Fig. 3.3 A). A positive control of efficient Proteinase K digestion for this particular experiment is missing, however, the efficiency of Proteinase K digestion of a fusion protein in general is shown for one of the variants (*Pf*AK2^{G2AC4A}/GFP in Fig. 3.7 C). After saponin treatment and Proteinase K treatment of the samples of both

transgenic parasite lines *Pf*SERP was detected in the supernatant fraction meaning that the PV was lysed as expected. *Pf*aldolase was detected in both the saponin pellet fraction treated with Proteinase K and the untreated saponin pellet fraction indicating an almost retention of an intact parasite. Similar to the result of the SLO treatment aldolase was also detected in the supernatant fraction of the *Pf*ARF1/GFP sample as a very faint band. Thus, a small amount of aldolase was released during the lysis procedure indicating some lysis of parasites during the saponin treatment. However, the majority of the protein was detected in the pellet fraction. *Pf*SERP could also be detected in the saponin pellet fraction, but the band of approximately 130 kDa disappeared upon Proteinase K treatment. This probably means that SERP sticks to membranes and was difficult to wash off the membrane despite many washing steps of the pellet fraction during sample preparation. Upon proteinase treatment it could be removed from sticking to the membrane. However, a band of ~ 50 kDa corresponding to the *Pf*ARF1/GFP and the *Pf*ARF1^{G2A}/GFP fusion protein, respectively, was found in the saponin pellet fraction when detected with an α-GFP antibody and in the saponin pellet treated with Proteinase K (Fig. 3.3 A). This indicates that the fusion protein was not accessible to Proteinase K digestion and therefore is not secreted beyond the parasite plasma membrane. This result corresponds to the fluorescence and co-localization studies showing that *Pf*ARF1 is solely found in the parasite cytosol and is not secreted beyond the parasite plasma membrane. To further support this observation the *Pf*ARF1/GFP transgenic parasite line was subjected to a co-localization study with an antibody against plasmodial ARF1, which was also used to detect the endogenous *Pf*ARF1 after SLO and saponin treatment, respectively. Indeed the antibody co-localized partially with the fusion protein *Pf*ARF1/GFP as can be seen in the overlapping dot-like structures, but also endogenous plasmodial ARF1 could be detected as punctuate structures in the parasite cytosol. Furthermore, a band corresponding to the endogenous *Pf*ARF1 of about 21 kDa and to the fusion protein of 50 kDa could be detected with the plasmodial α-ARF1 antibody in both the SLO and saponin pellet fractions (Fig. 3.3 C). Furthermore, the bands were also detected in each of the fractions, which were treated with Proteinase K. The endogenous ARF1 and the *Pf*ARF1/GFP fusion protein were not affected by Proteinase K treatment indicating that they were protected within the parasite cytosol. A small amount of the endogenous ARF

protein could also be detected in the supernatant fraction after SLO and saponin treatment, respectively. This indicates that some of the parasites were lysed during each of the treatment why some of the endogenous ARF protein could be detected in the supernatant fraction similar to the amount of the marker protein aldolase found in the supernatant fraction. A possible reason why the GFP-tagged ARF protein was not found in the supernatant might be that the amount of protein episomally expressed might be far less than the amount of the expression of the endogenous aldolase and ARF protein in the parasite, why despite some lysis of the parasites during the procedures the amount of GFP-tagged ARF was too less to be detected. This explanation is furthermore supported by the intensity of the bands of the endogenous ARF compared to the GFP-tagged version. However, a band of around 35 kDa appears strongly in the supernatant fraction after SLO and saponin treatment, but also to a less extent in the SLO pellet fractions (+/- Proteinase K). This could be the result of cross-reactivity of the antibody to exported parasite proteins in the host cell or host cell proteins and also within the parasite (Fig. 3.3 C). Images of the immunofluorescence study also occasionally, but not always revealed a weak detection of structures in the host cell cytosol by the plasmodial α-ARF1 antibody. Taken together, although *Pf*ARF1 was hypothesized to be localized to the PV according to the PV proteome approach, fluorescence and biochemical analyses revealed its localization solely within the parasite cytosol to compartments of the classical secretory pathway.

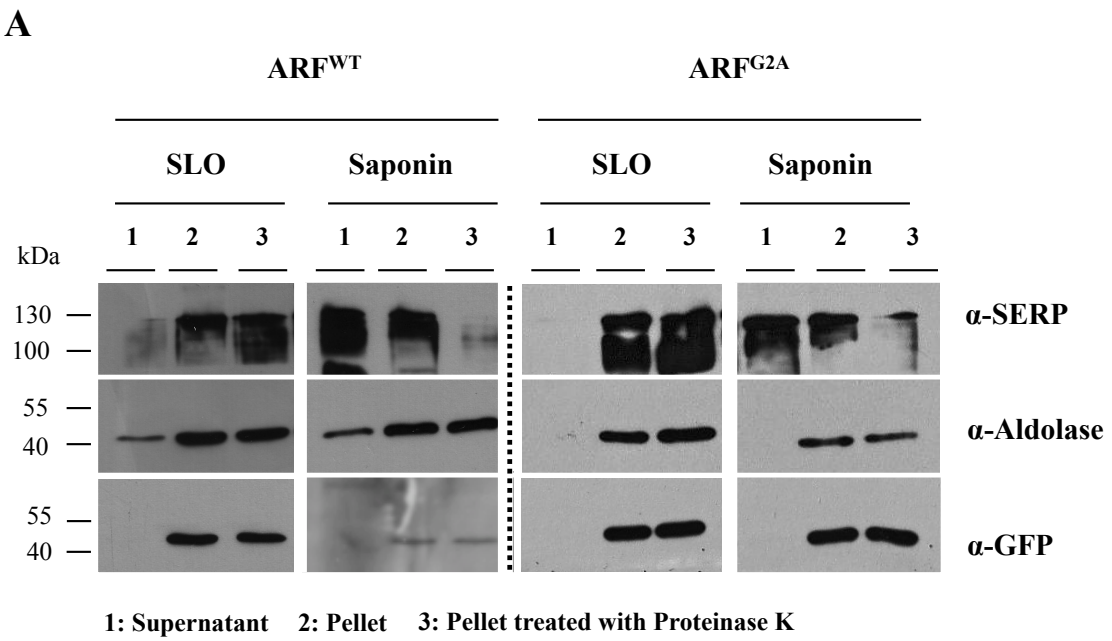

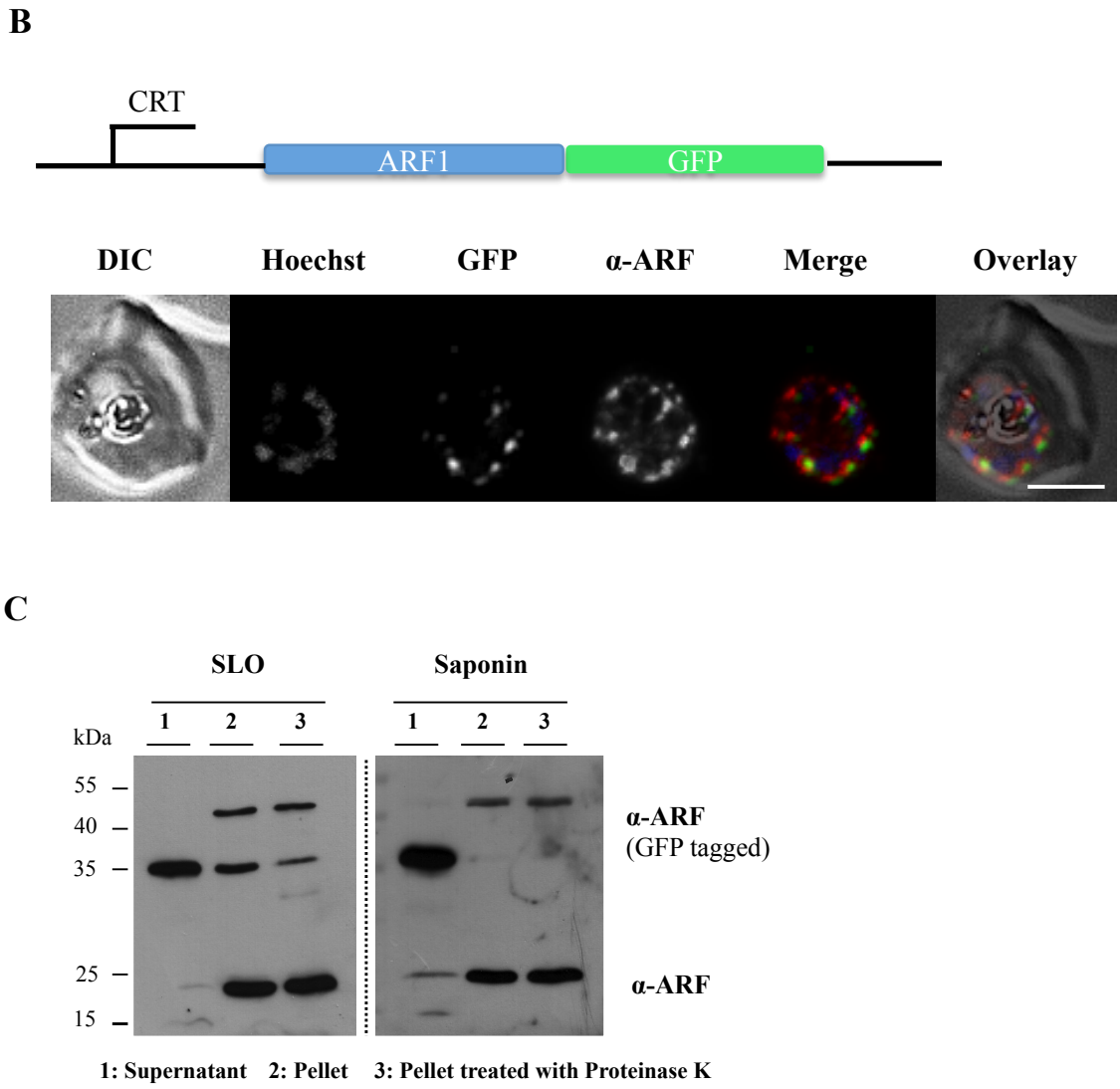

Figure 3.3 *Pf*ARF1/GFP is not secreted beyond the parasite plasma membrane according to a biochemical approach

(A) The *Pf*ARF1/GFP transgenic parasites and the respective variant were both subjected to SLO and saponin lysis, followed by a protease protection assay. *Pf*SERP and *Pf*aldolase were used as controls as a PV marker protein and parasite marker protein, respectively. All of the marker proteins could be detected with their respective antibodies after SLO and saponin lysis of the two transgenic parasite lines predominantly in the expected compartments. However, lysis of some parasites did occur during the SLO and saponin treatment, respectively, why a small amount of aldolase was also detected in the supernatant fraction. The fusion proteins *Pf*ARF1/GFP and *Pf*ARF1^{G2A}/GFP were detected with an α-GFP antibody after SLO and saponin lysis, respectively, in the pellet fractions and also the pellet fractions treated with Proteinase K. (B) Co-localization between the *Pf*ARF1/GFP and an α-ARF1 antibody directed against the plasmodial endogenous ARF1 (which will also detect the fusion protein tagged with GFP) can be seen in the fluorescence images. According to the biochemical approach the plasmodial α-ARF1 antibody

detected a strong band at 21 kDa and a weaker band of approximately 50 kDa in the SLO and saponin pellet fractions (-/+ Proteinase K addition). A small amount of the endogenous ARF protein was also detected in the supernatant fraction, which might be due to lysis of some parasites during the procedure. A strong protein band of ~ 35 kDa was also detected in the supernatant fraction and in both pellet fractions (-/+ Proteinase K) of saponin treated *Pf*ARF1/GFP parasites which might result from cross-reactivity of the antibody with other parasite proteins. DIC channel for high-contrast; in merge: green (GFP), red (α-ARF1), blue (Hoechst = nucleus dye). Scale bar – 3 µm.

3.2 Is *Pf*AK2 secreted beyond the parasite plasma membrane?

Similar to the reporter construct studies designed for *Pf*Prefoldin, *Pf*CDPK4 and *Pf*ARF1 Ma and colleagues generated fusion proteins with the full-length *Pf*AK2 fused to GFP and created a variant of it, the *Pf*AK2^{G2A}/GFP. In the variant the *N*-myristoylation site was removed by changing the glycine residue at the N-terminus of the protein to alanine. Both of these constructs were transfected individually into the *P. falciparum* 3D7 strain and were episomally expressed with the low-expression promoter CRT by Ma and colleagues. A repetition of the fluorescence analysis of the *Pf*AK2/GFP transgenic parasite line and the *Pf*AK2^{G2A}/GFP - first shown by Ma and colleagues (Ma et al., 2012) - was performed in this study to visualize the difference between the wildtype phenotype of the *Pf*AK2/GFP fusion protein and the *Pf*AK2^{G2A}/GFP fusion protein and for subsequent comparison with the following variants made and analyzed in this study. Interestingly, the phenotypes of the *Pf*AK2/GFP fusion protein and *Pf*AK2^{G2A}/GFP fusion protein differed in their protein localization pattern when visualized by fluorescence microscopy. While the *Pf*AK2/GFP showed a ring-like structure around the parasite with a knob-like protrusion, which are referred to as 'loops' the signal from the *Pf*AK2^{G2A}/GFP was rather found to be evenly distributed in the cytosol of the parasite (Fig. 3.4 A and Ma et al., 2012). This indicates that the *N*-myristoylation site has an effect on the localization of *Pf*AK2. These findings were further analyzed via hypotonic lysis by Ma and colleagues with samples of both transgenic parasite lines (*Pf*AK2/GFP and *Pf*AK2^{G2A}/GFP, respectively). While the AK2/GFP fusion protein was found in the membrane fraction consistent with the role of membrane-anchoring due to myristate, the variant form, where the *N*-myristoylation site was removed, was found entirely in

the soluble fraction (Ma et al., 2012). Further, Ma and colleagues proposed that the full-length AK2 localizes to the PVM. This was shown by a co-localization study of *Pf*SERP and *Pf*Exp1 with the *Pf*AK2/GFP parasite line by the overlap of the signals of *Pf*Exp1 and *Pf*AK2/GFP in the merged image (Ma et al., 2012). However, biochemical evidence on the subcellular localization of *Pf*AK2 and further explanation on the secretion process of *Pf*AK2 are still missing.

To verify the findings of Ma and colleagues the transgenic parasite lines of *Pf*AK2/GFP and *Pf*AK2^{G2A}/GFP were subjected to Streptolysin O and saponin lysis before being analyzed by SDS-PAGE, western blotting and immunodetection. SLO treatment was performed on the sample of the *Pf*AK2/GFP transgenic parasite line (Fig. 3.4 B). The pellet fraction after SLO lysis contains the intact PV and parasite and the permeabilised RBCM, while the SLO supernatant fraction only contains the erythrocyte cytosol. The band of approximately 60 kDa detected in the SLO pellet fraction by an α-GFP antibody corresponds to the size of the fusion protein consisting of the full-length *Pf*AK2 (32.5 kDa) and GFP (27 kDa). Proteinase K treatment of the SLO pellet fraction did not lead to the disappearance of the band indicating that the fusion protein *Pf*AK2/GFP was not digested by Proteinase K, hence it is not located at the outer face of the PVM. Bands corresponding to the size of the marker proteins *Pf*SERP and *Pf*aldolase were each found in the pellet fractions meaning that the PV was not lysed after SLO treatment of the parasitized cells but remained intact. In a next step the saponin lysis in combination with Proteinase K treatment was performed to figure out whether or not the AK2 protein was secreted beyond the PPM. Saponin treatment of parasitized cells leads to the retention of an intact parasite and to disintegration of the RBCM and PVM resulting in the release of the erythrocyte cytosol and the vacuolar content (supernatant fraction). Hence the pellet fraction after saponin treatment contains the intact parasite, the permeabilized PVM and RBCM, while the supernatant fraction after saponin treatment contains the erythrocyte cytosol and the vacuolar content. After saponin treatment bands corresponding to the size of the the marker proteins of both compartments - PV (marker protein: SERP) and parasite (marker protein: aldolase) - were found predominantly in the expected fractions. A positive control of efficient Proteinase K digestion for this particular experiment is missing, however, the efficiency

of Proteinase K digestion of a fusion protein is shown for one of the variants (*Pf*AK2^{G2AC4A}/GFP in Fig. 3.7 C).

Although a band of 130 kDa corresponding to *Pf*SERP could also be detected in the saponin pellet fraction of the *Pf*AK2/GFP parasitized cells the band disappeared after Proteinase K treatment indicating that SERP sticks to membranes and was not properly removed during the washing steps after saponin treatment. Also a small amount of aldolase was detected in the supernatant fraction after saponin treatment, the majority of aldolase was found in the pellet fraction. This is a general issue of this procedure which could also be seen in different *P. falciparum* studies (Ansorge et al., 1997; Spielmann et al., 2006; Heiber et al., 2013). However, the band of ~ 60 kDa in the saponin pellet fraction of the sample from the *Pf*AK2/GFP transgenic parasite line when treated with Proteinase K disappeared. This indicates that Proteinase K had access to the fusion protein (Fig 3.4 B) what indicates that AK2 fused to GFP was not protected by the parasite plasma membrane. This finding corresponds to the findings of Ma and colleagues in which they claim *Pf*AK2 to be located beyond the PPM. To further support the role of *N*-myristoylation in the secretion process beyond the PPM the *Pf*AK2^{G2A}/GFP variant was analyzed in the same manner. Since the marker proteins of the PV (SERP) and parasite (aldolase), respectively, were almost found in the expected fractions after SLO and saponin treatment, respectively, an almost proper lysis did take place. However, similar as observed for the saponin treated *Pf*AK2/GFP parasites, the PV marker protein SERP also was detected in the pellet fraction, but almost disappeared in the saponin pellet fraction treated with Proteinase K. This suggets that SERP sticks to membranes and is difficult to remove despite many washing steps during sample preparation. However, the band in the saponin pellet fraction of the variant *Pf*AK2^{G2A}/GFP still could be detected by an α-GFP antibody after Proteinase K treatment. This indicates that the fusion protein was not digested by proteinase and that Proteinase K had no access to the fusion protein. From this observation it can be concluded that the *N*-myristoylation site indeed plays a role in the localization of the *P. falciparum* AK2 protein. Two different phenotypes could be observed in the fluorescence analyses comparing the wildtype protein and one where the *N*-myristoylation site was removed (Ma et al., 2012). This is consistent with the findings of the biochemical approach in which the wildtype fusion protein was found

digested upon Proteinase K treatment after saponin lysis. This indicates that the wildtype protein is secreted into the PV, while the variant of this protein, which lacks the *N*-myristoylation site, remained protected within the parasite cytosol (Fig. 3.4).

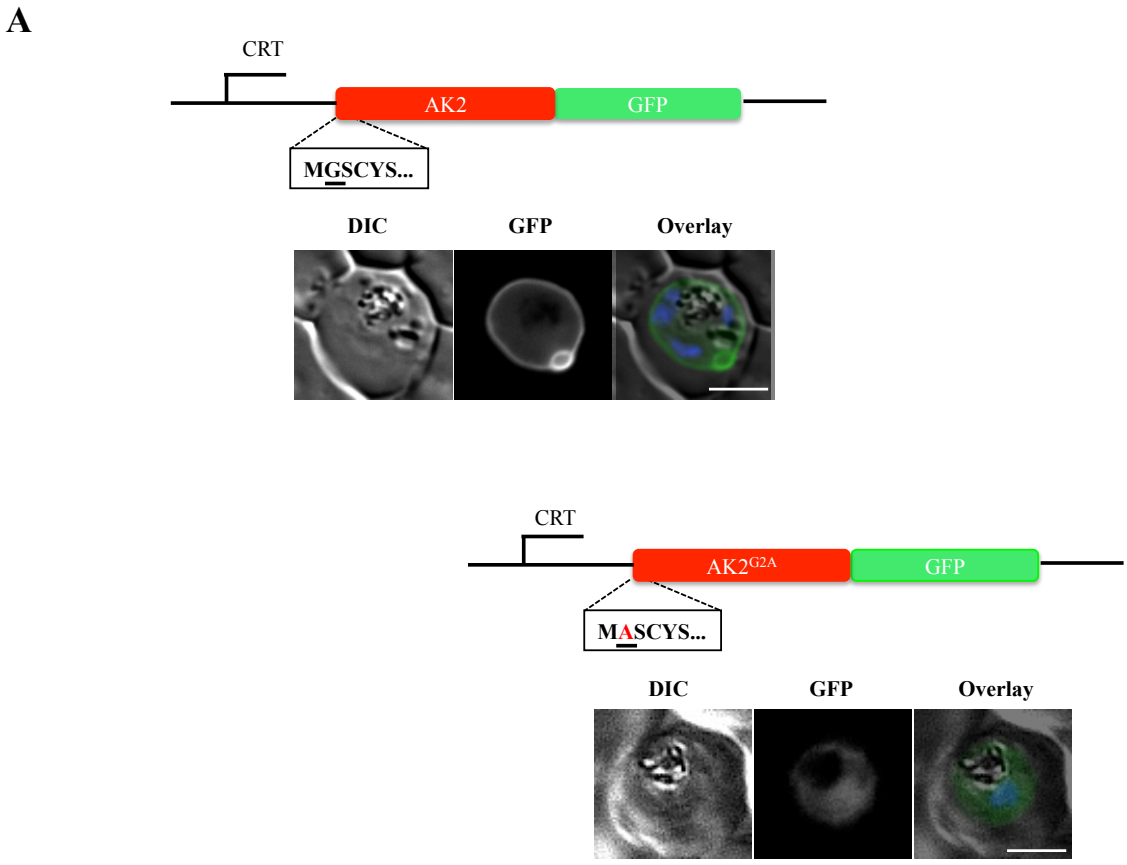

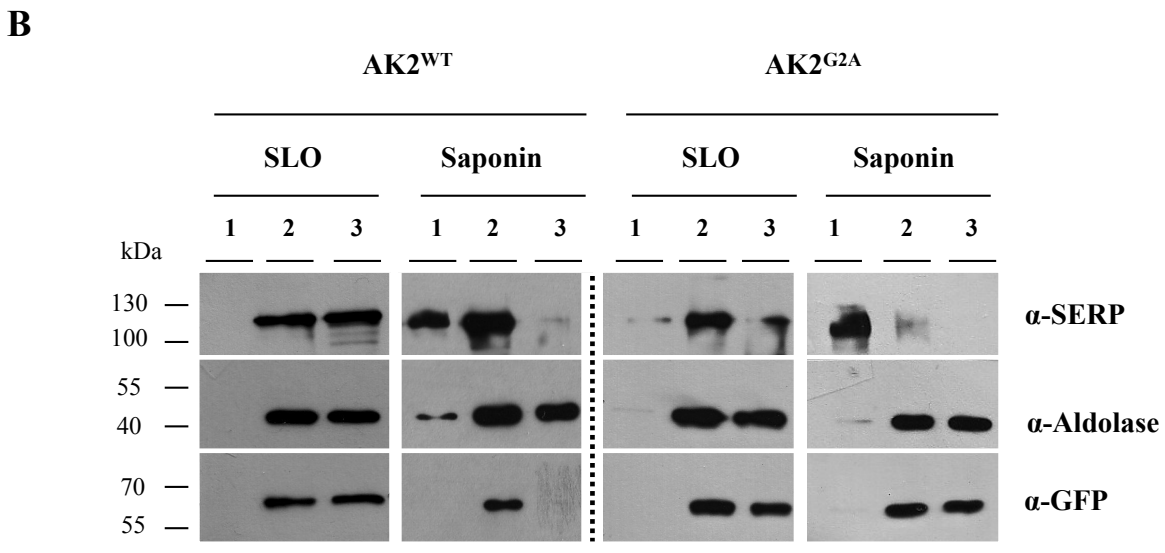

1: Supernatant 2: Pellet 3: Pellet treated with Proteinase K

Figure 3.4 Live cell imaging and a biochemical approach of the *Pf*AK2/GFP transgenic parasite line and the variant *Pf*AK2^{G2A}/GFP
(A) Live cell imaging of the *Pf*AK2/GFP expressing parasites reveals a ring-like structure of the fusion protein, while the signal of the fusion protein of the *Pf*AK2^{G2A}/GFP parasites appears to be cytosolic. DIC channel for high-contrast; overlay (green =GFP; Hoechst = nucleus dye). Scale bar – 3 µm. (B) The *Pf*AK2/GFP transgenic parasites and the respective variant were both subjected to SLO and saponin lysis, followed by a protease protection assay. *Pf*SERP and *Pf*aldolase were used as PV marker protein and parasite marker protein, respectively. All of the marker proteins could be detected with their respective antibodies predominantly in the expected compartments after SLO and saponin lysis. However, aldolase was also sometimes detected in the supernatant fraction, which indicates that a small amount of parasites did lyse during the whole procedure. The fusion proteins *Pf*AK2/GFP and *Pf*AK2^{G2A}/GFP were detected with an α-GFP antibody after SLO and saponin lysis in the SLO pellet fraction and also the pellet fraction treated with Proteinase K. However, while the variant of the fusion protein *Pf*AK2^{G2A}/GFP was detected in both saponin pellet fractions (-/+ Proteinase K addition), the wildtype fusion protein could not be detected in the saponin pellet fraction treated with Proteinase K. This indicates that the protein was accessible to Proteinase K. The size-marker is presented in kDa.

3.2.1 A multiple sequence alignment

Ma and colleagues already performed a multiple sequence alignment with *Pf*AK2, *Pf*AK1, the two *Pf*AKLPs, *Pf*GAK and the human AK6, in which they showed that the N-terminus of *Pf*AK2 differed from the N-termini of the other aligned proteins (Ma et al., 2012). In this study, a further multiple sequence alignment (MSA) of *Pf*AK2 with putative adenylate kinase 2 proteins of other *Plasmodium* species and other Apicomplexa was performed. Except for *Plasmodium cynomolgi* (B strain) – a *Plasmodium* species known to infect monkeys – which harbours the adenylate kinase 2 protein, only putative adenylate kinase 2 proteins were identified for the other *Plasmodium* species. Interestingly, other parasitic protozoa such as *Babesia bovis* and some *Leishmania* species also contain an adenylate kinase 2 protein. That is why *Babesia bovis* and *Leishmania infantum* were also included in the MSA.
Only the N-terminus (1-50 positions) is presented in the following graphic (Fig. 3.5). The entire sequence alignment can be found in the appendix. The N-terminus of *Pf*AK2 clearly revealed motifs, which are missing in the N-terminus of *Pf*AK1, but also in the N-termini of the other adenylate kinase 2 proteins of the other *Plasmodium* species and the other parasitic protozoa. Apart from the glycine residue at the N-terminus, which

has already been shown to be myristoylated by plasmodial NMT (Rahlfs et al., 2009), a cysteine residue at the 4th position was found at the N-terminus of plasmodial AK2 indicative for a putative palmitoylation site. According to the 'two-step model' a stable membrane anchoring of a myristoylated protein requires either a palmitoylation site or a polybasic cluster of amino acids close by. The N-terminus of *Pf*AK2 harbours in addition to a putative palmitoylation site a polybasic cluster of lysine residues at the N-terminus. These motifs might play a role in stable protein anchoring and secretion beyond the parasite plasma membrane as was already shown for the *Leishmania* HASPB and the *Plasmodium* CDPK1: both proteins contained in addition to a *N*-myristoylation site a palmitoylation site at their N-terminus (Denny et al., 2000; Möskes et al., 2004). However, these motifs were not found in the other verified and putative adenylate kinase 2 proteins aligned.

```
                  1                                                  50
PfAK2             MGSC----------YSRKNKVSTISLDEEEKKKE--KKKKKKIYILNGAS
PfAK1             MNE-------------NLENFSTIDLLNELKRRYACLSKPDGRYIFLGAP
PBANKA_AK2_p      MVP--------------------------------PPPKKKVYIMNGPP
PCHAS_AK2_p       MVS--------------------------------Q-KKKKVYIMNGPP
PKH_AK2_p         MEQ----------------------------------KKGPKVFILNGAA
PVX_AK2_p         MSD-------------NLEKFSTVDLLNELKRRYSCLSKPDGRYIFLGAP
PYYM_AK2_p        MVS--------------------------------QKKKKKVYIINGPP
PCYB_AK2          MSD-------------NLEKFSTVDLLNELKRRYSCLSKPDGRYIFLGAP
BbAK2             MIFLRVLSLLFFATMSGLHGYETQTLVEELRRRYDCLSKPQGNFIFMGAP
LiAK2             M-------------------------------------KIVMEGPP
                  *                                        :: *..
```

Figure 3.5 A multiple sequence alignment of the N-terminus of *Pf*AK2 and other verified and putative adenylate kinase 2, respectively, in other *Plasmodium* species and other parasitic protozoa
*Pf*AK2 (PF3D7_0816900) was aligned to *Pf*AK1 (*Pf*3D7_1008900), *Pb*AK2, putative (PBANKA_071390), *Pc*AK2, putative (PCHAS_072300), *Pk*AK2, putative (PKH_051560), *Pv*AK2, putative (PVX_094660), *Py*AK2, putative (PYYM_071400), *Pc*AK2 (PCYB_081850), *Bb*AK2 (bbov|XP_001609458.1) and *Li*AK2 (linf|LinJ.34.0130). The N-terminus of *Pf*AK2 clearly differs from the N-termini of the other aligned proteins, insofar as it contains a verified *N*-myristoylation site (Rahlfs et al., 2009), a putative palmitoylation site at the 4th position and a polybasic cluster of lysine residues (each motif marked in grey). None of the other AK2 proteins contain either of these motifs. The alignment was created using ClustalW and only the first 50 positions are shown. The entire sequence alignment can be found in the appendix.

3.2.2 A putative palmitoylation site at the N-terminus of *Pf*AK2

In order to figure out whether or not *Pf*AK2 has a putative palmitoylation site at the N-terminus the cysteine residue at position 4 was changed to alanine. The resultant *Pf*AK2^{C4A}/GFP transgenic parasite line was first visualized by fluorescence microscopy before being subjected to hypotonic, SLO and saponin lysis followed by SDS-PAGE, western blotting and immunodetection. Fluorescence analysis of the *Pf*AK2^{C4A}/GFP transgenic parasites reveals a different phenotype to the wildtype *Pf*AK2/GFP (Fig. 3.4 A). Instead a ring-like structure as visualized for the wildtype *Pf*AK2/GFP expressing parasites the GFP signal of this variant lacking the putative palmitoylation site appears cytosolic. Interestingly, patch-like accumulation at some regions within the parasite cytosol can be seen especially in the early trophozoite stage of the parasite (marked with a white arrow in Fig. 3.6 A), but also in late-stage parasites. This observation coincides with the findings of the hypotonic lysis, which was used to distinguish between soluble and membrane fraction of the parasitized cells. For the soluble fraction the plasmodial aldolase was used as a marker protein, while for the membrane fraction the *Pf***E**xported **p**rotein 1 (Exp1) - an integral membrane protein of the PVM (Günther et al., 1991)- was used as a marker protein. A band of about 60 kDa could be detected with an α-GFP antibody in both fractions corresponding to the size of the fusion protein *Pf*AK2^{C4A}/GFP. A soluble and membrane-bound pool of this protein could be detected. Antibodies against *Pf*Exp1 and *Pf*aldolase were used to detect these proteins in the soluble and membrane fraction, respectively, as a control for proper separation (Fig. 3.6 B). SLO treatment of the transgenic parasites of the *Pf*AK2^{C4A}/GFP line revealed that the GFP chimera was found in both SLO pellet fractions (+/- Proteinase K). This indicates that no digestion of the fusion protein took place. A positive control of efficient Proteinase K digestion for this particular experiment is missing, however, the efficiency of Proteinase K digestion of a fusion protein in general is shown for one of the variants (*Pf*AK2^{G2AC4A}/GFP in Fig. 3.7 D). The detection of the marker proteins *Pf*SERP and *Pf*aldolase by their respective antibodies in the SLO pellet fraction indicates that proper lysis by SLO had occured since their correct localization indicates an intact PV. A strong GFP signal was obtained in the pellet fraction of saponin treated *Pf*AK2^{C4A}/GFP transgenic parasites, which was detected by the α-GFP antibody. The band in the saponin pellet fraction treated with Proteinase K was of similar size and

intensity indicating that the fusion protein lacking the putative palmitoylation site was protected by the parasite plasma membrane, hence not secreted beyond the PPM. Also the compartments seem to be almost intact after saponin treatment of the parasitized cells since the bands corresponding to the size of *Pf*SERP and *Pf*aldolase were predominantly detected in the expected fractions. Again SERP sticks to the membrane in the saponin pellet fraction but almost disappeared after Proteinase K treatment. Here also a small amount of aldolase is detected in the supernatant fraction indicating some lysis of the parasites during the treatment. From these observations it can be concluded that the *Pf*AK2^{C4A} variant exists in a soluble and membrane-bound form possibly resulting from the unstable binding of the myristoyl moiety to a membrane. This can be seen by the fluorescence images due to some patch-like accumulation of the GFP signal in the overall cytosolic signal inside the parasite. Further, a partial soluble and membrane-bound pool of the protein was found after hypotonic lysis. The lack of the cysteine residue at the N-terminus prevented secretion of the protein beyond the parasite plasma membrane as indicated by saponin lysis and the protease protection assay.

A

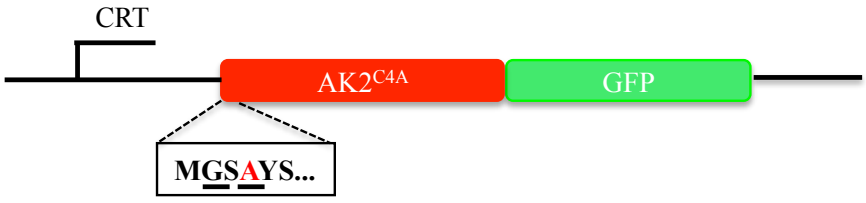

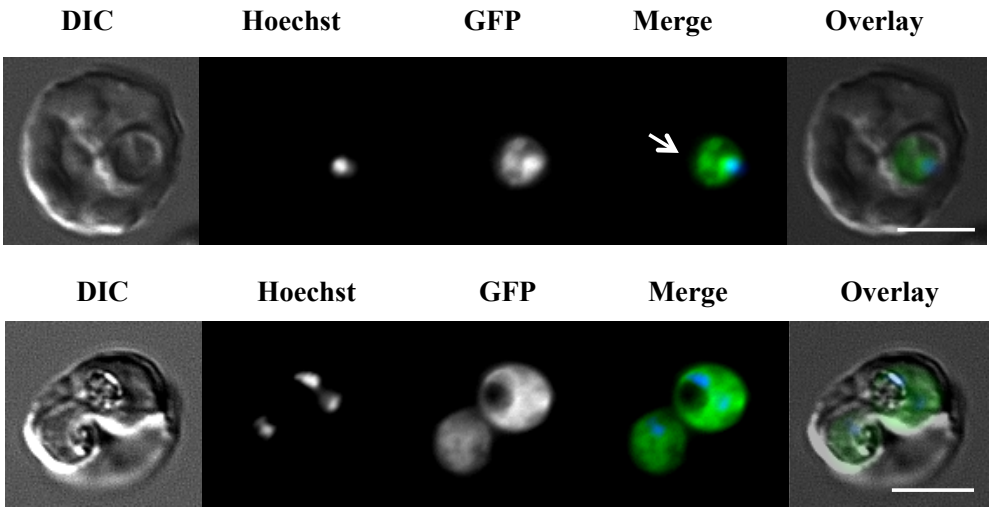

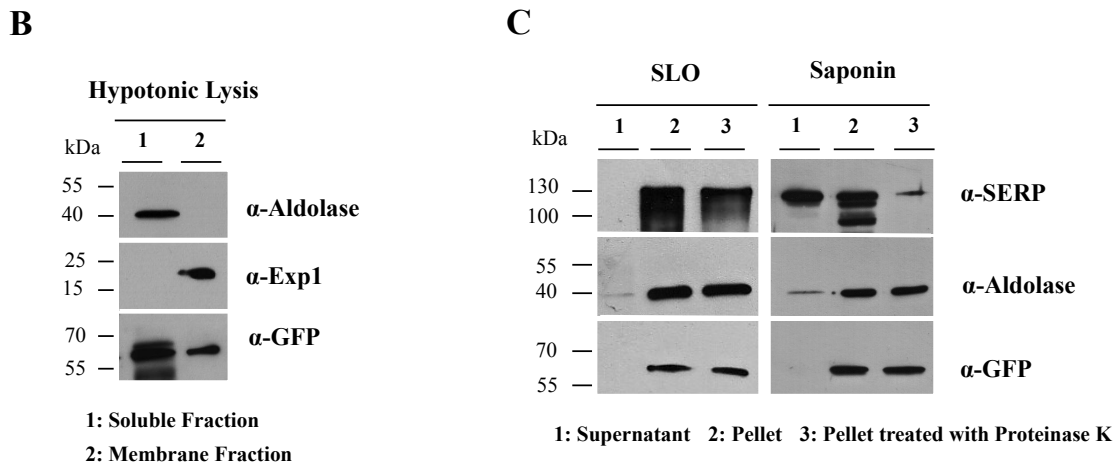

Figure 3.6 The *Pf*AK2^{C4A}/GFP transgenic parasite line shows a cytosolic localization and is not secreted beyond the parasite plasma membrane

(A) Live cell imaging of the *Pf*AK2^{C4A}/GFP parasite line in early and late trophozoite stages show patch-like structures within the parasite, which is different to the wildtype phenotype. DIC channel for high-contrast; in merge: green (GFP), blue (Hoechst = nucleus dye). Scale bar – 3 µm. (B) After hypotonic lysis a band corresponding to the size of the fusion protein could be detected in the soluble and membrane fraction. *Pf*aldolase was used as a control for the soluble fraction and *Pf*Exp1 was used as a control for the membrane fraction. (C) *Pf*AK2^{C4A}/GFP parasites were subjected to SLO and saponin lysis. The marker proteins *Pf*SERP of the PV and *Pf*aldolase of the parasite were both found predominantly in the expected fractions indicating an almost proper SLO lysis and saponin lysis, respectively. However, minimal amounts of aldolase could also be detected in the supernatant fraction and a small amount of SERP was also found in the saponin pellet fraction even after Proteinase K treatment. This indicates that some parasites did indeed lyse during the whole procedure. The size markers are presented in kDa.

3.2.3 The *Pf*AK2^{G2AC4A} expressing parasites localize to the parasite cytosol

To further examine the role of the *N*-myristoylation site and the putative palmitoylation site a further transfectant line was generated. Therefore the *N*-myristoylation and the putative palmitoylation site were removed from *Pf*AK2 by changing the respective sites to alanine. The resultant *Pf*AK2^{G2AC4A}/GFP transgenic parasite line was visualized by fluorescence microscopy and then subjected to biochemical analyses. The *Pf*AK2^{G2AC4A}/GFP parasites showed a strong cytosolic signal of the fusion protein when observed by fluorescence microscopy (Fig. 3.7 A), which differs in location from the GFP signal seen with the wildtype transgenic parasite strain. The cytosolic localization of the GFP chimera is further supported by the hypotonic lysis study where a band corresponding to the *Pf*AK2^{G2AC4A}/GFP of 60 kDa could be detected in the soluble

fraction by an α-GFP antibody. *Pf*Exp1 was detected in the membrane fraction, while *Pf*aldolase was detected in the soluble fraction showing that a clear separation took place during the lysis procedure (Fig 3.7 B). The parasites were subjected to SLO and saponin lysis. This time the pellet fraction of the SLO and saponin lysis, respectively, were equally divided into for samples and were treated as followed: 1) untreated (control), 2) addition of Proteinase K, 3) addition of Proteinase K and Triton X-100 and 4) addition of Triton X-100 and PIC/PMSF. Triton X-100 was used to permeabilize the PPM giving Proteinase K access to degrade the GFP chimera, once it is released upon Triton X-100 treatment of the cells. This positive control shows the efficacy of Proteinase K digestion of the fusion protein (disappearance of the protein band in this fraction). Treatment of the parasizited cells with only Triton X-100 showed that the protein band of the GFP chimera is still present meaning that Triton X-100 is not causing the disappearance of the protein band (negative control). PIC and PMSF were added to prevent degradation of the fusion protein by endogenous proteases. The fusion protein was affected by Triton X-100 permeabilization and Proteinase K treatment, but not by Triton X-100 permeabilization alone. In the SLO and saponin treated samples of the *Pf*AK2^{G2AC4A}/GFP transgenic parasite line, respectively, the GFP chimera was detected in the pellet fraction treated with Proteinase K and in the untreated one. This indicates that the fusion protein is not secreted beyond the PVM and the PPM, respectively. The marker proteins ensuring correct lysis and correct performance of the protease protection assay were detected predominantly in the expected fractions. However, in the SLO treated samples a small amount of SERP could also be detected in the supernatant fraction indicating that some lysis during the SLO treatment of the parasitized cells did occur (Fig. 3.7 C). In saponin treated samples a minimal amount of *Pf*aldolase and the GFP chimera could also be detected in the supernatant fraction, however the protein signal detected was much weaker compared to the signal found in the pellet fraction (Fig. 3.7 C). This indicates that some parasites were lysed during this sensitive procedure. This extended biochemical analysis of *Pf*AK2^{G2AC4A}/GFP was performed with a positive control for verification of Proteinase K efficacy towards the fusion protein. In conclusion, it can be stated that these findings are similar to the findings of the *Pf*AK2^{G2A}/GFP variant, which lacks the *N*-myristoylation site and was also localized to the cytosol of the parasite. The *N*-myristoylation motif seems crucial

for membrane binding and probably membrane targeting. This conclusion can be made since no membrane bound pool of proteins could be detected following hypotonic lysis.

A

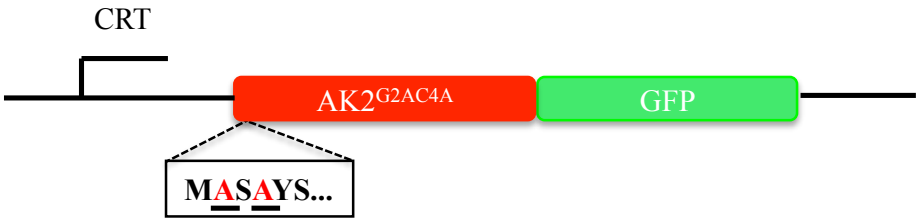

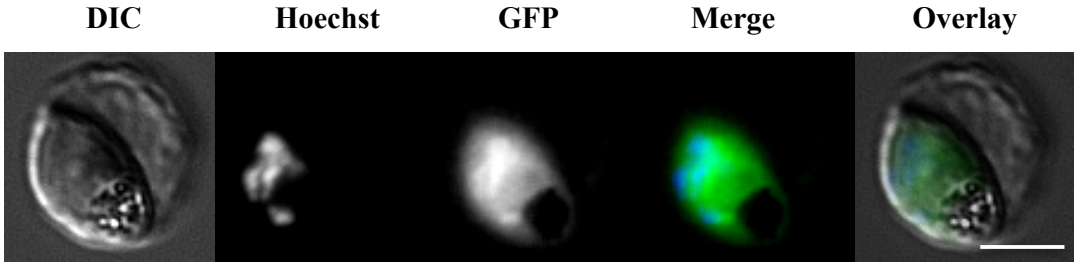

B

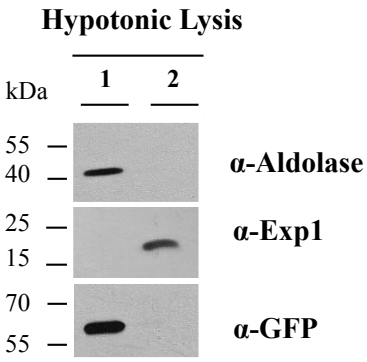

1: Soluble Fraction

2: Membrane Fraction

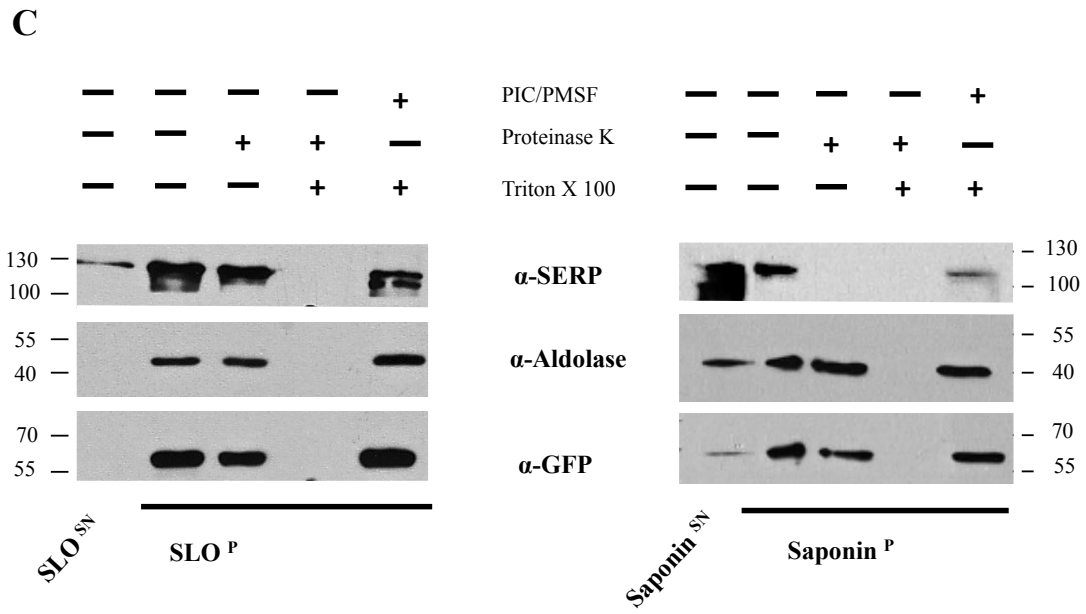

Figure 3.7 Removal of acylation sites at the N-terminus of *Pf*AK2 localizes the fusion protein to the cytosol of the parasite(A) Fluorescence analyses of the *Pf*AK2^{G2AC4A}/GFP parasites clearly showed a cyotosolic localization of the fusion protein *Pf*AK2$^{G2AC4A/}$GFP. DIC channel for high-contrast; in merge: green (GFP), blue (Hoechst = nucleus dye). Scale bar – 3 µm. (B) After hypotonic lysis performed on this transgenic parasite line a band of approximately 60 kDa corresponding to the GFP chimera was detected solely in the soluble fraction with an α-GFP antibody. *Pf*aldolase was used as a marker protein for the soluble fraction and *Pf*Exp1 was used as a marker protein for the membrane fraction. (C) The parasites were subjected to SLO and saponin lysis. The pellet fraction of the SLO and saponin lysis, respectively, were equally divided into for samples and were treated as followed: 1) untreated (control), 2) addition of Proteinase K, 3) addition of Proteinase K and Triton X-100 and 4) addition of Triton X-100 and PIC/PMSF. Triton X-100 was used to permeabilize the PPM so that Proteinase K is able to degrade the GFP chimera, once it is released upon Triton X-100 treatment of the cells. This positive control shows the efficacy of Proteinase K degradation of the fusion protein (disappearance of the protein band in this fraction). Treatment of the parasizited cells with only Triton X-100 showed that the protein band of the GFP chimera is still present meaning that Triton X-100 is not causing the disappearance of the protein band (negative control). PIC and PMSF were added to prevent degradation of the fusion protein by endogenous proteases. *Pf*SERP of the PV and *Pf*aldolase of the parasite were both found predominantly in the expected fractions indicating an almost proper SLO lysis and saponin lysis, respectively. However, aldolase was also found in the supernatant fraction of saponin treated parasitized cells and a small amount of SERP was detected in the supernatant fraction of SLO treated samples. This indicates that some of the parasites did lyse during the procedures. Both proteins were affected by Triton X-100 permeabilization and Proteinase K treatment, but not by Triton X-100 permeabilization alone. The size markers are presented in kDa.

3.2.4 Is a third motif involved in the secretion process of *Pf* AK2?

The MSA revealed a stretch of lysine residues (ten lysines with one interspersed glutatmate residue) at the N-terminus of *Pf*AK2 at close proximity to the *N*-myristoylation site. According to the 'two-step model' of membrane binding by myristoylated proteins a polybasic stretch of amino acids in addition to the myristoyl moiety leads to a stable membrane anchoring of myristoylated proteins to a membrane (Murray et al., 1997). To investigate the role of the lysine residues at the N-terminus of *Pf*AK2 these amino acids were deleted via overlapping extension PCR and the resultant construct *Pf*AK2$^{\Delta 21\text{-}30}$/GFP was transfected into the 3D7 *P. falciparum* line. Live cell imaging showed a ring-like structure with a protrusion similar to the wildtype GFP chimera, although the protrusion is less prominent compared to the wildtype *Pf*AK2/GFP (Fig. 3.8 A). Subsequent analyses on the subcellular localization of this protein were performed via hypotonic lysis, SLO and saponin lysis followed by SDS-PAGE, western blotting and immunodetection. The hypotonic lysis clearly separated the soluble from the membrane fraction of proteins, since *Pf*aldolase was detected in the soluble fraction and *Pf*Exp1 was found in the membrane fraction. The GFP signal from the *Pf*AK2$^{\Delta 21\text{-}30}$/GFP fusion protein could be detected with an α-GFP antibody in the membrane fraction showing that this variant protein is membrane-bound, which is in accordance with the findings of the fluorescence analyses (Fig. 3.8 B). In the SLO treated samples a band corresponding to the size of the GFP chimera could be detected in both the untreated SLO pellet fraction and the SLO pellet fraction treated with Proteinase K. This indicates that *Pf*AK2$^{\Delta 21\text{-}30}$/GFP is not secreted beyond the PVM. Faint bands observed with a slightly lower molecular weight than the *Pf*AK2/GFP fusion protein possibly are degradation products. A positive control of efficient Proteinase K digestion for this particular experiment is missing, however, the efficiency of Proteinase K digestion of a fusion protein was shown for one of the variants (*Pf*AK2^{G2AC4A}/GFP in Fig. 3.7 C).

Surprisingly, a band of ~ 60 kDa was detected with an α-GFP antibody in the saponin pellet fraction treated with Proteinase K and in the untreated saponin pellet fraction. This indicates that the fusion protein was protected by the PPM. The marker proteins for each compartment – PV (marker protein: SERP) and parasite (marker protein: aldolase) – were found predominantly in the expected fractions, although a faint band of

*Pf*aldolase could also be detected in the supernatant fraction after SLO and saponin treatment, respectively. However, the signal detected in the pellet fraction was much stronger indicating that the parasites almost remained intact after SLO and saponin treatment, respectively. A faint band of *Pf*SERP could also be detected in the pellet fraction but almost disappeared after Proteinase K treatment. This indicates that SERP stuck to the membrane and was not fully removed during the washing steps after saponin treatment (Fig. 3.8 C).

Although a stable membrane anchoring was achieved with the *Pf*AK2$^{\Delta 21\text{-}30}$/GFP fusion protein in the parasitized cells as evidenced by fluorescence and hypotonic lysis, no secretion of the GFP chimera was found based on the results of the saponin treatment. From this, it can be concluded that the variant chimeric protein is stably bound to the parasite plasma membrane by the myristoyl moiety and by potential palmitoylation. However, the lack of the lysine residues seem to prevent the secretion of this protein beyond the PPM.

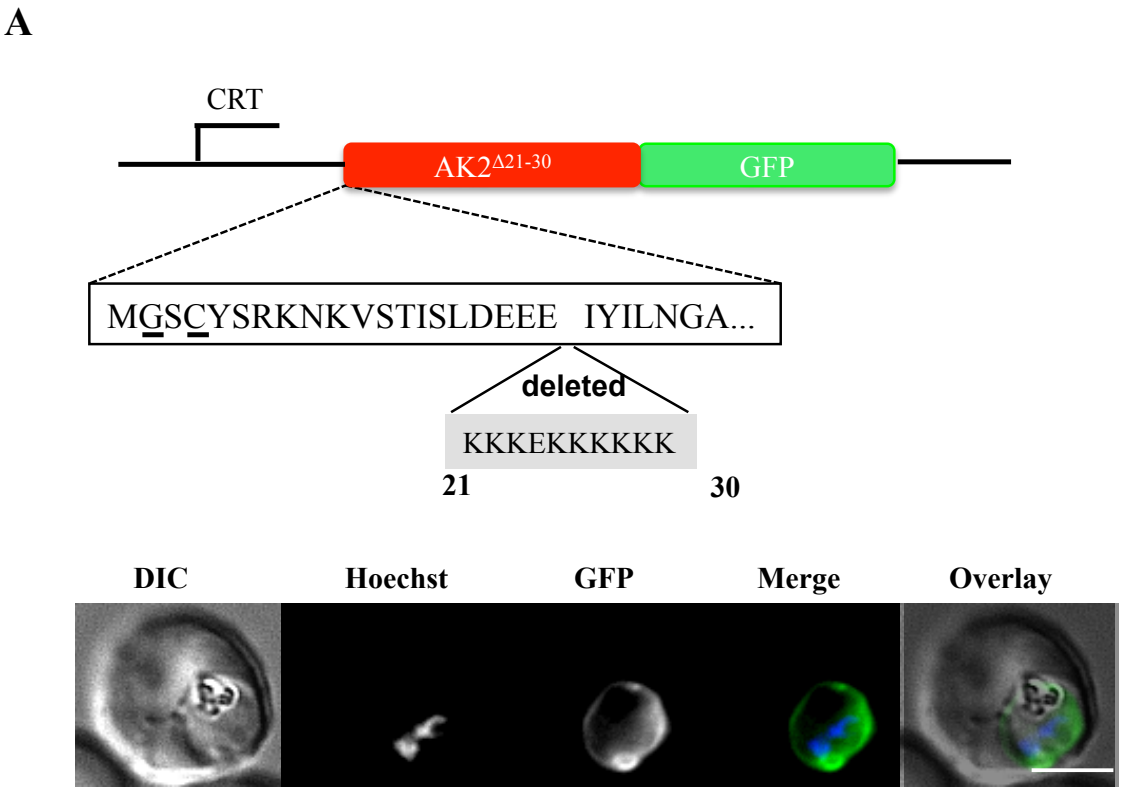

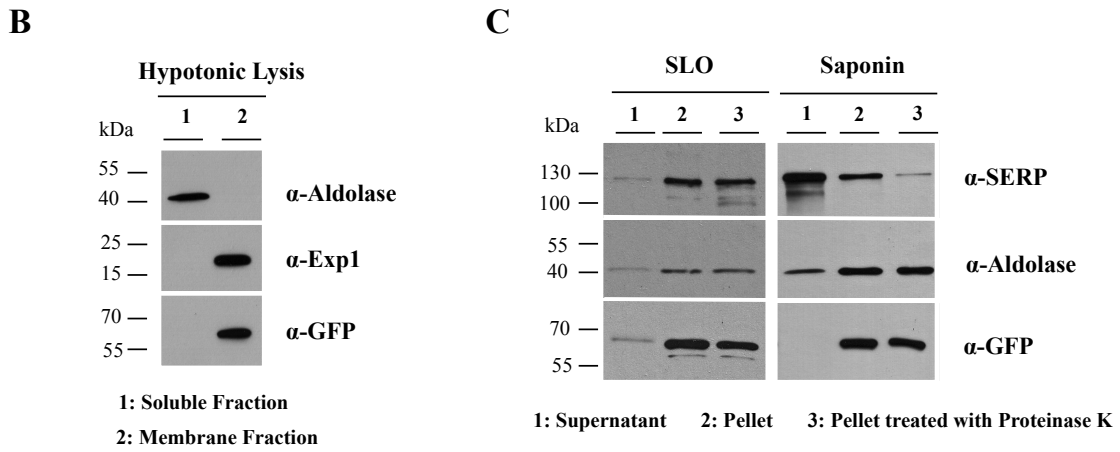

Figure 3.8 Deletion of a polybasic-cluster at the N-terminus of *Pf*AK2 prevents secretion beyond the parasite plasma membrane

(A) Live cell imaging of *Pf*AK2$^{\Delta 21\text{-}30}$/GFP parasites showed a ring-like structure of the fusion protein with a knob-like protrusion similar to the wildtype *Pf*AK2/GFP. DIC channel for high-contrast; in merge: green (GFP), blue (Hoechst = nucleus dye). Scale bar – 3 µm. (B) After hypotonic lysis of the *Pf*AK2$^{\Delta 21\text{-}30}$/GFP parasites a band of ~ 60 kDa could be detected with an α-GFP antibody in the membrane fraction. *Pf*aldolase was used as a marker protein for the soluble fraction and *Pf*Exp1 was used as a marker protein for the membrane fraction. (C) The parasites were also subjected to SLO and saponin lysis. *Pf*SERP of the PV and *Pf*aldolase of the parasite were both found predominantly in the expected fractions indicating proper SLO and saponin lysis, respectively. The band corresponding to the size of the fusion protein *Pf*AK2$^{\Delta 21\text{-}30}$/GFP was detected with an α-GFP antibody in the SLO and saponin pellet fraction (+/- Proteinase K addition). The size markers are presented in kDa.

3.2.5 Is the N-terminus of *Pf*AK2 - containing a *N*-myristoylation site, a putative palmitoylation site and a polybasic cluster of amino acids - sufficient for protein secretion?

The preceding mutagenesis analyses of *Pf*AK2 revealed that a *N*-myristoylation site is required for membrane binding and that a putative palmitoylation site likely plays a role in stabilizing the membrane anchoring of this protein. However, secretion of *Pf*AK2 beyond the PPM was not achieved when a polybasic cluster of amino acids was removed indicating its potential role in the secretion mechanism. To figure out whether or not these three motifs found at the N-terminus of *Pf*AK2 are sufficient for an atypical secretion pathway the following chimeric construct was designed: the 1-37 amino acids of the *Pf*AK2 protein sequence containing all three above mentioned motifs was fused

to GFP in the pARL2 vector and then transfected into the 3D7 *P. falciparum* parasite line. Fluorescence analyses of the respective transgenic parasite line revealed a similar phenotype to the wildtype AK2 that is a ring-like structure with a clear knob-like protrusion (Fig. 3.9 A). Furthermore, live cell imaging of the schizont-stage of the parasite showed a ring-like structure around each individual parasite (Fig. 3.9 A). Hypotonic lysis performed on this parasite line revealed that the GFP chimera was in the membrane-bound fraction. Faint bands of low molecular weight in the supernatant fraction could be degradation products of the fusion protein. *Pf*aldolase was used as a marker protein for the soluble fraction and *Pf*Exp1 was used as a marker protein for the membrane fraction. Both proteins were found in the expected fractions (Fig. 3.9 B). The SLO treated sample of the *Pf*AK2$^{1\text{-}37}$/GFP transgenic parasite line revealed a band of approximately 25 kDa detected with an α-GFP antibody corresponding to the size of the fusion protein in the untreated SLO pellet fraction and the SLO pellet fraction treated with Proteinase K. Low molecular weight bands which appear in both pellet fractions possibly are degradation products. The detection of the marker proteins with the respective antibodies revealed their localization predominantly to the respective compartments displaying an almost proper SLO lysis, thus an intact PV and parasite. However, a a small amount of SERP was also detected in the supernatant fraction after SLO treatment indicating that some parasites did lyse during the SLO procedure.

Interestingly, a GFP signal was found in the saponin pellet fraction, but not in the saponin pellet fraction treated with Proteinase K. This indicates that the protein was not protected by the PPM and was accessible to Proteinase K digestion. The marker proteins assuring proper saponin lysis were detected with an α-SERP antibody and an α-aldolase antibody in the expected fractions: SERP in the supernatant fraction, whereby the signal detected in the pellet fraction was almost removed after Proteinase K treatment. This means that SERP sticks to membranes and was not sufficiently washed off despite many washing steps. Aldolase, however, was predominantly found in the pellet fractions (sample treated with Proteinase K and untreated sample), and only a faint band was also detected by an α-aldolase antibody in the supernatant fraction (Fig. 3.9 B) indicating that some of the parasites did lyse during the procedure. These results indicates that the N-terminus of *Pf*AK2 is sufficient for secreting the GFP chimera across and to the outer face of the PPM.

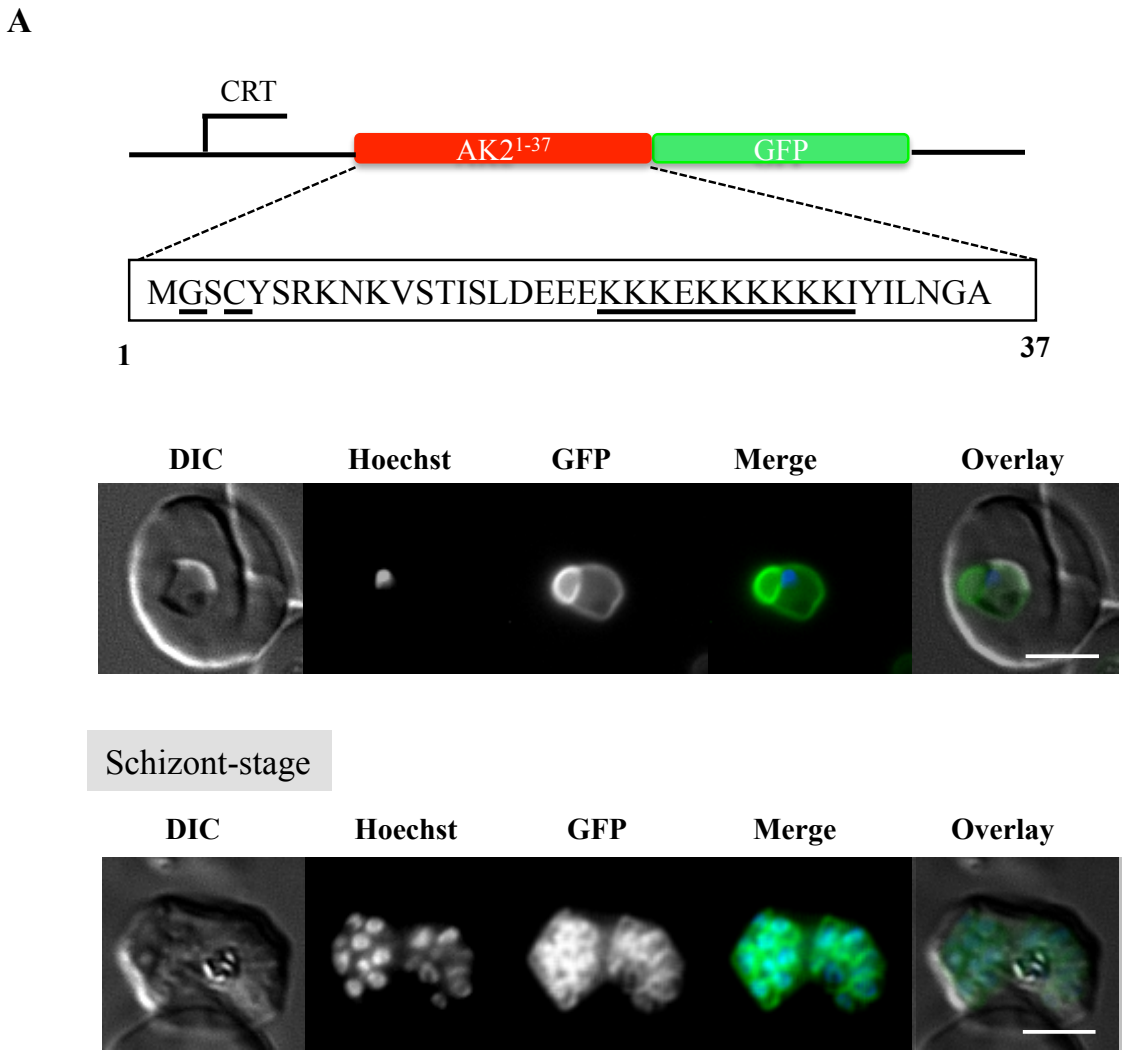
A
CRT
AK2 1-37
GFP
MGSCYSRKNKVSTISLDEEEKKKEKKKKKKIYILNGA
1
37
DIC
Hoechst
GFP
Merge
Overlay
Schizont-stage
DIC
Hoechst
GFP
Merge
Overlay
B
Hypotonic Lysis
kDa
1
2
55
40
25
15
25
15
α-Aldolase
α-Exp1
α-GFP
1: Soluble Fraction
2: Membrane Fraction
C
SLO
Saponin
kDa
1
2
3
1
2
3
130
100
55
40
25
15
α-SERP
α-Aldolase
α-GFP
1: Supernatant 2: Pellet 3: Pellet treated with Proteinase K

Figure 3.9 Live cell imaging and biochemical analyses of the *Pf*AK2$^{1-37}$/GFP transgenic parasite line
(A) The fluorescence analyses of the *Pf*AK2$^{1-37}$/GFP parasites showed a ring-like structure with a clear knob-like protrusion of the fusion protein very similar to the phenotype of the wildtype *Pf*AK2/GFP parasites. The schizont-stage of these parasites showed a clear signal of the fusion protein around each of the individual daughter cells. DIC channel for high-contrast; in merge: green (GFP), blue (Hoechst = nucleus dye). Scale bar – 3 µm. (B) Biochemial analyses showed the fusion protein to be membrane-bound, since the GFP chimera could be detected in the membrane fraction after hypotonic lysis. *Pf*aldolase was used as a marker protein for the soluble fraction and *Pf*Exp1 was used as a marker protein for the membrane fraction and were found in the expected fractions. Faint bands in the supernantant fractions might be degradation products of the fusion protein (C) The parasites were also subjected to SLO and saponin lysis. The marker protein of the PV *Pf*SERP and the marker protein of the parasite *Pf*aldolase were both found predominantly in the expected fractions after SLO lysis and saponin lysis, respectively. The band corresponding to the size of the fusion protein *Pf*AK2$^{1-37}$/GFP was detected by an α-GFP antibody in the SLO pellet fractions (+/- Proteinase K addition) and in the saponin pellet fraction. However, no band could be detected in the saponin pellet fraction treated with Proteinase K. The size markers are presented in kDa.

3.2.6 The ARF1-AK2/GFP chimera is targeted to the parasite plasma membrane

Plasmodial ARF1 contains a *N*-myristoylation site and it has been shown that it localizes to compartments of the early secretory pathway (by fluorescence analyses) and is partially membrane-bound (by hypotonic analyses). In contrast to *Pf*AK2 plasmodial ARF1 lacks a putative palmitoylation site and a polybasic cluster of amino acids at the N-terminus. To figure out whether these two motifs are sufficient for secretion of *N*-myristoylated proteins to the plasma membrane and subsequent secretion beyond the parasite plasma membrane a chimeric construct consisting partially of the N-terminus of ARF1 and partially of the N-terminus of AK2 was generated and fused to GFP in the pARL2 vector prior to transfection in the *P. falciparum* 3D7 strain. Fluorescence analyses showed a phenotype similar to the wildtype AK2 with a ring-like structure containing a 'loop' like protrusion. However, occasionally also a ring-like structure with a dot-like protrusion was also observed (Fig. 3.10 A). Live cell imaging of the schizont-stage of the *Pf*ARF1$^{1-17/+4C/-V5}$AK2^{+18-37}/GFP parasites showed a ring-like structure around the individual parasites (Fig. 3.10 B). According to the results of the hypotonic lysis a strong GFP signal corresponding to the size of the GFP chimera could be detected in the membrane fraction and a faint band could also be seen in the soluble fraction. The soluble amount of the protein indicate some degradation products or it

could result from the pool of protein which at the time-point of harvest was not anchored to the membrane. However, the majority of this protein was found membrane-bound. The marker proteins *Pf*aldolase and *Pf*Exp1 were detected in the respective fractions ensuring that proper separation of soluble and membrane fraction by hypotonic lysis had occured (Fig. 3.10 C). A proper SLO lysis on the *Pf*ARF1$^{1\text{-}17/+C4/\text{-}V5}$AK2$^{+18\text{-}37}$/GFP line was performed since the marker proteins *Pf*SERP and *Pf*aldolase were both predominantly found in the pellet fractions. However, a small amount of SERP was also found in the supernatant fraction, which indicates that some of the parasites did lyse during the procedure, however the majority of the SERP protein was detected in the pellet fractions. The protease protection assay was almost efficient since a strong *Pf*Exp1 signal could be detected in the pellet fraction and only a faint band was found in the pellet fraction treated with Proteinase K. A saponin treatment was also performed on the respective transgenic parasite strain where aldolase could be detected solely in both pellet fractions (-/+Proteinase K treatment), while *Pf*SERP was found in the supernatant and the pellet fraction. A strong GFP signal in the saponin pellet fraction without Proteinase K addition could be detected by an α-GFP antibody, but was also found present in the Proteinase K treated pellet fraction. This indicates that the *Pf*ARF1$^{1\text{-}17/+C4/\text{-}V5}$AK2$^{+18\text{-}37}$/GFP fusion protein was protected by the parasite plasma membrane and that the protein is not secreted into the PV (Fig. 3.10 D). These results initially seem contradictory, since the phenotype of *Pf*ARF1$^{1\text{-}17/+C4/\text{-}V5}$AK2$^{+18\text{-}37}$/GFP resembles that of the wildtype *Pf*AK2/GFP but the protease protection assay showed no secretion of the GFP chimera of this transgenic parasite line compared to the wildtype fusion protein. One possible explanation might be that although the additional cysteine residue and the polybasic cluster of lysine residues added to the N-terminus of plasmodial ARF1 seem to traffic the chimeric protein to the parasite plasma membrane (determined by fluorescence analyses) and leads to a stable membrane anchoring (determined by hypotonic lysis), further amino acids in the N-terminal region of *Pf*AK2 also seem to play a role in the secretion process. The N-terminal part of *Pf*ARF1 modified by the addition of the two AK2 motifs (cysteine residue at position 4 and a stretch of lysine residues with one interspersed glutamate residue) still differs by 11 amino acids from the N-terminus of *Pf*AK2.

A

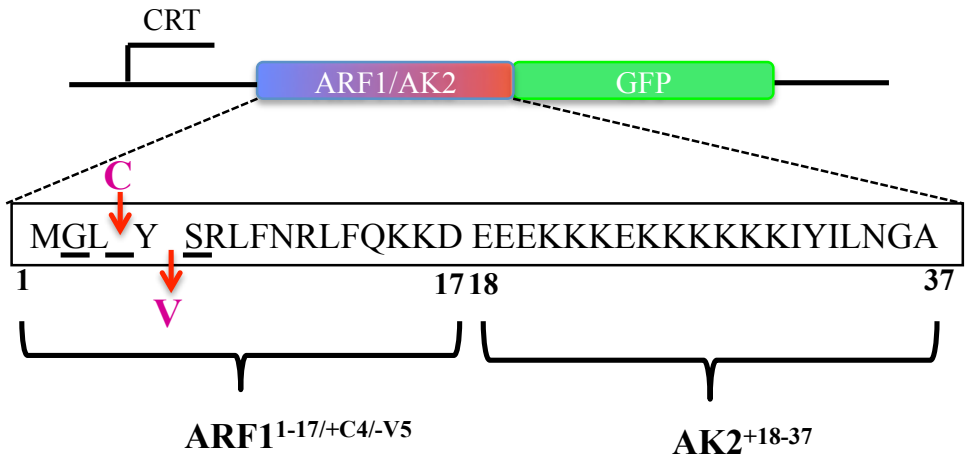

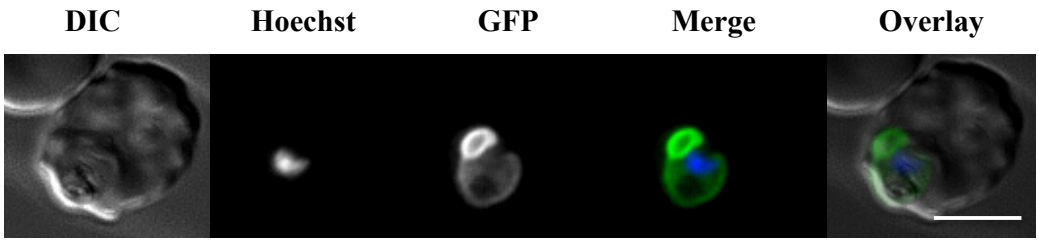

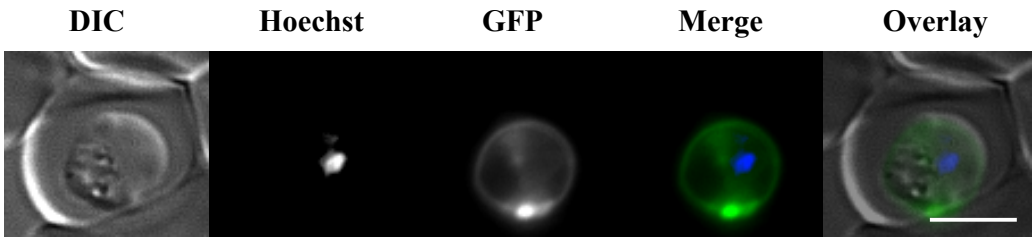

B

Schizont-stage

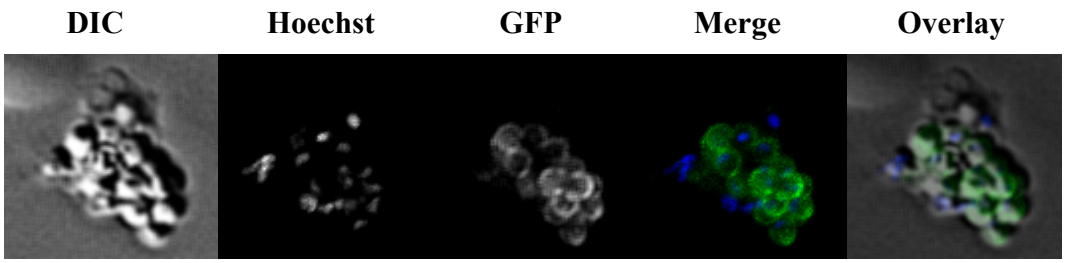

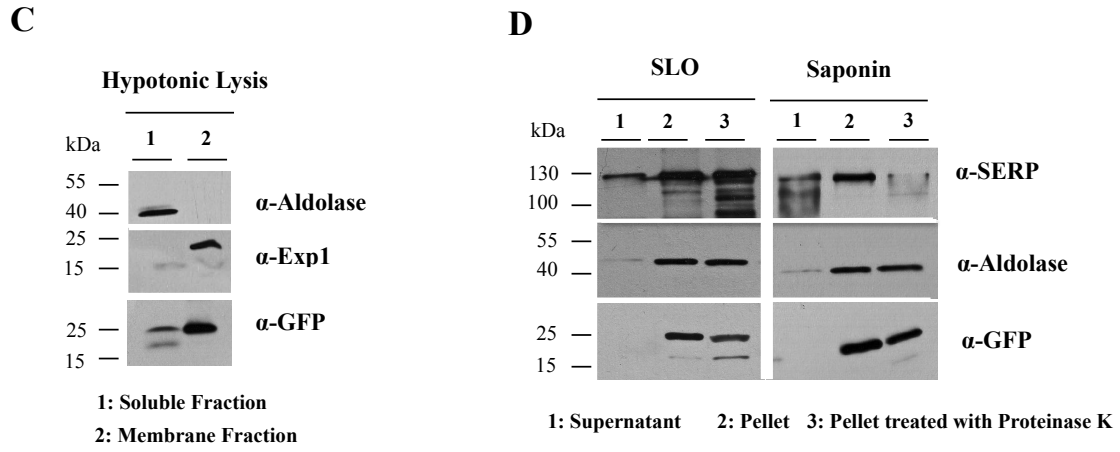

Figure 3.10 Fluorescence and biochemcial analyses of the *Pf*ARF1$^{1\text{-}17/+C4/\text{-}V5}$AK2$^{+18\text{-}37}$/GFP transgenic parasite line

(A) Live cell imaging of the *Pf*ARF1$^{1\text{-}17/+C4/\text{-}V5}$AK2$^{+18\text{-}37}$/GFP parasite line showed two slightly different phenotypes: some of the parasites show a ring-like structure with a knob-like protrusion, while others rather revealed just a ring-like structure with a prominent dot at one edge of the parasite. (B) Live cell imaging on the schizont stage of this parasite line showed a ring-like structure around each of the individual parasites separately. DIC channel for high-contrast; in merge: green (GFP), blue (Hoechst = nucleus dye). Scale bar – 3 µm. (C) Biochemial analyses showed the fusion protein to be predominantly membrane-bound, since the GFP chimera could be detected in the membrane fraction after hypotonic lysis. However, a small amount of the fusion protein was also detected in the soluble fraction and a low molecular weight band might be degradation products. *Pf*aldolase was used as a marker protein for the soluble fraction and *Pf*Exp1 was used as a marker protein for the membrane fraction. (D) The parasites were also subjected to SLO and saponin lysis. *Pf*SERP of the PV and *Pf*aldolase of the parasite were both found predominantly in the expected fractions after SLO lysis and saponin lysis, respectively. However, SERP was also detected in the SLO supernatant fraction meaning that some lysis of the parasite did take place during the SLO treatment. A small amount of aldolase was also found in the SLO and saponin supernatant fractions, respectively, which also indicates that some lysis of the parasites did occur. However, the majority of SERP and aldolase still could be detected in the expected fractions. The band corresponding to the size of the fusion protein *Pf*ARF1$^{1\text{-}17/+C4/\text{-}V5}$AK2$^{+18\text{-}37}$/GFP was detected with an α-GFP antibody in the SLO and saponin pellet fractions (+/- Proteinase K addition), respectively. The size markers are presented in kDa.

3.3 The mDHFR fusion system

Dihydrofolate reductase is a ubiquitous eukaryotic enzyme responsible for the catalysis of dihydrofolate to tetrahydrofolate in a NADP-dependent manner. It is also known to be involved in the *de novo* synthesis of certain amino acids (Schnell et al., 2004). Interestingly, Eilers and Schatz used the murine DHFR as an experimental system to analyze the folding state of a protein regarding import into mitochondria. They found that mDHFR could be stabilized in its tertiary structure in the presence of a folate analogue and was not unfolded even in the presence of chaperones (Eilers and Schatz, 1986; Salvador et al., 2000). This characteristic feature of mDHFR was used to study the translocation of mitochondrial proteins into mitochondria by fusing the pre-sequence of a mitochondrial protein to mDHFR and detecting its localization in the absence and presence of a folat analogue, respectively (Eilers and Schatz, 1986). Since then the mDHFR system has been used to study the folding state of proteins and to understand translocation mechanisms in various compartments, such as mitochondria and glycosomes (Eilers and Schatz, 1986; Häusler et al., 1996).

To analyze the folding state and the possible involvement of a translocon in the secretion process of *Pf*AK2 beyond the PPM the protein was fused to mDHFR in addition to GFP, cloned into the pARL2 vector and the plasmid was then transfected into the *P. falciparum* 3D7 line. These parasites were not negatively affected by WR treatment, since they expressed a hDHFR. Fluorescence and biochemical analyses were performed. The following fluorescence images show *Pf*AK2/mDHFR/GFP expressing parasites in the presence of WR after incubation at 37 °C for 12 hours and in the absence of WR (control). According to the microscopical pictures no differences between the WR treated and untreated parasites could be seen (Fig. 3.11 A). Both parasite cultures show a similar phenotype corresponding to the wildtype *Pf*AK2/GFP parasite strain indicating that the addition of WR does not seem to have an effect on protein localization. This observation was supported with further analyses by hypotonic and saponin lysis, SDS-PAGE, western blotting and immunodetection. Hypotonic lysis performed on the *Pf*AK2/mDHFR/GFP parasites (+/-WR) revealed a band corresponding to the size of the GFP chimera in both samples, which was detected with an α-GFP antibody solely in the membrane fraction in the WR treated and untreated parasites. The marker proteins, *Pf*aldolase and *Pf*Exp1 were detected in the respective

fractions ensuring that proper separation of soluble and membrane fraction by hypotonic lysis had occured. To analyze the subcelluar localization of the fusion protein in the WR treated and untreated parasites saponin lysis was performed. *Pf*aldolase was detected in both pellet fractions (-/+Proteinase K treatment), while *Pf*SERP was found in the supernatant and the pellet fraction indicating that proper lysis was achieved. A strong GFP signal in the saponin pellet fraction without proteinase K addition could be detected with an α-GFP antibody, but was not found in the Proteinase K treated pellet fraction of both parasite cultures: + WR and – WR. This indicates that the *Pf*AK2/mDHFR/GFP fusion protein was not protected by the parasite plasma membrane in the absence and presence, respectively, of WR.

A

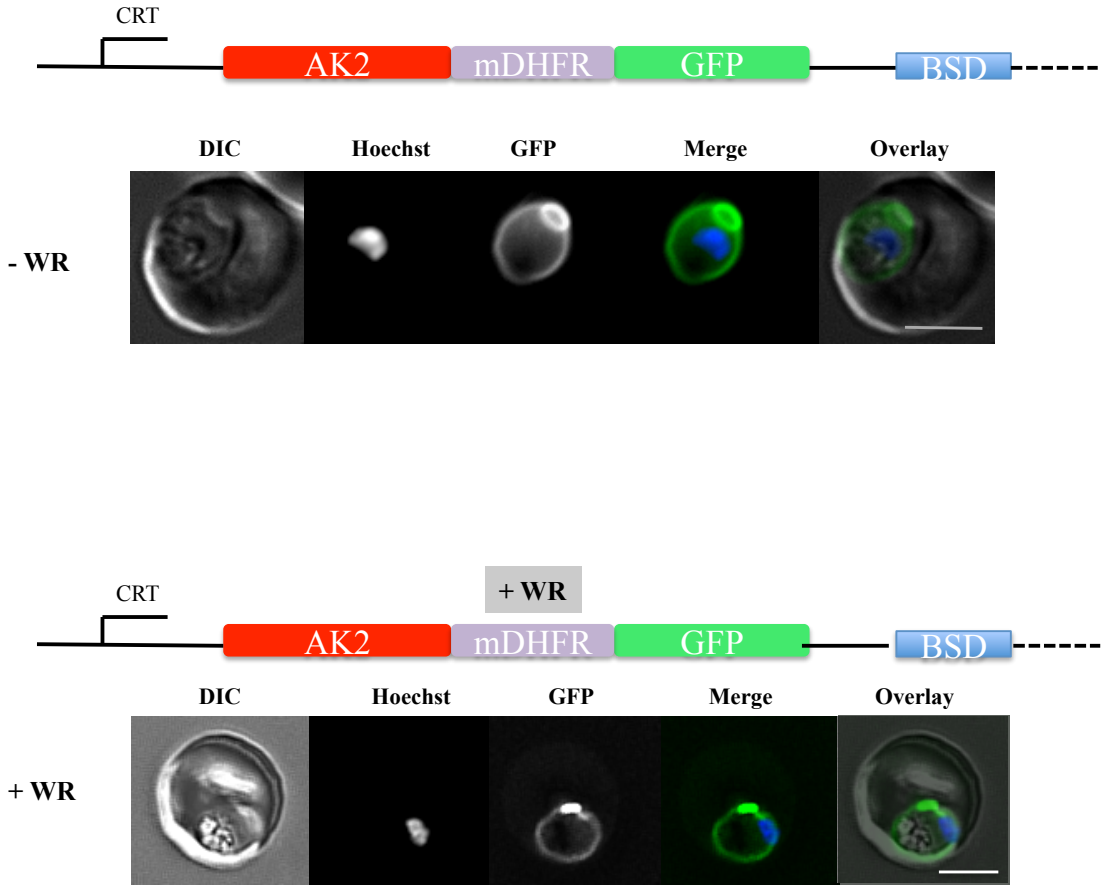

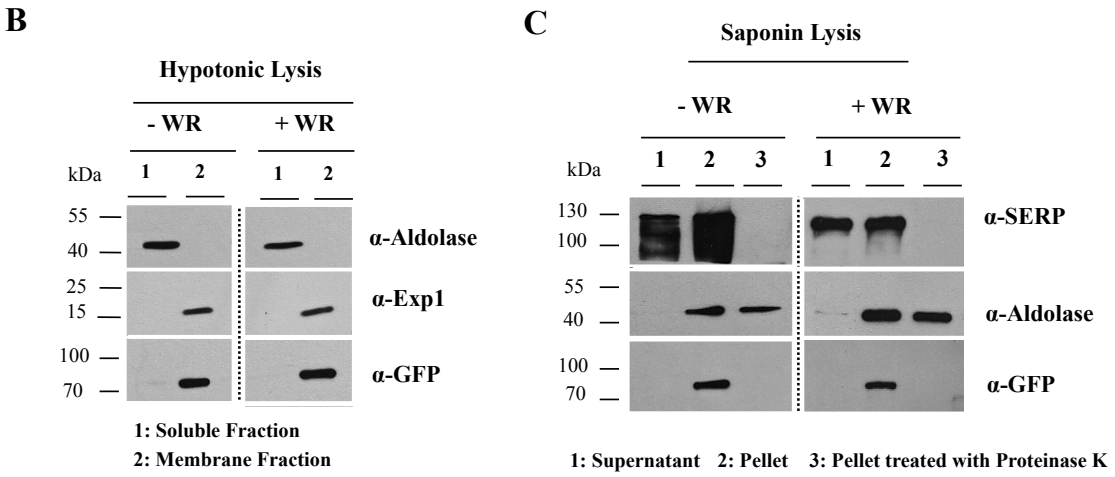

Figure 3.11 The mDHFR system was used to analyze the folding state of the *Pf*AK2 protein in the blood-stage parasite

The *Pf*AK2/mDHFR/GFP parasites were split into two cultures: one was treated with the folate analogue WR for 6 hours, while the other parasite culture was left untreated (control). After 6 hours the cells were visualized via fluorescence microscopy (A) and harvested for biochemical analyses (B). (A) Live cell imaging on the *Pf*AK2/mDHFR/GFP parasites in the absence and presence of WR, respectively, was performed showing a ring-like structure with a loop distribution of the fusion-protein. The phenotypes did not differ from each other regardless of WR addition. DIC channel for high-contrast; in merge: green (GFP), blue (Hoechst = nucleus dye). Scale bar – 3 µm. (B) After hypotonic lysis a band corresponding to the size of the fusion protein was detected in the membrane fraction with an α-GFP antibody in the WR treated and untreated sample, respectively. *Pf*aldolase was used as a marker protein for the soluble fraction and *Pf*Exp1 was used as a marker protein for the membrane fraction and both proteins were detected in the expected fractions. (C) After saponin treatment of each of the *Pf*AK2/mDHFR/GFP parasites (-/+WR) a band corresponding to AK2/mDHFR/GFP was only detected in the saponin pellet fraction, but not in the saponin pellet fraction treated with Proteinase K indicating that the fusion protein was not protected by the PPM. *Pf*SERP of the PV and *Pf*aldolase of the parasite were both found predominantly in the respective fractions after saponin lysis. The size markers are presented in kDa.

4 Discussion

Over the years more and more light has been shed on the secretion and export mechanisms for secretory proteins expressed by *P. falciparum* in infected RBCs. In particular, the existence of the PV, which separates the parasite from the host cell, calls for further secretory signals apart from the classical signal peptide. The identification of recessed hydrophobic domains instead of the classical signal peptide in many exported parasite proteins was an early hallmark of the parasite's atypical protein secretory mechanisms (Lingelbach, 1993). The discovery of the PEXEL/HT motif in exported proteins led to the *in silico* identification of approximately 250 proteins, which were predicted to be exported to the host cell (malarial 'exportome') (Marti et al., 2004; Hiller et al., 2004). The PEXEL/HT motif resembles a motif (RxLR) found in some proteins of fungal plant pathogens, which are exported to the host plant cells (Dou et al., 2008).

Some parasite proteins exported to the host cell such as for example the SBP1, REX1 and REX2 lack a classical N-terminal signal sequence and the PEXEL motif and are generally termed PEXEL negative exported proteins (PNEPs) (Saridaki et al., 2009; Haase et al., 2009). The number of PNEPs are steadily growing indicating the possible existence of pathways different from the classical secretory pathway in the malaria parasite (Heiber et al., 2013). The importance of understanding the secretory mechanisms in parasite protein trafficking is based on the fact that many of these exported proteins are key players in the pathogenesis and the adherence properties of the infected RBC.

Therefore the identification of unconventional secretory mechanisms - like found for a small number of proteins in other eukaryotic systems (see introductory section 1.4) - of the parasite and the components involved increases the chances of finding a suitable potential drug-target for the development of antimalarial drugs against the intraerythrocytic stage.

This study deals with the analysis of *P. falciparum* parasite proteins, which lack a signal peptide or a hydrophobic stretch of amino acids at the N-terminus but were found secreted beyond the parasite plasma membrane, with a focus on the *P. falciparum* adenylate kinase 2 (Ma et al., 2012). This protein was proposed to contain a *N*-myristoylation site at its N-terminus, which was hypothesized to play a role in the secretion mechanism. This hypothesis was followed up in this work by further reporter construct studies, co-localization studies and biochemical analyses and the results are discussed here.

4.1 The secretion hypothesis is based on the result of a preceding PV proteome analysis

The parasitophorous vacuole is a compartment with a very small lumen surrounding the parasite and separating it from the host cell cytosol (Lingelbach and Joiner, 1998). An experimental approach to identify proteins of the PV already revealed 27 vacuolar proteins assigning many of them via *in silico* analysis as chaperones and proteases (Nyalwidhe and Lingelbach, 2006). Since it has already been shown that many exported proteins, which contain the PEXEL motif, cross the PVM before entering the host cell it can be hypothesized that chaperones might play a role in the unfolding of these proteins (Ansorge et al., 1996; Wickham et al., 2001; Gehde et al., 2009; Nyalwidhe and Lingelbach, 2006). A second vacuolar proteome analysis of the parasite from a similar proteomic study of the PV enabled the identification of ~ 200 vacuolar proteins, from which 96 proteins were analyzed for topogenic signals. Approximately 50 % of these proteins lacked any distinguishable signal peptide. To further validate these findings two proteins from the latter group were randomly selected, fused to GFP and their subcellular localization was analyzed. Indeed both of the proteins were found secreted confirming the proteomic results, although the mode of secretion was not understood. More interestingly, 5 % of the proteins of the PV proteome analysis which lacked any known signal peptide contained instead a putative *N*-myristoylation site indicating the role of *N*-myristoylation in protein secretion. The role of *N*-myristoylation in protein secretion has already been shown for *P. falciparum* CDPK1 (Möskes et al., 2004) and the *Leishmania* HASPB (Denny et al., 2000). Both studies showed by mutational

analyses that the *N*-myristoylation site at the N-terminus of CDPK1 and HASPB, respectively, is a prerequisite for membrane attachment.

4.1.1 Does the 'Met-Gly...' motif at the N-terminus of *Pf*Prefoldin (PF3D7_0904500), *Pf*CDPK4 (PF3D7__0717500) and *Pf*ARF1 (PF3D7_1020900) affect their subcellular localization?

One of the selected proteins from the proteome analysis is the chaperone Prefoldin (PF3D7_0904500), which contains a 'Met-Gly...' motif at the N-terminus. Although the secretion of a chaperone into the PV would fit a role of being a resident PV protein due to its function in promoting protein folding, the Myristoylator prediction tool did not predict Prefoldin to be myristoylated. This prediction was confirmed experimentally: a reporter construct study showed no difference in the subcellular localization of the fusion protein between the wildtype phenotype and the variant. In the variant the putative myristoylation site was removed by exchange of the glycine residue to alanine at the N-terminus of the protein. According to the GFP fluorescence analysis it seems like Prefoldin is located in the parasite cytosol. Due to the limited resolution of epifluorescence microscopy it cannot be completely ruled out that a small portion of Prefoldin is also located beyond the parasite plasma membrane indicating a dual localization of the protein. However, according to the fluorescence analysis the majority of the protein was localized to the parasite cytosol. Hypotonic lysis and cell fractionation should be performed to examine the solubility of this protein in order to find out whether or not this protein is completely soluble or a small amount of it is also membrane-bound, which however cannot be distinguished via live-cell imaging. If a membrane-bound population would be identified this could mean that the protein is able to bind to a membrane due to a myristate moiety and further experiments could involve metabolic labelling or recombinant expression of *Pf*Prefoldin and *Pf*NMT together in bacterial cells with subsequent analysis of myristoylation. This would help to find out whether or not *Pf*Prefoldin is capable of being *N*-myristoylated. After these experiments are performed a biochemical analysis involving SLO and saponin lysis could be carried out to identify the accurate localization of *Pf*Prefoldin. Although these experiments seem to be reasonable to perform recombinant expression of *P. falciparum* proteins in

bacterial cells is often tricky and difficult to conduct due to the high AT-content of the parasite genes (Gardner et al., 2002).

*Pf*CDPK4 (PF3D7__0717500) was also hypothesized to be *N*-myristoylated based on the 'Met-Gly...' motif at the N-terminus and predicted to be myristoylated according to the myristoylator prediction tool. In addition, a second *P. falciparum* CDPK, CDPK1, was shown to be secreted across the PPM and the process involved *N*-myristoylation (Möskes et al., 2004). CDPKs are found only in plants and Alveolates (including ciliates and Apicomplexa) and protein kinases of protists generally are evolutionarily remote to human kinases, which is why they are considered to be suitable drug targets (Tsekoa et al., 2009). Although CDPK4 is predicted to be *N*-myristoylated the fluorescence analysis showed no difference in the location of the fusion protein between the wildtype phenotype and the G2A variant. This result differs from the findings for CDPK1. The CDPK1 fusion protein showed a ring-like structure around the parasite compared to the parasites expressing the *Pf*CDPK1^{G2A} protein where the signal was found to be cytosolic (Möskes et al., 2004). As found for Prefoldin, CDPK4 seem to be predominantly located in the parasite cytosol, however, the protein was only recently verified to be *N*-myristoylated (Wright et al., 2013). Therefore further analysis of the accurate subcellular localization of *Pf*CDPK4 are required.

ARF1 is another protein, which was identified in the proteome analysis of the PV and was proposed to be secreted into the PV. In contrast to *Pf*Prefoldin and *Pf*CDPK4 the fluorescence images of the *Pf*ARF1 (PF3D7_1020900) transgenic parasites clearly showed 1 to 2 dot-like structures of the fusion protein in the parasite cytosol. However, the exchange of the glycine residue to alanine at the N-terminus altered the localization of *Pf*ARF1^{G2A}/GFP in the parasite to completely soluble. Since ARF1 is ubiquitous in eukaryotic cells and highly conserved among eukaryotes (Boman and Kahn, 1995) it can be hypothesized that *Pf*ARF1 is myristoylated as well, since *N*-myristoylation is crucial for its biological role. Cook and colleagues have already shown that similar to human ARF1, *Pf*ARF1 also contains a helix at the N-terminus, which is important for the biological function of ARFs (Cook et al., 2010). Hence, it is not surprising to see an effect on the subcellular localization of the G2A variant upon removal of the

N-myristoylation site. Furthermore, the results of the hypotonic lysis revealed a membrane-bound *Pf*ARF1/GFP in the *Pf*ARF1/GFP transgenic parasites in contrast to the *Pf*ARF1^{G2A}/GFP form, where a membrane-bound pool of the fusion protein was absent. This indicates that upon myristoylation the protein is able to associate with a membrane once it is activated by GTP. GTP is hydrolyzed by ARFGAPs and in the GDP-bound form the protein is predominantly cytosolic (Stafford et al., 1996; Memon, 2004). Although the fluorescence images (dot-like structures of *Pf*ARF1/GFP within the parasite) suggest a greater membrane-bound pool of the GFP chimera in the *Pf*ARF1/GFP parasites, the cell fractionation study shows a more prominent band in the soluble fraction. This discrepancy possibly results from the low resolution of the epifluorescence microscopy in which the membrane-associated pool of the ARF1/GFP chimera compared to the soluble pool cannot be distinguished. This observation can be supported by further studies on human ARF1 where it is postulated that the Golgi membrane actually presents a platform for the exchange of GTP and GDP to take place (Franco et al., 1996; Weiss et al., 1989). This indicates that the GDP-bound form of *Pf*ARF1 is in close proximity to the GTP-bound form, but is still cytosolic. Application of for example super resolution microscopy would help to provide a better visualization of the ratio of membrane-bound to cytosolic *Pf*ARF1 in the parasite.

In summary it can be concluded that the findings of the proteome analysis contradicts to the results of the fluorescence analysis of the reporter constructs. Analyzing the PV proteome with the given methods (high-throughput-analysis) is not only a very difficult challenge but also has a high probability of identifying false-positives during the entire procedure. This is mainly because the PV has a very small lumen and contamination is likely to occur with proteins of the parasite cytosol or host cell cytosol, respectively, during the experimental procedure. However, with the given methods it cannot be completely ruled out that Prefoldin or CDPK4 do not have a dual localization. It could be that a very small amount of this protein is also present in the PV, and this is why it was detected in the proteome analysis. However, as mentioned before further analysis of the localization of these proteins are required.

Since ARF proteins are structurally and functionally well conserved in eukaryotes (Boman and Kahn, 1995) their physiological role is probably the same across all eukaryotic organisms including *P. falciparum*. That is why it is quite surprising that this protein was detected in the PV, since its function is to mediate vesicular formation and trafficking in the early secretory pathway (Boman and Kahn, 1995). Although recombinant *Pf*ARF1 was expressed in *E. coli* and characterized (Stafford et al., 1996) and its structure even determined (Cook et al., 2010) a localization study of this protein is still missing.

4.1.2 Analysis of the subcellular localization of *Pf*ARF1 in *P. falciparum*-infected RBC

According to the co-localization studies with marker proteins of the early secretory pathway *Pf*ARF1 shows partial co-localization with the ER-marker *Pf*Sec12 and the *trans*-Golgi-marker *Pf*Rab6. A strong co-localization could be observed with *Pf*Grasp1, the *cis*-Golgi marker. These results are in accordance with what is known about the role of ARF1 in vesicular trafficking in eukaryotes. The human ARF1 for instance has been shown to be mostly present at the *cis*-Golgi complex according to immunofluorescence and electronmicroscopy studies (Stearns et al., 1990). Furthermore, the protein is involved in vesicle formation and trafficking mainly from the Golgi to the ER and also between the Golgi cisternae (D'Souza-Schorey and Chavrier, 2006). Since ARF1 proteins are structurally and functionally highly conserved across eukaryotes the localization and function of this protein will possibly be similar in *P. falciparum.* This is probably the reason why the signal of the *Pf*ARF1/GFP chimera shows a strong overlap with the signal of the *Pf*GRASP1/mCherry chimera. *Pf*ARF1 also shows partial co-localization with *Pf*Rab6, a protein found to be ubiquitous across eukaryotes and involved in *trans*-Golgi trafficking (Martinez and Goud, 1998). Although the Golgi-complex in *P. falciparum* is less elaborate compared to its counterpart in higher eukaryotes a trafficking pathway via the Golgi exists within the parasite. That is why the dot-like signals of *Pf*ARF1 overlapped predominantly with *Pf*Grasp1, but also with *Pf*Rab6. In accordance with its function in retrograde trafficking a partial co-localization of *Pf*ARF1 with the ER-marker *Pf*Sec12 – a protein, which has already been shown to localize to the ER of *Plasmodium* (Lee et al., 2008) – was also detected.

As found in the study of Lee and colleagues the distribution of *Pf*Sec12/mCherry was perinuclear (Lee et al., 2008). All of these results strongly support the localization of *Pf*ARF1 to the early secretory system of the parasite rather than a PV localization. In addition, a co-localization study with the PVM marker Exp1 clearly showed no overlap of the GFP signal of *Pf*ARF1/GFP with the signal of the PVM marker *Pf*Exp1/mCherry. The biochemical analysis of the fusion protein *Pf*ARF1/GFP supports the findings of the fluorescence analysis. The results obtained from the SLO and saponin lysis analyses in combination with the protease protection assay revealed that *Pf*ARF1/GFP is not secreted beyond the parasite plasma membrane. Using a plasmodial α-ARF1 antibody against the endogenous protein also showed the presence of *Pf*ARF1 in the parasite cytosol according to the biochemical analysis. This indicates that the endogenous protein is protected by the parasite plasma membrane. Taken together, the localization of *Pf*ARF1 can be assigned exclusively to the parasite cytosol according to the fluorescence study, the co-localization study and the biochemical analysis. This finding very much fits with the general physiological role of ARF1, which is the vesicular shuttling between compartments of the secretory pathway (Boman and Kahn, 1995). The finding of *Pf*ARF1 in the PV according to the preceding proteomic approach falls into the category of a false-positive candidate.

4.2 Is *Pf*AK2 a candidate protein of an alternative secretory pathway?

Ma and colleagues created a reporter construct consisting of the adenylate kinase 2 (PF3D7_0816900) fused to GFP in a pARL vector and transfected the plasmid into 3D7 parasites. The fluorescence image clearly showed a ring-like structure with 'loops' of the fusion protein. They proposed that this protein is localized to the PV (Ma et al., 2012). However, the AK2 protein lacks a signal peptide or any other known signal motif typical for the parasite which would drive secretion into the PV. Interestingly, earlier studies had already revealed AK2 to be a substrate of the *Pf*NMT indicating that this protein is myristoylated (Rahlfs et al., 2009). To find out whether *N*-myristolyation plays a role in secretion they generated another reporter construct, where the *N*-myristoylation site was removed (*Pf*AK2^{G2A}/GFP). The plasmid was transfected into

3D7 parasites and in these transgenic parasites the subcellular localization of the GFP chimera was clearly altered to being cytosolic and different from the ring-like structure seen for the fusion protein *Pf*AK2/GFP. Further analysis of the *Pf*AK2/GFP parasites revealed co-localization with Exp1, the integral membrane protein of the PVM, but not with the soluble serine rich protein (SERP) located in the PV. From this Ma and colleagues concluded that *Pf*AK2 is localized to the PVM and with the membrane stain Bodipy-TR-ceramide the 'loops' were identified as membranous structures (Ma et al., 2012). Their hypothesis was that this protein is secreted into the PV driven by *N*-myristoylation similar to the findings of *Pf*CDPK1 (Möskes et al., 2004). Möskes and colleagues showed that *Pf*CDPK1 was myristoylated *in vivo* and proposed its localization to the PV according to reporter construct and immunoelectron microscopy studies. In a further mutational analysis the N-terminal glycine residue was replaced with valin and the fusion protein CDPK1^{VG2}/GFP relocated entirely to the parasite cytosol indicating the role of *N*-myristoylation in targeting and localization of this protein to the parasite plasma membrane (Möskes et al., 2004). Apart from *P. falciparum* CDPK1 the *Leishmania* HASPB is another candidate protein where it was shown via reporter construct studies that a myristate moiety at the N-terminus of this protein is a prerequisite for membrane anchoring (Denny et al., 2000).

To further investigate the results of the *P. falciparum* AK2 protein the current study focused on biochemical analyses of both transgenic parasite lines obtained from Ma and colleagues. The biochemical analyses consisting of SLO and saponin lysis of the parasitized cells combined with a protease protection assay showed that the *Pf*AK2/GFP protein was protected by the PVM, but not by the PPM after Proteinase K treatment. This indicates that the fusion protein is located either at the outer leaflet of the parasite plasma membrane or at the inner leaflet of the PVM. However, to date, no method is known to distinguish between these two locations. The biochemical analysis further revealed that the *Pf*AK2^{G2A}/GFP protein was not secreted to the outer face of the PPM, which is consistent with the findings of Ma and colleagues. This indicates that the *N*-myristoylation site affects the subcellular localization of the AK2/GFP protein similar to the finding for CDPK1 and the *Leishmania* HASPB. Further, the removal of the *N*-myristoylation site prevents membrane attachment and leads to a cytosolic localization of the AK2 protein.

In a next step Ma and colleagues performed a multiple sequence alignment (MSA) of *Pf*AK2 with *Pf*adenylate kinase 1, adenylate kinase-like proteins of *P. falciparum* and adenylate kinases of other species. They showed that the N-terminus of *Pf*AK2 clearly differed from the N-termini of the other adenylate kinases (Ma et al., 2012). The N-terminus of *Pf*AK2 contained in addition to the glycine residue at the N-terminus, which is a requirement for *N*-myristoylation, also a cysteine residue at the 4th position and a stretch or polybasic cluster of lysine residues. In the current study the MSA was extended by including putative adenylate kinases of other *Plasmodium* species, a verified adenylate kinase 2 of *P. cynomolgi* and adenylate kinase 2 of two other parasitic protozoa: *Babesia bovis* and *Leishmania infantum*. The sequence alignment showed that only *Pf*AK2 differs in the N-terminus from the N-termini of the other adenylate kinase 2 proteins. *Pf*AK2 is the only protein, which contains the aforementioned motifs in contrast to the AK2 proteins of the other species, which were analyzed in the MSA.

To further investigate the additional motifs of the *Pf*AK2 protein of *P. falciparum* different variants of the *Pf*AK2 protein were generated. The role of the putative palmitoylation site and the polybasic cluster of lysine residues at the N-terminus of *Pf*AK2 were analyzed. Protein, which are known to be N-myristoylated are usually also dually acylated proteins meaning that they are modified at their N-terminus with myristate and palmitate. For example members of the Src family contain this 'two-signal model' which enables membrane binding (Resh, 1999). Analysis of the *Pf*AK2^{C4A}/GFP protein showed a different signal to the *Pf*AK2/GFP fusion protein indicating that the cysteine residue close to the N-terminus affects the subcellular localization of this protein. This was further supported by biochemical analyses. The fusion protein was found to be soluble and membrane-bound and compared to the *Pf*AK2/GFP fusion protein was not translocated across the PPM. The C4A variant was protected within the parasite according to the SLO and saponin analyses in combination with the Proteinase K treatment. The equal amount of membrane-bound to soluble protein indicates that although the *N*-myristoylation site is present and membrane-anchoring can take place, the low binding energy of the myristate to the phospholipids of its target membrane is not sufficient to achieve a stable membrane anchoring (Peitzsch and McLaughlin, 1993). However, protein palmitoylation in addition to *N*-myristoylation is known to lead

to a stable membrane anchoring of a myristoylated protein due to the increased hydrophobicity of the protein (Resh, 2006). That is possibly why an equal amount of soluble to membrane-bound fraction of the *Pf*AK2^{C4A}/GFP chimera was found in the cell fractionation study. A similar phenotype to the *Pf*AK2^{C4A}/GFP chimera was also found with the *Pf*CDPK1^{AC3}/GFP (putative palmitoylation site was removed) chimera in the studies of Möskes and colleagues and with a palmitoylation-deficient mutant of the *Leishmania* HASPB (Denny et al., 2000). In the studies of Denny and colleagues they observed some association of the palmitoylation-deficient mutant - which was still able to be myristoylated - with the outer leaflet of the Golgi, why they proposed a model where HASPB is co-translationally myristoylated in the cytoplasm, then trafficked to the Golgi membrane to be palmitoylated by a putative palmitoyltransferase at the outer leaflet of the Golgi before being targeted and translocated across the plasma membrane (Denny et al., 2000).

Another variant of this protein was generated where both the *N*-myristoylation site and the palmitoylation site were removed: *Pf*AK2^{G2AC4A}/GFP. Biochemical analysis revealed no membrane-bound fraction of this protein and no secretion to the outer face of the PPM due to the lack of the potential dual acylation sites. Similar to the study of the *Pf*CDPK1 by Möskes and colleagues the studies on these three variant proteins - *Pf*AK2^{G2A}/GFP (Ma et al., 2012), *Pf*AK2^{C4A}/GFP and *Pf*AK2^{G2AC4A}/GFP –showed that a *N*-myristoylation site and the putative palmitoylation site are required for membrane-targeting, correct localization to the parasite plasma membrane and stable membrane-anchoring. The analyses of these proteins strongly suggests that stable membrane anchoring can only take place when the protein is dually acylated as for example known for members of the Src family (Resh, 1999). Intriguingly, a third motif present at the N-terminus of the AK2 protein – a polybasic cluster of lysine residues – also affects the subcellular localization of the fusion protein. Although the phenotype of the *Pf*AK2$^{\Delta 21-30}$/GFP transgenic parasites is similar to the wildtype phenotype of AK2 according to live cell imaging, the biochemical analysis revealed no secretion of this protein beyond the PPM. A polybasic cluster in proximity to a *N*-myristoylation site seems to increase the membrane anchoring due to the electrostatic interactions between the positively charged amino acids of the protein and the phospholipids of the parasite plasma

membrane (Resh, 2006). A similar feature was observed for MARCKS protein which uses a cluster of basic residues at the N-terminus in close proximity to the *N*-myristoylation site to achieve stable membrane anchoring (Resh, 1999).

A removal of the lysine residue stretch at the N-terminus still enabled a stable membrane-anchoring by myristate and possibly palmitate of the protein. This is consistent with the result of the hypotonic lysis of the parasitized cells, where only a membrane-bound fraction of this protein was detected. The absence of the lysine residues at the N-terminus prevents secretion of the protein beyond the PPM indicating a possible role of the cluster of basic amino acids in the translocation process of *Pf*AK2 across the PPM. This observation corresponds to the findings with the CDPK1 protein, which also contains these three membrane anchoring features, which were shown to be required for membrane binding and membrane anchoring (Möskes et al., 2004).

To further analyze these findings the N-terminus of the AK2 protein (residues 1 to 37 amino acids) was fused to GFP, the plasmid was transfected into 3D7 parasites and the subcellular localization of this fusion protein was analyzed. The *Pf*AK2$^{1-37}$/GFP fusion protein showed a similar phenotype to *Pf*AK2/GFP when visualized by live cell imaging. Furthermore, observation of the late-stage parasites showed that the signal of the fusion protein was found around each of the merozoites. Biochemical analysis also revealed a secretion of this protein to the outer face of the PPM, but not beyond the PVM. These results are similar to the findings for the *Pf*AK2/GFP fusion protein by Ma and colleagues. This indicates that the N-terminus of the AK2 protein is sufficient for secretion of this protein beyond the PPM. These findings are similar to what is known about the *Leishmania* HASPB. Dual acylation of this protein has been shown to be important for plasma membrane targeting and plasma membrane anchoring. Furthermore, the N-terminus of this protein (residues 1 to 18 amino acids) fused to GFP was sufficient for translocation across the plasma membrane (Denny et al., 2000). These results are similar to the findings with *Pf*AK2/GFP. This indicates that the *P. falciparum* AK2 protein belongs to the small number of proteins, which is secreted by an alternative secretory pathway involving dual acylation to the ER/Golgi route.

4.2.1 How much of the N-terminus of *Pf*AK2 is required for targeting other myristoylated proteins like *Pf*ARF1 to the PPM and beyond?

Compared to *Pf*AK2 *N*-myristoylated *Pf*ARF1 localizes to the Golgi-membrane. The targeting mechanisms of myristoylated proteins to a specific membrane, however, is not understood (Murray et al., 1998). Interestingly, the study of the *Pf*ARF1$^{1\text{-}17/+C4/\text{-}V5}$AK2$^{+18\text{-}37}$/GFP transgenic parasites – the fusion protein consists of the N-terminus of ARF with incorporation of a putative palmitoylation site and a polybasic cluster of lysine residues - showed a similar phenotype to the wildtype fusion protein when visualized by epifluorescence microscopy. Also a predominant membrane-bound fraction was found as a result of the hypotonic lysis indicating that this protein is strongly anchored to the PPM. However, the biochemical analysis did not show any secretion of this protein to the outer face of the PPM. The schizont-stage also showed that the fusion protein localizes individually around the newly formed individual merozoites. This would indicate that the protein is indeed targeted to the parasite plasma membrane. A stable membrane-anchoring is also achieved, however, the additional putative palmitoylation site and the polybasic cluster of amino acids are not sufficient to secrete this protein beyond the PPM. These findings suggest that the PPM targeting and membrane anchoring are driven by the three motifs found at the N-terminus of *Pf*AK2: a *N*-myristoylation site, a putative palmitoylation site and a polybasic cluster of lysine residues. However, the N-terminus of the modified *Pf*ARF1 still differs in approximately 11 amino acid positions from the AK2 N-terminus. This indicates that also other amino acids at the N-terminus of *Pf*AK2 are possibly involved in the secretion process for the AK2 protein. Further variants of AK2 should be generated to find out which other amino acids apart from the already identified crucial motifs are required and involved in the secretion of this protein. Furthermore, it should be kept in mind that only the N-terminus of *Pf*ARF1 was analyzed and modified. Whether or not the full-length *Pf*ARF1 would show the same phenotype (PPM targeting instead of Golgi-membrane localization) upon N-terminal modification is not clear according to these results. Another experiment with the full-length ARF1 and the additional AK2 motifs should be performed to see whether or not the results will be consistent.

More interestingly, two slightly different phenotypes could be observed for the ARF1$^{1\text{-}17/+C4/\text{-}V5}$AK2$^{+18\text{-}37}$/GFP transgenic parasites. The fluorescence signal of the fusion

protein showed a clear 'loop' structure in some of the parasites similar to the findings with *Pf*AK2/GFP. On the other hand, the signals of the fusion protein in some parasites was a less prominent 'dot' like structure instead of the 'loop'. Since it is not known what causes the 'loops' it is also is not clear why parasites expressing the same fusion protein can show slightly different fluorescence patterns. To analyze the 'loop' structure, the ratio between these two phenotypes should first be determined by live cell imaging.

4.2.2 An analysis about the folding state of *Pf*AK2 as it translocates from the parasite cytosol into the PV

Eilers and Schatz applied the mDHFR system to investigate the translocation state of mitochondrial proteins. They could show that mDHFR fused to a mitochondrial presequence must be kept in a 'translocation-competent' state (unfolded) before crossing the membrane (Eilers and Schatz, 1986). Gehde and colleagues applied the mDHFR system for the first time in the investigation of cytosolic *P. falciparum* proteins, which were known to be trafficked to the host cell. They succeeded in showing that the GFP chimera consisting of the N-terminus of the soluble protein GBP130 - which is known to enter the host cell – and mDHFR and GFP have to be unfolded prior to entering the host cell. Therefore they postulated that soluble proteins destined to be secreted beyond the PVM possibly require a translocon for translocation across the PVM (Gehde et al., 2009). Indeed, an ATP-driven translocon, the so-called PTEX machinery, was found in the PVM and was proposed to be a possible candidate of protein translocation for soluble proteins (de Koning-Ward et al., 2009; Bullen et al., 2012).

The mDHFR system was applied to analyze the folding state of the *Pf*AK2 protein and the possible involvement of a translocon before the protein is secreted from the cytoplasmic site of the PPM into the PV. Fluorescence analysis showed no difference between the phenotype of the fusion protein of *Pf*AK2/mDHFR/GFP transgenic parasites in the presence and absence of WR. A ring-like structure with a knob-like protrusion was observed. Since SLO lysis of the *Pf*AK2/GFP wildtype parasites had already shown that the protein was not secreted beyond the PVM, this time the analysis was performed only with saponin treated lysates. It was investigated whether or not the protein is unfolded when it passes the PPM in order to enter the PV, which could mean that the secretion mechanism involves a translocon located in the PPM. Biochemical

analysis could show that the addition of the folate analogue WR, which is known to stabilize the tertiarty structure of mDHFR had no effect on the localization of the fusion protein. As found in the biochemical analysis of the *Pf*AK2/GFP parasites, the *Pf*AK2/GFP fusion protein was secreted beyond the PPM. This indicates that the protein did translocate across the PPM in a possibly folded configuration and was degraded upon exposure to Proteinase K. Although a positive control in this particular experiment is missing - to verify that WR indeed was able to bind to mDHFR and stabilize it - this experiment was performed in a way consistent with the protocol of prior mDHFR experiments with parasite proteins. Furthermore, the mDHFR system was usually applied to cytosolic proteins (Eilers and Schatz, 1986; Salvador et al., 2000) and not to membrane-attached proteins. The possible strong parasite plasma membrane attachment via the dual acylation sites and the polybasic cluster of lysine residues of the *Pf*AK2 protein would rather suggest a different mode of translocation.

4.2.3 A model for *Pf*AK2 protein anchoring to the PPM and secretion

The study of Ma and colleagues already showed that *N*-myristoylation plays a key role in the secretion process of *Pf*AK2 into the PV (Ma et al., 2012). The current study has further confirmed these findings by creating and analyzing different variants of the AK2 protein. Thereby, a putative palmitoylation site and a polybasic cluster of amino acids were also found to be involved in the secretion process of this protein. However, a gene expression profile of the AK2 protein (PF3D7_0816900) during *P. falciparum*'s life-cycle based on a high-density oligonucleotide array showed that this protein is not highly expressed during the erythrocytic asexual stages (Le Roch et al., 2003). Instead, a low gene expression was proposed in the first sexual stages of the parasite, the gametocytes, based on the transcriptome data (using a microarray approach) (Young et al., 2005) (see appendix).

Although these high-throughput genomic and proteomic screening approaches enable a better understanding of gene and protein expression patterns in the different stages of *P. falciparum's* life-cycle, incorrect findings cannot be excluded. This could mean that a gene is incorrectly given a low expression value, although it might be expressed in the asexual erythrocytic stage. In case of *Pf*AK2 (PF3D7_0816900) a further approach consisting of designing an antibody against *Pf*AK2 would give a clue about whether or

not this protein is expressed in the asexual erythrocytic stages. Nevertheless, the findings of the reporter construct study of the AK2 protein still mirrors an atypical secretory signal of a secretory pathway involving *N*-myristoylation similar to the findings of *Pf*CDPK1 (Möskes et al., 2004) and *Leishmania* HASPB (Denny et al., 2000). In the following the results of the experiments with *Pf*AK2 and its variant forms are summarized in an illustration as a model for a potential novel secretory pathway in *P. falciparum*:

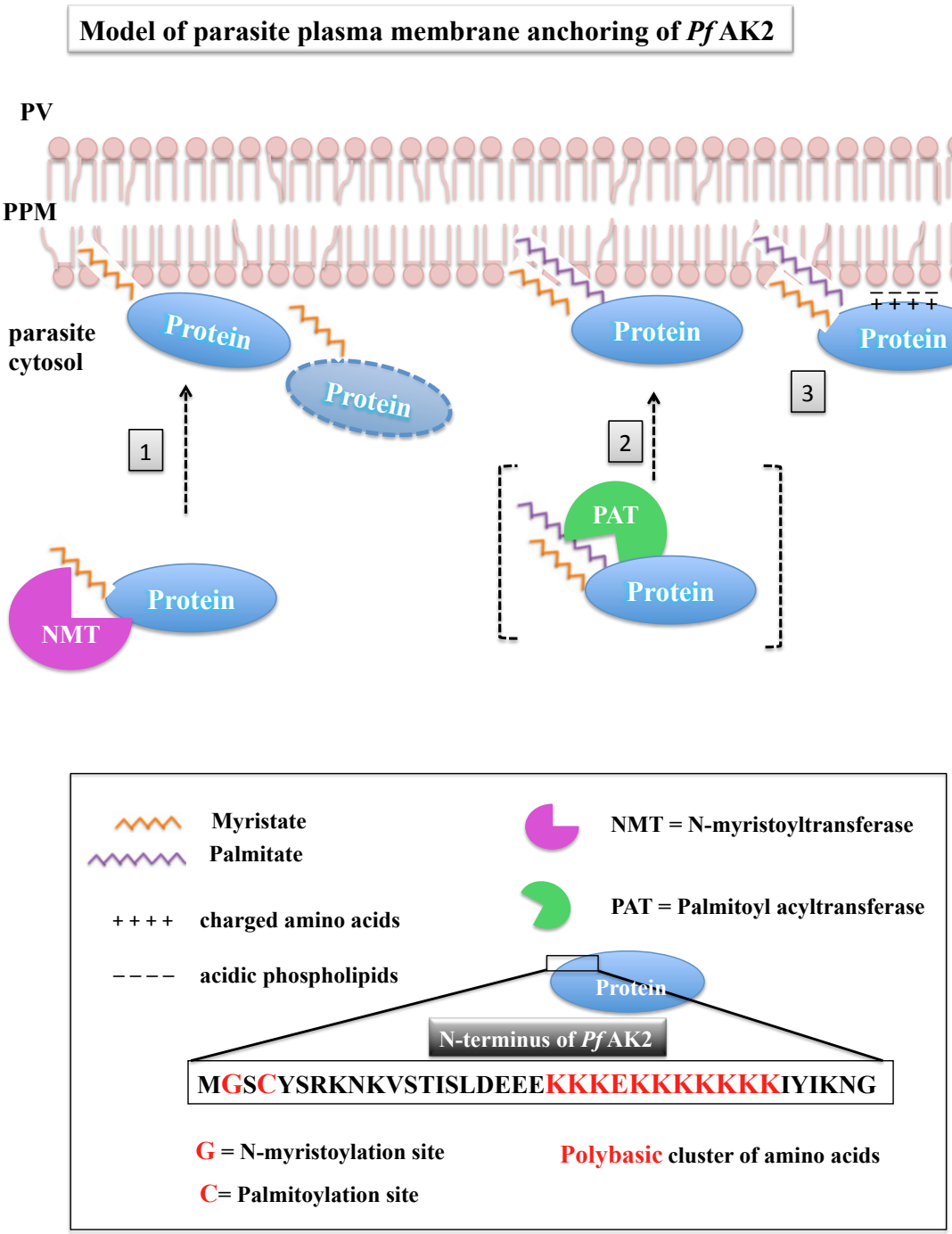

Figure 4.1 A hypothetical model how *Pf*AK2 is anchored to the parasite plasma membrane
Initially the 14-carbon saturated fatty acid (myristate) is irreversibly attached to the glycine residue at the second position of the N-terminus of *Pf*AK2 by the *N*-myristoyltransferase (NMT). (1) Due to the low binding energy of myristate the protein ist not stably anchored and can dissociate from the parasite plasma membrane. 2) To achieve stable membrane anchoring a 16-carbon saturated fatty acid (palmitate) is attached to a cysteine residue of a putative palmitoylation site at the N-terminus of *Pf*AK2 via palmitoyl transferase (PAT). However, palmitoylation can also occur in the absence of PAT if palmitoyl-CoA is present (alternative palmitoylation mechanism), which is why this step is shown in brackets. 3) In the case of *Pf*AK2 a third motif – a polybasic cluster of lysine residues at the N-terminus – is also involved in plasma membrane anchoring and subsequent translocation across the PPM.

4.3 Concluding remarks on the analysis of *Pf*AK2 as a candidate protein of an alternative secretory pathway in *P. falciparum*

The initial experiments with *Pf*AK2 were performed by Ma and colleagues who proposed a PVM localization of this fusion protein (shown by co-localization study with *Pf*Exp1). The biochemical approach of the current study suggests a localization either at the outer leaflet of the PPM or the inner leaflet of the PVM. The generation and subsequent analysis of variants of AK2 revealed that the N-terminus of this protein is important for parasite plasma membrane anchoring and subsequent secretion. Interestingly, the phenotypes of the fusion proteins of the *Pf*AK2$^{\Delta 21\text{-}30}$/GFP parasites and the *Pf*ARF1$^{1\text{-}17/+C4/\text{-}V5}$AK2$^{+18\text{-}37}$/GFP parasites were similar to the phenotype of the fusion protein of the *Pf*AK2/GFP parasites (Ma et al., 2012) when visualized by epifluorescence microscopy. All showed a ring-like structure with a clearly visible knob-like protrusion. However, they differed in their subcellular localization according to biochemical analyses: the *Pf*AK2/GFP fusion protein is located beyond the PPM, while the variant proteins were located at the cytoplasmic site of the PPM. These findings indicate that the *N*-myristoylation site, the putative palmitoylation site and the cluster of basic residues are involved in plasma membrane targeting, anchoring and subsequent translocation across the PPM. However further amino acids at the N-terminal region between the palmitoylation site and the row of basic amino acids also seem to be involved in the secretion process of this protein.

A difference in the localization between PPM and PVM via conventional fluorescence microscopy cannot be made due to the limited resolution. Electronmicroscopy or super resolution microscopy techniques might help further investigation of the proposed PVM localization of the fusion protein by Ma and colleagues similar to the proposal of this study which is localization of *Pf*AK2 at the outer leaflet of the PPM or at the inner leaflet of the PVM.

The knob-like protrusion which was observed in many of the cells expressing the variant proteins still remain an enigma. These 'extensions' have not been seen before with other parasite proteins fused to GFP. However, it is not known whether or not this observation is related to GFP expression, the expression of AK2 itself, or is a result of parasite plasma membrane anchoring via dual acylation of the fusion protein.

One more important aspect regarding the biochemical analysis should be taken into consideration. The biochemical approach involving saponin treatment of the parasite is technically challenging. Although the SLO and saponin concentrations used for each of the experiment was not altered a proper lysis after SLO and saponin treatment, respectively, was most of the time not achieved. To achieve lysis of the PVM and to prevent lysis of the PPM at the same time required extensive titration of the saponin concentration to find out the right concentration to disintegrate the RBCM and the PVM and to avoid rupture of the PPM at the same time. Even then, a proper lysis without lysis of some parasites during the procedure was not achieved. As can be seen from the results minimal amounts of the marker protein aldolase, the parasite internal control, was frequently detected in the supernatant fraction after SLO and saponin treatment, respectively, indicating that during the procedure some parasites were lysed. However, the majority of aldolase could still be detected in the SLO and saponin pellet fractions indicating that most of the parasites remained intact. The marker protein of the PV - the soluble serine rich protein (SERP) - was always detected after saponin treatment not only in the supernatant fraction as expected, but also in the pellet fraction. This indicates that this protein sticks to membranes and is difficult to remove despite many washing steps during sample preparation. This explanation is likely to be valid, since Proteinase K treatment of the saponin pellet fraction led to the removal of SERP in the

saponin pellet fraction. The difficulty to achieve proper lysis is a general issue since the parasite internal control aldolase and the soluble PV protein SERP are never found completely in the expected fractions as could be shown for different localization studies of *P. falciparum* proteins involving these two lysis methods (Ansorge et al., 1997; Spielmann et al., 2006; Heiber et al., 2013). The efficacy of Proteinase K digestion in the SLO and saponin pellet fractions was performed on one of the variant form, the *Pf*AK2^{G2AC4A}/GFP transgenic parasites. Therefore the parasite plasma membrane was permeabilized with Triton X 100 with and without Proteinase K addition. In the detergent permeabilized parasites Proteinase K was able to degrade the fusion protein indicating its efficiency to degrade the fusion protein. However, a weak-point of all of these results might be the lack of positive control for all of the experiments performed individually, although the efficiency of Proteinase K digestion of an acylated protein (*Pf*AK2) and a non-acylated protein (*Pf*AK2^{G2AC4A}/GFP) was shown. An indirect evidence that Proteinase K treatment worked for each of the experiment is that in saponin treated cells the SERP protein disappeared from the pellet fraction (possibly sticking to membranes) compared to the saponin pellet fraction treated with Proteinase K indicating the efficiency of Proteinase K digestion.
Although the majority of the control proteins in each of the experiment was detected in the expected fractions after SLO and saponin treatment, respectively, indicating that the majority of the parasites analyzed remained intact during SLO and saponin treatment the results should still be carefully interpreted, especially because they mostly represent 1-2 experiments where the SLO and saponin treatment almost worked properly meaning that a statistical significant result is missing.

Most surprising is the fact that the N-terminus of *Pf*AK2 differs from the N-terminus of the other adenylate kinases and that it was found localized beyond the PPM. These findings are surprising, especially because adenylate kinase 2 is usually found located at the intermembrane space of mitochondria of various tissue cells as for the human AK2, which is known to play an important role in the energy metabolism (Dzeja and Terzic, 2009). It is difficult to speculate on why the parasite expresses the AK2 protein with a clearly different N-terminus compared to other AK2 proteins and why the N-terminus drives this protein into the PV. Nevertheless, the results of analysis for *Pf*AK2 reveals

*Pf*AK2 as a further candidate protein using a different pathway to the conventional ER/Golgi route with a similar mechanism found for *Pf*CDPK1 (Möskes et al., 2004) and *Leishmania* HASPB (Denny et al., 2000).

A screening of the *P. falciparum* genome for proteins with a predicted *N*-myristoylation site, a putative palmitoylation site and a large number of basic amino acids of the first 50 amino acids of the N-terminus revealed quite a few potential proteins as candidates of this putative secretory pathway. In the following five of these proteins (including *Pf*AK2 and *Pf*CDPK1), which were found in the screening are listed (a list with further candidate proteins can be found in the appendix). It would be interesting to perform similar experiments with these candidate proteins in a future study.

Table 4.1 Potential proteins of the *P. falciparum* genome as candidates of a novel secretory pathway

	N-Myristoy-lation	Palmitoy-lation	Basic residues	Acidic residues	Blood stage	Sexual stage
***Pf* adenylate kinase 2** (PF3D7_0816900)	✓	✓	17	7	----	✓
***Pf* calpain** (PF3D7_0502300)	✓	✓	15	11	----	✓
***Pf* protein phosphatase, putative** (PF3D7_0810300)	✓	✓	14	11	✓	✓
***Pf* CDPK1** (PF3D7_0217500)	✓	✓	13	5	✓	✓
***Pf* cAMP-dependent protein kinase** (PF3D7_1223100)	✓	✓	12	13	✓	✓

5 Outlook

Interestingly, a large number of atypical signal sequences and secretion mechanisms of parasite proteins were discovered as a result of the analyses of parasite protein secretion to the parasite's different compartments (Lingelbach, 1993; Marti et al., 2004; Hiller et al., 2004). However, the secretion mechanisms of many parasite proteins into the PV or even to destinations in the host cell are still not understood.

In this study two *N*-myristoylated proteins were analyzed as candidate proteins of an alternative secretory pathway: the *Pf*ADP-ribosylation factor 1 and the *Pf*adenylate kinase 2. While the results strongly support the localization of *Pf*ARF1 to compartments of the early secretory pathway, *Pf*AK2 was found to be targeted to the plasma membrane of the parasite (PPM) and subsequently translocated across the PPM. Further analyses of the *Pf*AK2 revealed the importance of a *N*-myristoylation site, a putative palmitoylation site and a polybasic cluster of lysine residues at its N-terminus for PPM targeting, membrane anchoring and subsequent secretion. The N-terminus of *Pf*AK2 (1-37 amino acids) was sufficient for trafficking this protein beyond the PPM. But the secretion of another *N*-myristoylated protein (*Pf*ARF1) was not achieved by the addition of the palmitoylation site and the polybasic cluster of amino acids (results of the analysis of the fusion protein of the *Pf*ARF1$^{1\text{-}17/+C4/\text{-}V5}$AK2$^{+18\text{-}37}$/GFP parasites). This indicates that other amino acids at the N-terminus of *Pf*AK2 also seem to play a role in the secretion process. Therefore more variants of AK2 should be generated and analyzed to figure out which other amino acids are important in the secretion process. However, the underlying mechanism of the secretion process for *Pf*AK2 is not understood so far.

Even if *Pf*AK2 appears to be not expressed in the erythrocytic stage of the parasite's life cycle (Le Roch et al., 2003) – this still needs to be verified via immunodetection with an antibody against *Pf*AK2 with samples prepared from the intraerythrocytic stage of the parasite - it still represents a novel mechanism of protein secretion similar to the

findings of the *Pf*CDPK1 (Möskes et al., 2004) and the *Leishmania* HASPB (Denny et al., 2000). Therefore it would be interesting to express this fusion protein in a mammalian system in regard to the anaylsis of the protein's subcellular localization.

Intriguingly, the *PfN*-myristoyltransferase appears to be a promising drug target since essential parasite proteins require *N*-myristoylation to perform their biological function (Möskes et al., 2004; Rees-Channer et al., 2006). Hence, current research is focused on the design and synthesis of inhibitors of *Pf*NMT and only recently *Pf*NMT was validated to be an antimalarial drug-target (Rackham et al., 2013; Wright et al., 2013). Therefore, the discovery of further *Pf*NMT candidate proteins contributes to the understanding of the importance and influence of *Pf*NMT in different cellular processes. In the case of *Pf*AK2/GFP *N*-myristoylation via *Pf*NMT seems to be a prerequisite for membrane targeting, membrane anchoring and protein secretion. Further experiments could include studies with NMT inhibitors to analyze their effect on the subcellular localization of *Pf*AK2/GFP.

6 References

Adisa, A., Rug, M., Klonis, N., Foley, M., Cowman, A.F., & Tilley, L. (2003). The signal sequence of exported protein-1 directs the green fluorescent protein to the parasitophorous vacuole of transfected malaria parasites. *The Journal of Biological Chemistry*, *278*(8), 6532-42.

Adisa, A., Frankland, S., Rug, M., Jackson, K., Maier, A. G., Walsh, P., Lithgow, T., Klonis, N., Gilson, P.R., Cowman, A.F., & Tilley, L. (2007). Re-assessing the locations of components of the classical vesicle-mediated trafficking machinery in transfected *Plasmodium falciparum*. *International Journal for Parasitology*, *37*(10), 1127-1141.

Aikawa, M. (1971). Parasitological review. *Plasmodium*: the fine structure of malarial parasites. *Experimental Parasitology*, *30*(2), 284–320.

Aikawa, M. (1988). Fine structure of malaria parasites in the various stages of development. In W. H. Wernsdorfer & I. McGregor (Eds.), *Malaria: Principles and practice of malariology* (pp. 97–129).

Aikawa, M., Uni, Y., Andrutis, A. T., & Howard, R. J. (1986). Membrane-Associated Electron-Dense Material of the Asexual Stages of *Plasmodium falciparum*: Evidence for Movement from the Intracellular Parasite to the Erythrocyte Membrane. *The American Journal of Tropical Medicine and Hygiene*, *35*, 30–36.

Albano, F. R., Foley, M., & Tilley, L. (1999). Export of parasite proteins to the erythrocyte cytoplasm: secretory machinery and traffic signals. *Novartis Found Symp.*, *226*, 157–72.

Alberts, B., Johnson, A., Lewis, J., Raff, M., Roberts, K., & Walter, P. (2008). Intracellular Compartments and Protein Sorting. In M. Anderson & S. Granum (Eds.), *Molecular Biology of the Cell* (5th Edition., pp. 695–748).

Amor, J. C., Harrison, D. H., Kahn, R. A., & Ringe, D. (1994). Structure of the human ADP-ribosylation factor 1 complexed with GDP. *Nature*, *372*, 704–8.

Andrei, C., Dazzi, C., Lotti, L., Torrisi, M. R., Chimini, G., & Rubartelli, A. (1999). The secretory route of the leaderless protein interleukin-1beta involves exocytosis of endolysosome-related vesicles. *Molecular Biology of the Cell*, *10*(5), 1463–75.

Ansorge, I., Benting, J., Bhakdi, S., & Lingelbach, K. (1996). Protein sorting in *Plasmodium falciparum*-infected red blood cells permeabilized with the pore-forming protein streptolysin O. *The Biochemical Journal*, *315*, 307–314.

Ansorge, I., Paprotka, K., Bhakdi, S., & Lingelbach, K. (1997). Permeabilization of the erythrocyte membrane with streptolysin O allows access to the vacuolar membrane

of *Plasmodium falciparum* and a molecular analysis of membrane topology. *Molecular and Biochemical Parasitology 84*(2), 259-61.

Atkinson, C. T., & Aikawa, M. (1990). Ultrastructure of malaria-infected erythrocytes. *Blood Cells*, *16*(2-3), 351–68.

Bannister, L., & Dluzewski, A. (1990). The ultrastructure of red cell invasion in malaria infections: a review. *Blood Cells*, *16*(2-3), 257–92.

Bañó, M. C., Jackson, C. S., & Magee, A. I. (1998). Pseudo-enzymatic S-acylation of a myristoylated yes protein tyrosine kinase peptide *in vitro* may reflect non-enzymatic S-acylation *in vivo*. *The Biochemical Journal*, *330 (Pt 2)*, 723–31.

Barlowe, C., & Schekman, R. (1993). Sec12 encodes a guanine-nucleotide-exchange factor essential for transport vesicle budding from the ER. *Letters to Nature*, *365*, 347–349.

Barr, F. A., Puype, M., Vandekerckhove, J., & Warren, G. (1997). GRASP65, a protein involved in the stacking of Golgi cisternae. *Cell*, *91*(2), 253–62.

Baruch, D. I., Pasloske, B. L., Singh, H. B., Bi, X., Ma, X. C., Feldman, M., Taraschi, T.F., & Howard, R. J. (1995). Cloning the *P. falciparum* gene encoding PfEMP1, a malarial variant antigen and adherence receptor on the surface of parasitized human erythrocytes. *Cell*, *82*(1), 77–87.

Baumgartner, F., Wiek, S., Paprotka, K., Zauner, S., & Lingelbach, K. (2001). A point mutation in an unusual Sec7 domain is linked to brefeldin A resistance in a *Plasmodium falciparum* line generated by drug selection. *Molecular Microbiology*, *41*(5), 1151–8.

Beaumelle, B. D., Vial, H. J., & Philippot, J. R. (1987). Reevaluation, using marker enzymes, of the ability of saponin and ammonium chloride to free *Plasmodium* from infected erythrocytes. *Journal of Parasitology Parasitology*, *73*(4), 743–8.

Beier, J. C. (1998). Malaria parasite development in mosquitoes. *Annual Review of Entomology*, *43*, 519–543.

Bender, A., van Dooren, G. G., Ralph, S. A., McFadden, G. I., & Schneider, G. (2003). Properties and prediction of mitochondrial transit peptides from *Plasmodium falciparum*. *Molecular and Biochemical Parasitology*, *132*(2), 59–66.

Benting, J., Mattei, D., & Lingelbach, K. (1994). Brefeldin A inhibits transport of the glycophorin-binding protein from *Plasmodium falciparum* into the host erythrocyte. *The Biochemical Journal*, *300 (Pt 3)*, 821–826.

Bhakdi, S., Tranum-Jensen, J., & Sziegoleit, A. (1985). Mechanism of Membrane Damage by Streptolysin-O. *Infection and Immunity*, *47*(1), 52–60.

Bhattacharjee, S., Stahelin, R. V, Speicher, K. D., Speicher, D. W., & Haldar, K. (2012). Endoplasmic reticulum PI(3)P lipid binding targets malaria proteins to the host cell. *Cell*, *148*(1-2) 201-212.

Blobel, G., & Dobberstein, B. (1975a). Transfer of proteins across membranes. II. Reconstitution of functional rough microsomes from heterologous components. *The Journal of Cell Biology*, *67*(3), 852–62.

Blobel, G., & Dobberstein, B. (1975b). Transfer of proteins across membranes I. Presence of Proteolytically Processed and Unprocessed Nascent Immunoglobulin Light Chains On Membrane-Bound Ribosomes of Murine Myeloma. *The Journal of Cell Biology*, *67*(3), 835–851.

Boddey, J. A., Hodder, A. N., Günther, S., Gilson, P. R., Patsiouras, H., Kapp, E. A., Pearce, J. A., de Koning-Ward, T.F., Simpson, R.J., Crabb, B.S., & Cowman, A. F. (2010). An aspartyl protease directs malaria effector protein to the host cell. *Nature*, *463*, 627-631.

Boman, A. L., & Kahn, R. A. (1995). Arf proteins: the membrane traffic police? *Trends in Biochemical Sciences*, *20*(4), 147–50.

Bullen, H. E., Charnaud, S. C., Kalanon, M., Riglar, D. T., Dekiwadia, C., Kangwanrangsan, N., Tori, M., Tsuboi, T., Baum, J., Ralph, S.A., Cowman, A.F., de Koning-Ward, T.F., Crabb, B.S., & Gilson, P. R. (2012). Biosynthesis, localization, and macromolecular arrangement of the *Plasmodium falciparum* translocon of exported proteins (PTEX). *The Journal of Biological Chemistry*, *287*(11), 7871-84.

Buser, C. A., Sigal, C. T., Resh, M. D., & McLaughlin, S. (1994). Membrane binding of myristoylated peptides corresponding to the NH2 terminus of Src. *Biochemistry*, *33*(44), 13093–101.

Cabral, M., Anjard, C., Malhotra, V., Loomis, W. F., & Kuspa, A. (2010). Unconventional secretion of AcbA in *Dictyostelium discoideum* through a vesicular intermediate. *Eukaryotic Cell*, *9*(7), 1009–17.

Carter, R., & Mendis, K. N. (2002). Evolutionary and Historical Aspects of the Burden of Malaria. *Clinical Microbiology Reviews*, *15*(4), 564-94.

Chang, H. H., Falick, A. M., Carlton, P. M., Sedat, J. W., DeRisi, J. L., & Marletta, M. A. (2008). N-terminal processing of proteins exported by malaria parasites. *Molecular and Biochemical Parasitology*, *160*(2), 107-15.

Charpian, S., & Przyborski, J. M. (2008). Protein transport across the parasitophorous vacuole of *Plasmodium falciparum*: into the great wide open. *Traffic*, *9*(2), 157–65.

Cook, W. J., Smith, C.D., Senkovich, O., Holder, A.A. & Chattopadhyay, D. (2010). Structure of *Plasmodium falciparum* ADP-ribosylation factor 1. *Acta Crystallographica. Structural Biology and Crystallization Communications*, *66*, 1426–1431.

Cooke, B. M., Lingelbach, K., Bannister, L. H., & Tilley, L. (2004). Protein trafficking in *Plasmodium falciparum*-infected red blood cells. *Trends in Parasitology*, *20*(12), 581–9.

Couffin, S., Hernandez-Rivas, R., Blisnick, T., & Mattei, D. (1998). Characterisation of PfSec61, a *Plasmodium falciparum* homologue of a component of the translocation machinery at the endoplasmic reticulum membrane of eukaryotic cells. *Molecular and Biochemical Parasitology*, *92*(1), 89–98.

Cowman, A. F., & Crabb, B. S. (2006). Invasion of red blood cells by malaria parasites. *Cell*, *124*(4), 755–66.

Cox-Singh, J., Davis, T. M. E., Lee, K.-S., Shamsul, S. S. G., Matusop, A., Ratnam, S., Rahman, H.A., Conway, D.J., & Singh, B. (2008). *Plasmodium knowlesi* malaria in humans is widely distributed and potentially life threatening. *Clinical infectious diseases: an official publication of the Infectious Diseases Society of America*, *46*(2), 165–71.

Crabb, B. S., Cooke, B. M., Reeder, J. C., Waller, R. F., Caruana, S. R., Davern, K. M., Wickham, M.E., Brown, G.V., Coppel, R.L., & Cowman, A. F. (1997). Targeted gene disruption shows that knobs enable malaria-infected red cells to cytoadhere under physiological shear stress. *Cell*, *89*(2), 287–96.

Crabb, B. S., de Koning-Ward, T. F., & Gilson, P. R. (2010). Protein export in *Plasmodium* parasites: from the endoplasmic reticulum to the vacuolar export machine. *International Journal for Parasitology*, *40*(5), 509–13.

Culvenor, J., Langford, C. J., Crewther, A. E., Saint, R. B., Coppel, R. L., Kemp, J., Anders, R.E., & Brown, G. V. (1987). *Plasmodium falciparum*: identification and localization of a knob protein antigen expressed by a cDNA clone. *Experimental Parasitology*, *67*, 58–67.

de Castro, F.A., Ward, G.E., Jambou, R., Attal, G., Mayau, V., Jaureguiberry, G., Braun-Breton, C., Chakrabarti, D., & Langsley G. (1996). Identification of a family of Rab G-proteins in *Plasmodium falciparum* and a detailed characterisation of pfrab6. *Molecular and Biochemical Parasitology*, *80*(1), 77–88.

de Koning-Ward, T. F., Gilson, P. R., Boddey, J. A., Rug, M., Smith, B.J., Papenfuss, A.T., Sanders, P.R., Lundie, R.J., Maier, A.G., Cowman, A. F., & Crabb, B. S. (2009). A novel protein export machine in malaria parasites. *Nature*, *459*(7249), 945–949.

Denny, P. W., Gokool, S., Russell, D. G., Field, M. C., & Smith, D. F. (2000). Acylation-dependent Protein Export in *Leishmania*. *Journal of Biological Chemistry*, *275*(15), 11017–11025.

Deponte, M., Hoppe, H. C., Lee, M. C. S., Maier, A. G., Richard, D., Rug, M., Spielmann, T. & Przyborski, J. M. (2012). Wherever I may roam: protein and membrane trafficking in *P. falciparum*-infected red blood cells. *Molecular and Biochemical Parasitology*, *186*(2), 95–116.

Dieckmann-Schuppert, A., Bender, S., Odenthal-Schnittler, M., Bause, E., & Schwarz, R. T. (1992). Apparent lack of N-glycosylation in the asexual intraerythrocytic stage of *Plasmodium falciparum*. *European Journal of Biochemistry / FEBS*, *205*(2), 815–25.

Dixon, M. W. A., Hawthorne, P. L., Spielmann, T., Anderson, K. L., Trenholme, K. R., & Gardiner, D. L. (2008). Targeting of the Ring Exported Protein 1 to the Maurer's Clefts is Mediated by a Two-Phase Process. *Traffic*, *9*(8), 1316–1326.

Dou, D., Kale, S.D., Wang, X., Rays, H.X.J., Bruce N.A., Arredondo, F.D., Zhang, X., & Tyler, B.M. (2008). RXLR-Mediated Entry of *Phytophthora sojae* Effector *Avr1b* into Soybean Cells Does Not Require Pathogen-Encoded Machinery. *Plant Cell*, *20*, 1930-1947.

Dowse, T. J., Koussis, K., Blackman, M. J., & Soldati-Favre, D. (2008). Roles of proteases during invasion and egress by *Plasmodium* and *Toxoplasma*. *Subcellular Biochemistry*, *47*, 121–139.

D'Souza-Schorey, C., & Chavrier, P. (2006). ARF proteins: roles in membrane traffic and beyond. *Nature reviews. Molecular Cell Biology*, *7*(5), 347-58.

Duran, J. M., Anjard, C., Stefan, C., Loomis, W. F., & Malhotra, V. (2010). Unconventional secretion of Acb1 is mediated by autophagosomes. *The Journal of Cell Biology*, *188*(4), 527–36.

Dvorak, J.A., Miller, L.H., Whitehouse, W.C., & Shiroishi, T. (1975). Invasion of erythrocytes by malaria merozoites. *Science*, *187*(4178), 748–750.

Dzeja, P., & Terzic, A. (2009). Adenylate kinase and AMP signaling networks: metabolic monitoring, signal communication and body energy sensing. *International Journal of Molecular Sciences*, *10*(4), 1729–72.

Eilers, M., & Schatz, G. (1986). Binding of a specific ligand inhibits import of a purified precursor protein into mitochondria. *Nature*, *322* (6076), 228–232.

Elmendorf, H. G., & Haldar, K. (1993). Identification and localization of ERD2 in the malaria parasite *Plasmodium falciparum*: separation from sites of sphingomyelin synthesis and implications for organization of the Golgi. *The EMBO Journal*, *12*(12), 4763–4773.

Franchi, L., Eigenbrod, T., Muñoz-Planillo, R., & Nuñez, G. (2009). The Inflammasome: A Caspase-1 Activation Platform Regulating Immune Responses and Disease Pathogenesis. *Nature Immunology*, *10*(3), 241.

Francis, S. E., Sullivan, D. J., & Goldberg, D. E. (1997). Hemoglobin metabolism in the malaria parasite *Plasmodium falciparum*. *Annual Review of Microbiology*, *51*, 97–123.

Franco, M., Chardin, P., Chabre, M., & Paris, S. (1996). Myristoylation-facilitated Binding of the G Protein ARF1GDP to Membrane Phospholipids Is Required for Its Activation by a Soluble Nucleotide Exchange Factor. *Journal of Biological Chemistry*, *271*(3), 1573–1578.

Gallup, J. L., & Sachs, J. D. (2001). The economic burden of malaria. *The American Journal of Tropical Medicine and Hygiene*, *64*(1-2 Suppl), 85–96.

Gardner, M. J., Hall, N., Fung, E., White, O., Berriman, M., Hyman, R. W., Carlton, J.M., Pain, A., Nelson, K. E., Bowman, S., Paulsen, I. T., James, K., Eisen, J.A., Rutherford, K., Salzberg, S.L., Craig, A., Kyes, S., Chan, M.-S., Nene, V., Shallom, S.J., Suh, B., Peterson, J., Angiuoli, S., Pertea, M., Allen, J., Selengut, J., Haft, D., Mather, M.W., Vaidya, A. B., Martin, D. M. A., Fairlamb, A. H., Fraunholz, M. J., Roos, D. S., Ralph, S. A., McFadden, G. I., Cummings, L. M., Subramanian, G. M., Mungall, C., Venter, J. C., Carucci, D. J., Hoffman, S. L., Newbold, C., Davis, R. W., Fraser, C. M., & Barrell, B. (2002). Genome sequence of the human malaria parasite *Plasmodium falciparum*. *Nature*, *419*(6906), 498–511.

Gehde, N., Hinrichs, C., Montilla, I., Charpian, S., Lingelbach, K., & Przyborski, J. M. (2009). Protein unfolding is an essential requirement for transport across the parasitophorous vacuolar membrane of *Plasmodium falciparum*. *Molecular Microbiology*, *71*(3), 613–28.

Glenister, F. K., Coppel, R. L., Cowman, A. F., Mohandas, N., & Cooke, B. M. (2002). Contribution of parasite proteins to altered mechanical properties of malaria-infected red blood cells. *Blood*, *99*(3), 1060–3.

Grieve, A. G., & Rabouille, C. (2011). Golgi bypass: skirting around the heart of classical secretion. *Cold Spring Harbor perspectives in biology*, *3*(4), 1–15.

Griffiths, G. M. (1996). Secretory lysosomes - a special mechanism of regulated secretion in haemopoietic cells. *Trends in Cell Biology*, *6*(9), 329–32.

Günther, K., Tümmler, M., Arnold, H., Ridley, R., Goman, M., Scaife, J. G., & Lingelbach, K. (1991). An exported protein of *Plasmodium falciparum* is synthesized as an integral membrane protein. *Molecular and Biochemical Parasitology*, *46*(1), 149–157.

Haase, S., Herrmann, S., Grüring, C., Heiber, A., Jansen, P. W., Langer, C., Treeck, M., Cabrera, A., Bruns, C., Struck, N.S., Kono, M., Engelberg, K., Ruch, U., Stunnenberg, H. G., Gilberger, T.-W., & Spielmann, T. (2009). Sequence requirements for the export of the *Plasmodium falciparum* Maurer's clefts protein REX2. *Molecular Microbiology*, *71*(4), 1003–17.

Häusler, T., Stierhof, Y. D., Wirtz, E., & Clayton, C. (1996). Import of a DHFR hybrid protein into glycosomes in vivo is not inhibited by the folate-analogue aminopterin. *The Journal of Cell Biology*, *132*(3), 311–24.

Heiber, A., Kruse, F., Pick, C., Grüring, C., Flemming, S., Oberli, A., Schoeler, H., Retzlaff, S., Mesen-Ramirez, P., Hiss, J.A., Kadekoppala, M., Hecht, L., Holder, A. A., Gilberger, T.-W. & Spielmann, T. (2013). Identification of New PNEPs Indicates a Substantial Non-PEXEL Exportome and Underpins Common Features in *Plasmodium falciparum* Protein Export. *PLoS Pathogens 9*(8), e1003546.

Hiller, N. L., Bhattacharjee, S., van Ooij, C., Liolios, K., Harrison, T., Lopez-Estraño, C., & Haldar, K. (2004). A host-targeting signal in virulence proteins reveals a secretome in malarial infection. *Science*, *306*(5703), 1934–7.

Hinterberg, K., Scherf, A., Gysin, J., Toyoshima, T., Aikawa, M., Mazie, J. C., Dasilva, L.P., & Mattei, D. (1994). *Plasmodium falciparum*: - The Pf332 Antigen Is Secreted from the Parasite by a Brefeldin A-Dependent Pathway and Is Translocated to the Erythrocyte Membrane via the Maurer′s Clefts. *Experimental Parasitology*, *79*(3), 279–291.

Ho, S. N., Hunt, H. D., Horton, R. M., Pullen, J. K., & Pease, L. R. (1989). Site-directed mutagenesis by overlap extension using the polymerase chain reaction. *Gene*, *77*(1), 51–9.

Howard, R.J, Uni, S., Aikawa, M., Aley, S.B., Leech, J.H., Lew, A.M., Wellems, T.E., Rener, J., & Tayler, D.W. (1986). Secretion of a malarial histidine-rich protein (Pf HRP II) from *Plasmodium falciparum*-infected erythrocytes. *The Journal of Cell Biology*, *103*(4), 1269-1277.

Kahn, R. A., Kern, F. G., Clark, J., Gelmann, P., & Rulka, C. (1991). Human ADP-Ribosylation Factors. A functional conserved family of GTP-binding proteins. *The Journal of Biological Chemistry*, *266*(4), 2606–2614.

Kats, L. M., Cooke, B. M., Coppel, R. L., & Black, C. G. (2008). Protein trafficking to apical organelles of malaria parasites - building an invasion machine. *Traffic*, *9*(2), 176–86.

Khoo, J. C., & Russell, P. J. (1972). Isoenzymes of adenylate kinase in human tissue. *Biochimica et Biophysica Acta*, *268*(1), 98–101.

Kinseth, M. A., Anjard, C., Fuller, D., Guizzunti, G., Loomis, W. F., & Malhotra, V. (2007). The Golgi-associated protein GRASP is required for unconventional protein secretion during development. *Cell*, *130*(3), 524–34.

Kirchhausen, T. (2000). Three ways to make a vesicle. *Nature Reviews. Molecular Cell Biology*, *1*(3), 187–98.

Kirk, K. (2001). Membrane transport in the malaria-infected erythrocyte. *Physiological Reviews*, *81(2), 495-537.*

Kumar, N., Koski, G., Harada, M., Aikawa, M., & Zheng, H. (1991). Induction and localization of *Plasmodium falciparum* stress proteins related to the heat shock protein 70 family. *Molecular and Biochemical Parasitology*, *48*(1), 47–58.

Kutner, S., Breuer, W. V, Ginsburg, H., Aley, S. B., & Cabantchik, Z. I. (1985). Characterization of permeation pathways in the plasma membrane of human erythrocytes infected with early stages of *Plasmodium falciparum*: association with parasite development. *Journal of Cellular Physiology*, *125*(3), 521–7.

La Greca, N., Hibbs, A. R., Riffkin, C., Foley, M., & Tilley, L. (1997). Identification of an endoplasmic reticulum-resident calcium-binding protein with multiple EF-hand motifs in asexual stages of *Plasmodium falciparum*. *Molecular and Biochemical Parasitology*, *89*(2), 283–93.

Lambros, C., & Vanderberg, J. P. (1979). Synchronization of *Plasmodium falciparum* erythrocytic stages in culture. *Journal of Parasitology*, *65*(3), 418–20.

Lanzer, M., Wickert, H., Krohne, G., Vincensini, L., & Braun-Breton, C. (2006). Maurer's clefts: A novel multi-functional organelle in the cytoplasm of *Plasmodium falciparum*-infected erythrocytes. *International Journal for Parasitology*, *36*(1), 23–36.

Lauer, S. A., Rathod, P. K., Ghori, N., & Haldar, K. (1997). A Membrane Network for Nutrient Import in Red Cells Infected with the Malaria Parasite. *Science*, *276*(5315), 1122–1125.

Lauer, S., VanWye, J., Harrison, T., McManus, H., Samuel, B. U., Hiller, N. L., Mohandas, N., & Haldar, K. (2000). Vacuolar uptake of host components, and a role for cholesterol and sphingomyelin in malarial infection. *The EMBO Journal*, *19*(14), 3556–64.

Lee, M. C. S., Moura, P. A., Miller, E. A., & Fidock, D. A. (2008). *Plasmodium falciparum* Sec24 marks transitional ER that exports a model cargo via a diacidic motif. *Molecular Microbiology*, *68*(6), 1535–46.

Le Roch, K. G., Zhou, Y., Blair, P. L., Grainger, M., Moch, J. K., Haynes, J. D., De La Vega, P., Holder, A.A., Batalov, S., Carucci, D.J. & Winzeler, E. A. (2003). Discovery of gene function by expression profiling of the malaria parasite life cycle. *Science*, *301*(5639), 1503–8.

Linder, M. E., & Deschenes, R. J. (2003). New insights into the mechanisms of protein palmitoylation. *Biochemistry*, *42*(15), 4311–20.

Lingelbach, K. R. (1993). *Plasmodium falciparum*: a molecular view of protein transport from the parasite into the host erythrocyte. *Experimental Parasitology*, *76*(3), 318–27.

Lingelbach, K. R., & Joiner, K. A. (1998). The parasitophorous vacuole membrane surrounding *Plasmodium* and *Toxoplasma*: an unusual compartment in infected cells. *Journal of Cell Science*, *111 (Pt 1)*, 1467–75.

Lippincott-Schwartz, J., Yuan, L. C., Bonifacino, J. S., & Klausner, R. D. (1989). Rapid redistribution of Golgi proteins into the ER in cells treated with brefeldin A: evidence for membrane cycling from Golgi to ER. *Cell*, *56*(5), 801–13.

Ma, J., Rahlfs, S., Jortzik, E., Schirmer, R. H., Przyborski, J. M., & Becker, K. (2012). Subcellular localization of adenylate kinases in *Plasmodium falciparum*. *FEBS letters*, *586*(19), 3037–43.

MacKenzie, A., Wilson, H. L., Kiss-Toth, E., Dower, S. K., North, R. A., & Surprenant, A. (2001). Rapid Secretion of Interleukin-1 beta by Microvesicle Shedding. *Immunity*, *15*(5), 825–835.

Maier, A. G., Cooke, B. M., Cowman, A. F., & Tilley, L. (2009). Malaria parasite proteins that remodel the host erythrocyte. *Nature Reviews. Microbiology*, *7*(5), 341–54.

Maier, A. G., Rug, M., O'Neill, M. T., Brown, M., Chakravorty, S., Szestak, T., Chesson, J., Wu, Y., Hughes, K., Coppel, R.L., Newbold, C., Beeson, J.G., Craig,

A., Crabb, B.S., & Cowman, A. F. (2008). Exported proteins required for virulence and rigidity of *Plasmodium falciparum*-infected human erythrocytes. *Cell*, *134*(1), 48–61.

Manjithaya, R., Anjard, C., Loomis, W. F., & Subramani, S. (2010). Unconventional secretion of *Pichia pastoris* Acb1 is dependent on GRASP protein, peroxisomal functions, and autophagosome formation. *The Journal of Cell Biology*, *188*(4), 537–46.

Marti, M., Good, R. T., Rug, M., Knuepfer, E., & Cowman, A. F. (2004). Targeting malaria virulence and remodeling proteins to the host erythrocyte. *Science*, *306*(5703), 1930–3.

Marti, M., Baum, J., Rug, M., Tilley, L., & Cowman, A. F. (2005). Signal-mediated export of proteins from the malaria parasite to the host erythrocyte. *The Journal of Cell Biology*, *171*(4), 587–92.

Martinez, O., & Goud, B. (1998). Rab proteins. *Biochimica et Biophysica Acta*, *1404*(1-2), 101–12.

Matuschewski, K. (2006). Getting infectious: formation and maturation of *Plasmodium* sporozoites in the *Anopheles* vector. *Cellular Microbiology*, *8*(10), 1547–56.

Maurer-Stroh, S., Eisenhaber, B., & Eisenhaber, F. (2002). N-terminal N-Myristoylation of Proteins: Prediction of Substrate Proteins from Amino Acid Sequence. *Journal of Molecular Biology*, *317*(4), 541–557.

Maurer-Stroh, S., & Eisenhaber, F. (2004). Myristoylation of viral and bacterial proteins. *Trends in Microbiology*, *12*(4), 178–85.

McGrath, J. P., & Varshavsky, A. (1989). The yeast STE6 gene encodes a homologue of the mammalian multidrug resistance P-glycoprotein. *Nature*, *340*(6232), 400–4.

McLaughlin, S., & Aderem, A. (1995). The myristoyl-electrostatic switch: a modulator of reversible protein-membrane interactions. *Trends Biochemical Sciences*, *20*(7), 272–276.

McPherson, R. A., Donald, D. R., Sawyer, W. H., & Tilley, L. (1993). Proteolytic digestion of band 3 at an external site alters the erythrocyte membrane organisation and may facilitate malarial invasion. *Molecular and Biochemical Parasitology*, *62*(2), 233–42.

Memon, A. R. (2004). The role of ADP-ribosylation factor and SAR1 in vesicular trafficking in plants. *Biochimica et Biophysica Acta*, *1664*(1), 9–30.

Ménard, R. (2005). Knockout malaria vaccine ? *Nature*, *433*, 6–7.

Miller, L. H., Baruch, D. I., Marsh, K., & Doumbo, O. K. (2002). The pathogenic basis of malaria. *Nature*, *415*(6872), 673–9.

Misumi, Y., Misumi, Y. Miki, K., Takatsuki, A., Tamura, G., & Ikehara, Y. (1986). Novel blockade by brefeldin A of intracellular transport of secretory proteins in

cultured rat hepatocytes. *The Journal of Biological Chemistry*, *261*(24), 11398–403.

Mitchell, D. A., Vasudevan, A., Linder, M. E., & Deschenes, R. J. (2006). Protein palmitoylation by a family of DHHC protein S-acyltransferases. *Journal of Lipid Research*, *47*(6), 1118–27.

Mohandas, N., & Gallagher, P. G. (2008). Red cell membrane: past, present, and future. *Blood*, *112*(10), 3939–48.

Möskes, C., Burghaus, P. A., Wernli, B., Sauder, U., Dürrenberger, M., & Kappes, B. (2004). Export of *Plasmodium falciparum* calcium-dependent protein kinase 1 to the parasitophorous vacuole is dependent on three N-terminal membrane anchor motifs. *Molecular Microbiology*, *54*(3), 676–91.

Mullis, K., Faloona, F., Scharf, S., Saiki, R., Horn, G., & Erlich, H. (1986). Specific enzymatic amplification of DNA in vitro: the polymerase chain reaction. *Cold Spring Harbor perspectives in biology*, *51*(1), 263–73.

Murphy, S. C., Samuel, B. U., Harrison, T., Speicher, K. D., Speicher, D. W., Reid, M. E., Prohaska, R., Low, P.S., Tanner, M.J., Mohandas, N., & Haldar, K. (2004). Erythrocyte detergent-resistant membrane proteins: their characterization and selective uptake during malarial infection. *Blood*, *103*(5), 1920–8.

Murray, D., Ben-Tal, N., Honig, B., & McLaughlin, S. (1997). Electrostatic interaction of myristoylated proteins with membranes: simple physics, complicated biology. *Structure*, *5*(8), 985–9.

Murray, D., Hermida-Matsumoto, L., Buser, C. A., Tsang, J., Sigal, C. T., Ben-Tal, N., Honig, B., Resh, M.D., & McLaughlin, S. (1998). Electrostatics and the membrane association of Src: theory and experiment. *Biochemistry*, *37*(8), 2145–59.

Nadolski, M. J., & Linder, M. E. (2007). Protein lipidation. *The FEBS Journal*, *274*(20), 5202–10.

Nickel, W. (2005). Unconventional secretory routes: direct protein export across the plasma membrane of mammalian cells. *Traffic*, *6*(8), 607–14.

Nickel, W. (2010). Pathways of unconventional protein secretion. *Current Opinion in Biotechnology*, *21*(5), 621–6.

Nyalwidhe, J., & Lingelbach, K. (2006). Proteases and chaperones are the most abundant proteins in the parasitophorous vacuole of *Plasmodium falciparum*-infected erythrocytes. *Proteomics*, *6*(5), 1563–73.

Nyalwidhe, J. O., Azimzadeh, O., Przyborski, J. M., Pachlatko, E., Beck, H.-P., Gilberger, T.-W., Spielman, T., Baumeister, S. & Lingelbach, K. (n.d.). Proteome analysis of the parasitophorous vacuole. *Manuscript in preparation.*

Palade, G. (1975). Intracellular aspects of the Process of Protein Synthesis. *Science*, *189*(4200), 347–58.

Papakrivos, J., Newbold, C. I., & Lingelbach, K. (2005). A potential novel mechanism for the insertion of a membrane protein revealed by a biochemical analysis of the *Plasmodium falciparum* cytoadherence molecule PfEMP-1. *Molecular Microbiology*, *55*(4), 1272–84.

Pasvol, G., Wilson, R. J., Smalley, M. E., & Brown, J. (1978). Separation of viable schizont-infected red cells of *Plasmodium falciparum* from human blood. *Annals of Tropical Medicine & Parasitology*, *72*(1), 87–88.

Paul, F., Roath, S., Melville, D., Warhurst, D. C., & Osisanya, J. O. S. (1981). Separation of malaria-infected erythrocytes from whole blood: use of a selective high-gradient magnetic separation technique. *The Lancet*, *318*(8237), 70–71.

Peitzsch, R. M., & McLaughlin, S. (1993). Binding of acylated peptides and fatty acids to phospholipid vesicles: Pertinence to myristoylated proteins. *Biochemistry*, *32*(39), 10436–43.

Pologe, L. G., Pavlovec, A., Shiot, H., & Ravetch, J. V. (1987). Primary structure and subcellular localization of the knob-associated histidine-rich protein of *Plasmodium falciparum*. *Proceedings of the National Academy of Sciences of the United States of America*, *84*(20), 7139–7143.

Przyborski, J. M., Miller, S. K., Pfahler, J. M., Henrich, P. P., Rohrbach, P., Crabb, B. S., & Lanzer, M. (2005). Trafficking of STEVOR to the Maurer's clefts in *Plasmodium falciparum*-infected erythrocytes. *The EMBO Journal*, *24*(13), 2306–17.

Rabouille, C., Malhotra, V., & Nickel, W. (2012). Diversity in unconventional protein secretion. *Journal of Cell Science*, *125*(Pt 22), 5251–5255.

Rackham, M. D., Brannigan, J. A, Moss, D. K., Yu, Z., Wilkinson, A. J., Holder, A. A, Tate, E.W. & Leatherbarrow, R. J. (2013). Discovery of novel and ligand-efficient inhibitors of *Plasmodium falciparum* and *Plasmodium vivax* N-myristoyltransferase. *Journal of Medicinal Chemistry*, *56*(1), 371–5.

Rahlfs, S., Koncarevic, S., Iozef, R., Mailu, B. M., Savvides, S. N., Schirmer, R. H., & Becker, K. (2009). Myristoylated adenylate kinase-2 of *Plasmodium falciparum* forms a heterodimer with myristoyltransferase. *Molecular and Biochemical Parasitology*, *163*(2), 77–84.

Rees-Channer, R. R., Martin, S. R., Green, J. L., Bowyer, P. W., Grainger, M., Molloy, J. E., & Holder, A. A. (2006). Dual acylation of the 45 kDa gliding-associated protein (GAP45) in *Plasmodium falciparum* merozoites. *Molecular and Biochemical Parasitology*, *149*(1), 113–6.

Resh, M. D. (1999). Fatty acylation of proteins: new insights into membrane targeting of myristoylated and palmitoylated proteins. *Biochimica et Biophysica Acta*, *1451*(1), 1–16.

Resh, M. D. (2006). Trafficking and signaling by fatty-acylated and prenylated proteins. *Nature Chemical Biology*, *2*(11), 584–90.

Roggwiller, E., Betoulles, M. E., Blisnick, T., & Braun-Breton, C. (1996). A role for erythrocyte band 3 degradation by the parasite gp76 serine protease in the formation of the parasitophorous vacuole during invasion of erythrocytes by *Plamodium falciparum*. *Molecular and Biochemical Parasitology*, *82*(1), 13–24.

Roth, E. J. (1990). *Plasmodium falciparum* carbohydrate metabolism: a connection between host cell and parasite. *Blood Cells*, *16*(2-3), 453–60.

Rothman, J. E. (1994). Mechanisms of intracellular protein transport. *Nature*, *372*(6501), 55–63.

Rubartelli, A., Cozzolino, F., Talio, M., & Sitia, R. (1990). A novel secretory pathway for interleukin-1 beta, a protein lacking a signal sequence. *The EMBO Journal*, *9*(5), 1503–1510.

Russo, I., Babbitt, S., Muralidharan, V., Butler, T., Oksman, A., & Goldberg, D. E. (2010). Plasmepsin V licenses *Plasmodium* proteins for export into the host erythrocyte. *Nature*, *463*(7281), 632–636.

Sachs, J., & Malaney, P. (2002). The economic and social burden of malaria. *Nature*, *415*(6872), 680–5.

Sallares, R., Bouwman, A., & Anderung, C. (2004). The spread of malaria to Southern Europe in antiquity: new approaches to old problems. *Medical History*, *48*(3), 311–328.

Salvador, N., Aguado, C., Horst, M., & Knecht, E. (2000). Import of a cytosolic protein into lysosomes by chaperone-mediated autophagy depends on its folding state. *The Journal of Biological Chemistry*, *275*(35), 27447–56.

Sambrook, J., & Russell, D. W. (2001). Molecular cloning: A laboratory manual (3rd ed.). *Cold Spring Harbor Laboratory Press,* New York.

Saridaki, T., Fröhlich, K. S., Braun-Breton, C., & Lanzer, M. (2009). Export of PfSBP1 to the *Plasmodium falciparum* Maurer's clefts. *Traffic*, *10*(2), 137–52.

Schäfer, T., Zentgraf, H., Zehe, C., Brügger, B., Bernhagen, J., & Nickel, W. (2004). Unconventional secretion of fibroblast growth factor 2 is mediated by direct translocation across the plasma membrane of mammalian cells. *The Journal of Biological Chemistry*, *279*(8), 6244–51.

Schnell, J. R., Dyson, H. J., & Wright, P. E. (2004). Structure, dynamics, and catalytic function of dihydrofolate reductase. *Annual Review of Biophysics and Biomolecular Structure*, *33*, 119–40.

Shortt, H. E. (1951). Life-cycle of the mammalian malaria parasite. *British Medical Bulletin*, *8*(1), 7–9.

Sigal, C. T., Zhou, W., Buser, C. A., McLaughlin, S., & Resh, M. D. (1994). Amino-terminal basic residues of Src mediate membrane binding through electrostatic interaction with acidic phospholipids. *Proceedings of the National Academy of Sciences of the United States of America*, *91*(25), 12253–7.

Singh, B., Kim Sung, L., Matusop, A., Radhakrishnan, A., Shamsul, S. S. G., Cox-Singh, J., Thomas, A., & Conway, D. J. (2004). A large focus of naturally acquired *Plasmodium knowlesi* infections in human beings. *Lancet*, *363*(9414), 1017–24.

Smotrys, J. E., & Linder, M. E. (2004). Palmitoylation of intracellular signaling proteins: regulation and function. *Annual Review of Biochemistry*, *73*, 559–87.

Spielmann, T., Hawthorne, P.L., Dixon, M.W.A., Hannemann, M., Klotz, K., Kemp, D.J., Klonis, N., Tilley, L., Trenholme, K.R. & Gardiner, D.L. (2006). A Cluster of Ring Stage–specific Genes Linked to a Locus Implicated in Cytoadherence in *Plasmodium falciparum* Codes for PEXEL-negative and PEXEL-positive Proteins Exported into the Host Cell. *Molecular Biology of the Cell 17*(8), 3613-3624.

Spielmann, T., & Gilberger, T.-W. (2010). Protein export in malaria parasites: do multiple export motifs add up to multiple export pathways? *Trends in Parasitology*, *26*(1), 6–10.

Spycher, C., Rug, M., Pachlatko, E., Hanssen, E., Ferguson, D., Cowman, A. F., Tilley, L. & Beck, H.-P. (2008). The Maurer's cleft protein MAHRP1 is essential for trafficking of PfEMP1 to the surface of *Plasmodium falciparum*-infected erythrocytes. *Molecular Microbiology*, *68*(5), 1300–14.

Stafford, W. H., Stockley, R. W., Ludbrook, S. B., & Holder, A. A. (1996). Isolation, expression and characterization of the gene for an ADP-ribosylation factor from the human malaria parasite, *Plasmodium falciparum*. *European Journal of Biochemistry / FEBS*, *242*(1), 104–13.

Stearns, T., Willingham, M. C., Botstein, D., & Kahn, R. A. (1990). ADP-ribosylation factor is functionally and physically associated with the Golgi complex. *Proceedings of the National Academy of Sciences of the United States of America*, *87*(3), 1238–42.

Stoorvogel, W., Kleijmeer, M. J., Geuze, H. J., & Raposo, G. (2002). The biogenesis and functions of exosomes. *Traffic*, *3*(5), 321–30.

Struck, N. S., de Souza Dias, S., Langer, C., Marti, M., Pearce, J. A., Cowman, A. F., & Gilberger, T. W. (2005). Re-defining the Golgi complex in *Plasmodium falciparum* using the novel Golgi marker *Pf*GRASP. *Journal of Cell Science*, *118*(Pt 23), 5603–13.

Struck, N. S., Herrmann, S., Langer, C., Krueger, A., Foth, B. J., Engelberg, K., Cabrera, A.L., Haase, S., Treeck, M., Marti, M., Cowman, A.F., Spielmann, T., & Gilberger, T. W. (2008a). *Plasmodium falciparum* possesses two GRASP proteins that are differentially targeted to the Golgi complex via a higher- and lower-eukaryote-like mechanism. *Journal of Cell Science*, *121*(Pt 13), 2123–9.

Struck, N. S., Herrmann, S., Schmuck-Barkmann, I., de Souza Dias, S., Haase, S., Cabrera, A. L., Treeck., M., Bruns, C., Langer, C., Cowman, A.F., Marti, M., Spielmann, T., & Gilberger, T. W. (2008b). Spatial dissection of the cis- and trans-Golgi compartments in the malaria parasite *Plasmodium falciparum*. *Molecular Microbiology*, *67*(6), 1320–30.

Sturm, A., Amino, R., van de Sand, C., Regen, T., Retzlaff, S., Rennenberg, A., Krueger, A., Pollok, J.-M., Menard, R., & Heussler, V. T. (2006). Manipulation of host hepatocytes by the malaria parasite for delivery into liver sinusoids. *Science*, *313*(5791), 1287–90.

Su, X. Z., Heatwole, V. M., Wertheimer, S. P., Guinet, F., Herrfeldt, J. A., Peterson, D. S., Ravetch, J.A., & Wellems, T. E. (1995). The large diverse gene family var encodes proteins involved in cytoadherence and antigenic variation of *Plasmodium falciparum*-infected erythrocytes. *Cell*, *82*(1), 89–100.

Taraschi, T. F., Trelka, D., Martinez, S., Schneider, T., & O'Donnell, M. E. (2001). Vesicle-mediated trafficking of parasite proteins to the host cell cytosol and erythrocyte surface membrane in *Plasmodium falciparum* infected erythrocytes. *International Journal for Parasitology*, *31*(12), 1381–91.

Temmerman, K., Ebert, A. D., Müller, H.-M., Sinning, I., Tews, I., & Nickel, W. (2008). A direct role for phosphatidylinositol-4,5-bisphosphate in unconventional secretion of fibroblast growth factor 2. *Traffic*, *9*(7), 1204–17.

Thelen, M., Rosen, A., Nairn, A., & Aderem, A. (1991). Regulation by phosphorylation of reversible association of a myristoylated protein kinase C substrate with the plasma membrane. *Nature*, *351*(6324), 320–2.

Tomasselli, A. G., Schirmer, R. H., & Noda, L. H. (1979). Mitochondrial GTP-AMP Phosphotransferase. *European Journal of Biochemistry*, *93*, 257–262.

Tonkin, C. J., van Dooren, G. G., Spurck, T. P., Struck, N. S., Good, R. T., Handman, E., Cowman, A.F., & McFadden, G. I. (2004). Localization of organellar proteins in *Plasmodium falciparum* using a novel set of transfection vectors and a new immunofluorescence fixation method. *Molecular and Biochemical Parasitology*, *137*(1), 13–21.

Trager, W., Rudzinska, M. A., & Bradbury, P. C. (1966). The fine structure of *Plasmodium falciparum* and its host erythrocytes in natural malarial infections in man. *Bulletin of the World Health Organization*, *35*(6), 883–5.

Trager, J., & Jensen, J. B. (1976). Human malaria parasites in continuous culture. *Science*, *193*(4254), 673–675.

Trelka, D. P., Schneider, T. G., Reeder, J. C., & Taraschi, T. F. (2000). Evidence for vesicle-mediated trafficking of parasite proteins to the host cell cytosol and erythrocyte surface membrane in *Plasmodium falciparum* infected erythrocytes. *Molecular and Biochemical Parasitology*, *106*(1), 131–45.

Tsekoa, T. L., Makungo, T., & Mancama, D. (2009). Molecular Modelling of Calcium Dependent Protein Kinase 4 (CDPK4) from *Plasmodium falciparum*. In *SAICSIT* (Vol. 4, pp. 12–14).

Ulschmid, J. K., Rahlfs, S., Schirmer, R. H., & Becker, K. (2004). Adenylate kinase and GTP:AMP phosphotransferase of the malarial parasite *Plasmodium falciparum*. *Molecular and Biochemical Parasitology*, *136*(2), 211–220.

Vainberg, I. E., Lewis, S. A., Rommelaere, H., Ampe, C., Vandekerckhove, J., Klein, H. L., & Cowan, N. J. (1998). Prefoldin, a chaperone that delivers unfolded proteins to cytosolic chaperonin. *Cell*, *93*(5), 863–73.

van Ooij, C., Tamez, P., Bhattacharjee, S., Hiller, N. L., Harrison, T., Liolios, K., Kooij, T., Ramesar, J., Balu, B., Adams, J., Waters, A., Janse, C.J., & Haldar, K. (2008). The malaria secretome: from algorithms to essential function in blood stage infection. *PLoS pathogens*, *4*(6), e1000084.

Van Wye, J., Ghori, N., Webster, P., Mitschler, R. R., Elmendorf, H. G., & Haldar, K. (1996). Identification and localization of rab6, separation of rab6 from ERD2 and implications for an "unstacked" Golgi, in *Plasmodium falciparum*. *Molecular and Biochemical Parasitology*, *83*(1), 107–20.

Waller, R. F., & McFadden, G. I. (2005). The apicoplast: a review of the derived plastid of apicomplexan parasites. *Current Issues in Molecular Biology*, *7*(1), 57–79.

Wedegaertner, P. B., & Bourne, H. R. (1994). Activation and depalmitoylation of Gs alpha. *Cell*, *77*(7), 1063–70.

Wegehingel, S., Zehe, C., & Nickel, W. (2008). Rerouting of fibroblast growth factor 2 to the classical secretory pathway results in post-translational modifications that block binding to heparan sulfate proteoglycans. *FEBS letters*, *582*(16), 2387–92.

Weiss, O., Holden, J., Rulka, C., & Kahn, R. A. (1989). Nucleotide binding and cofactor activities of purified bovine brain and bacterially expressed ADP-ribosylation factor. *The Journal of Biological Chemistry*, *264*(35), 21066–72.

Wenk, P., & Renz, A. (2003). *Parasitologie, Biologie der Humanparasiten*. Thieme Verlag.

Wickert, H., & Krohne, G. (2007). The complex morphology of Maurer's clefts: from discovery to three-dimensional reconstructions. *Trends in Parasitology*, *23*(10), 502–9.

Wickham, M. E., Rug, M., Ralph, S. A., Klonis, N., McFadden, G. I., Tilley, L., & Cowman, A. F. (2001). Trafficking and assembly of the cytoadherence complex in *Plasmodium falciparum*-infected human erythrocytes. *The EMBO Journal*, *20*(20), 5636–5649.

Wilson, D., Povey, S., & Harris, H. (1976). Adenylate kinases in man: evidence for a third locus. *Annals of Human Genetics*, *39*(3), 305–13.

World Health Organization. (2011). *World Malaria Report*. Geneva.

World Health Organization. (2013). *World Malaria Report*. Geneva.

Wright, M. H., Heal, W. P., Mann, D. J., & Tate, E. W. (2010). Protein myristoylation in health and disease. *Journal of Chemical Biology*, *3*(1), 19–35.

Wright, M. H., Clough, B., Rackham, M. D., Rangachari, K., Brannigan, J. A., Grainger, M., Moss, D.K., Bottrill, A.R., Heal, W.P., Broncel, M., Serwa, R.A.,

Brady, D., Mann, D.J., Leatherbarrow, R.J., Tewari, R., Wilkinson, A.J., Holder, A.A. & Tate, E. W. (2013). Validation of *N*-myristoyltransferase as an antimalarial drug target using an integrated chemical biology approach. *Nature Chemistry*, *6*(2), 112-21.

Wu, Y., Sifri, C. D., Lei, H. H., Su, X. Z., & Wellems, T. E. (1995). Transfection of *Plasmodium falciparum* within human red blood cells. *Proceedings of the National Academy of Sciences of the United States of America*, *92*(4), 973–7.

Young, J. A., Fivelman, Q. L., Blair, P. L., de la Vega, P., Le Roch, K. G., Zhou, Y., Carucci, D.J., Baker, D.A., & Winzeler, E. A. (2005). The *Plasmodium falciparum* sexual development transcriptome: a microarray analysis using ontology-based pattern identification. *Molecular and Biochemical Parasitology*, *143*(1), 67–79.

Zacharias, D. A., Violin, J. D., Newton, A. C., & Tsien, R. Y. (2002). Partitioning of lipid-modified monomeric GFPs into membrane microdomains of live cells. *Science*, *296*(5569), 913–6.

Zehe, C., Engling, A., Wegehingel, S., Schäfer, T., & Nickel, W. (2006). Cell-surface heparan sulfate proteoglycans are essential components of the unconventional export machinery of FGF-2. *Proceedings of the National Academy of Sciences of the United States of America*, *103*(42), 15479–84.

Zha, J., Weiler, S., Oh, K. J., Wei, M. C., & Korsmeyer, S. J. (2000). Posttranslational N-Myristoylation of BID as a Molecular Switch for Targeting Mitochondria and Apoptosis. *Science*, *290*(5497), 1761–1765.

Websites:

Hompepage: center for disease control and prevention (www.cdc.gov/malaria/)

7 Appendix

7.1 Coding sequences (PlasmoDB, version 10.0)

Sequence encoding the *Pf*ADP-ribosylation factor 1 (ARF1) (PF3D7_1020900)

```
ATGGGTTTATATGTAAGTAGGTTATTTAATCGTTTATTTCAAAAAAAAGATGTACGTATT
TTAATGGTTGGATTAGATGCTGCTGGAAAAACTACAATATTATATAAAGTAAAACTTGGT
GAAGTTGTTACGACTATTCCAACAATAGGTTTCAATGTTGAAACTGTCGAATTTCGTAAC
ATTTCATTTACCGTATGGGATGTAGGAGGACAAGATAAGATCCGACCTTTATGGAGACAT
TATTATTCCAACACAGACGGATTAATATTTGTCGTAGATAGTAATGATAGAGAAAGAATA
GATGATGCTCGTGAAGAATTACATAGAATGATAAATGAAGAAGAATTAAAAGATGCTATA
ATTTTAGTCTTCGCTAATAAACAAGATTTACCAAATGCTATGTCAGCAGCTGAAGTTACA
GAGAAATTACACCTTAACACTATAAGGGAAAGGAACTGGTTTATTCAATCCACCTGTGCC
ACAAGGGGTGACGGATTGTACGAAGGTTTTGATTGGCTAACCACACACTTAAATAATGCC
AAATAA
```

(Sequence length: 546 bp)

Predicted protein sequence of *Pf*ARF1

```
MGLYVSRLFNRLFQKKDVRILMVGLDAAGKTTILYKVKLGEVVTTIPTIGFNVETVEFRN
ISFTVWDVGGQDKIRPLWRHYYSNTDGLIFVVDSNDRERIDDAREELHRMINEEELKDAI
ILVFANKQDLPNAMSAAEVTEKLHLNTIRERNWFIQSTCATRGDGLYEGFDWLTTHLNNA
K
```

(Sequence length: 181 aa)

Sequence encoding the *Pf*adenylate kinase 2 (AK2) (PF3D7_0816900)

```
ATGGGATCATGTTATAGTAGAAAAAATAAAGTATCAACAATATCATTAGATGAAGAGGAA
AAAAAAAAAGAAAAAAAGAAGAAAAAAAAAATATATATTTTAAATGGAGCATCTGGGTCA
GGAAAAGATACACAATGTAGATTATTAGAAAAAAAAATACAATTATAAAATAATTTGTATA
AGTAAATTATTAAAAGAATATAAAGAAGAATATAATAAAGAAAATGTATTAAATGAAGAA
GAAAATTATTTTGATGAAATAGAAAAATGTATGATAGATGGATCTTTAGTTAATGATCAA
ATTGTTATAGAGATATTTCATAAACAATTGAACAAATATATAAATGATGATAAATATAAT
GGTATTATAATAAATGGTTTTCCTAGAAATTATGAACAAGCTTTATTAATTATACAAAAC
AATATAAGTATAACGAAATTTATAAATATACAAGTAGGAAAAGATACTCTATGGACAAGA
ATAAATAATAGAATTATCGATCCAATTACAAATATAAGTTATAATGAAAATATAATACAA
ATAATTAAAAAAAAAAAGAGAAGGACAAGAACTATCAGACAAAGAACAAAAACAATTGATC
ATAGACAATCATTTATATAATAATTTAAGTAATGATATTTTAGAAAGATTAACAAAAAGA
AAAGATGACGAAGAACAGGTTTTCAATAAAAGGTTTCAATTATATATAGAAAGCGAACAA
AAAATTAATTCTCTATTTAAAAATATTTGTAAAAATGTTGATGGAGAAAAATCGATAAAT
GATATATTTGATCAAATATGCTCCATTATAGATGATAACCCCAATTAA
```

Sequence length (828 bp)

Predicted protein sequence of *Pf*AK2

```
MGSCYSRKNKVSTISLDEEEKKKEKKKKKKIYILNGASGSGKDTQCRLLEKKYNYKIICI
SKLLKEYKEEYNKENVLNEEENYFDEIEKCMIDGSLVNDQIVIEIFHKQLNKYINDDKYN
GIIINGFPRNYEQALLIIQNNISITKFINIQVGKDTLWTRINNRIIDPITNISYNENIIQ
IIKKKREGQELSDKEQKQLIIDNHLYNNLSNDILERLTKRKDDEEQVFNKRFQLYIESEQ
KINSLFKNICKNVDGEKSINDIFDQICSIIDDNPN
```

(Sequence length: 275 aa)

7.2 Multiple sequence alignment (Clustal W: T-coffee)

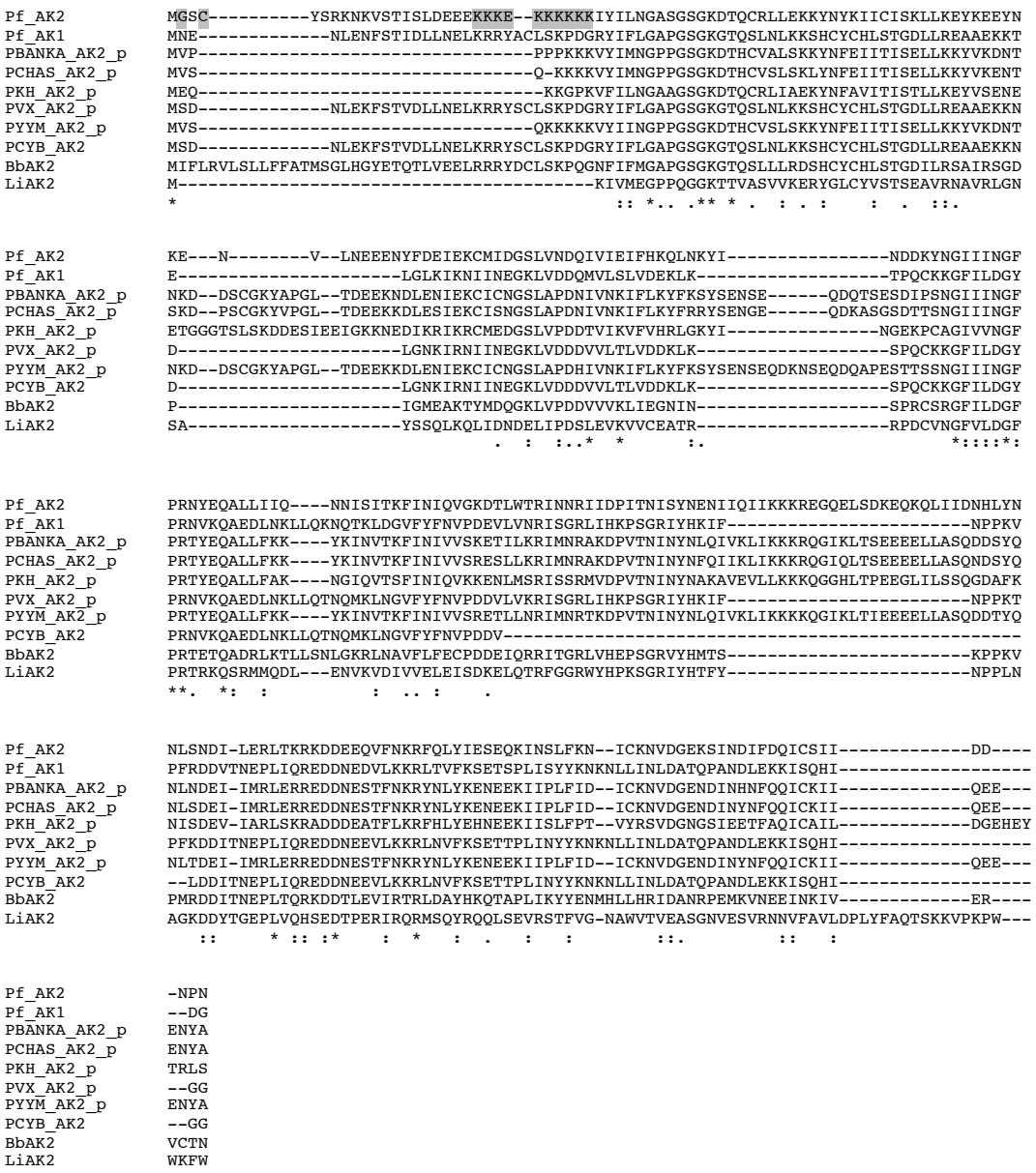

Figure A-1 A multiple sequence alignment of *Pf*AK2 and other verified and putative adenylate kinase 2 proteins, respectively, in other *Plasmodium* species and other parasitic protozoa

*Pf*AK2 (PF3D7_0816900) was aligned to *Pf*AK1 (*Pf*3D7_1008900), *Pb*AK2, putative (PBANKA_071390), *Pc*AK2, putative (PCHAS_072300), *Pk*AK2, putative (PKH_051560), *Pv*AK2, putative (PVX_094660), *Py*AK2, putative (PYYM_071400), *Pc*AK2 (PCYB_081850), *Bb*AK2 (bbov|XP_001609458.1) and *Li*AK2 (linf|LinJ.34.0130). The N-terminus of *Pf*AK2 clearly differs from the N-termini of the other aligned proteins, insofar as it contains a verified *N*-myristoylation site (Rahlfs et al., 2009), a putative palmitoylation site at the 4th position and a polybasic cluster of lysine residues (each motif marked in grey). None of the other AK2 proteins contain either of these motifs. The alignment was created using ClustalW (T-coffee).

7.3 Expression profiles of *Pf*AK2 (PlasmoDB 10.0 version)

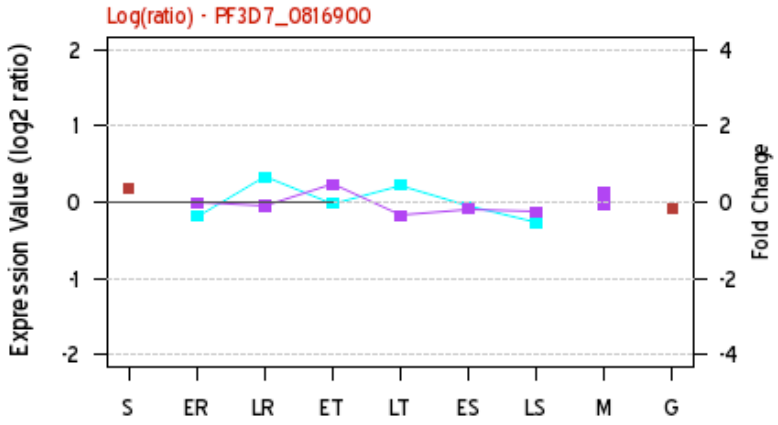

Figure A-2 Expression profile of PF3D7_0816900 (*Pf*AK2)

The expression profile of PF3D7_0816900 is based on a oligonucleotide microarray analysis (Le Roch et al., 2003). In blue: Sorbitol-synchronized 3D7 parasites; in purple: Temperature-synchronized 3D7 parasites. Different stages of *P. falciparum's* life-cycle were analysed (x-axis): ER= Early Rings; LR = Late Rings; ET= Early Trophs; LT= Late Trophs; ES=Early schizonts; LS= Late Schizonts; M=Merozoites; S=Sporozoites; G=Gametocytes. Y-axis: Log (base 2) ratio of Affymetrix RMAExpress expression value (normalized by experiment) to average RMAExpress value for all time points for a gene.

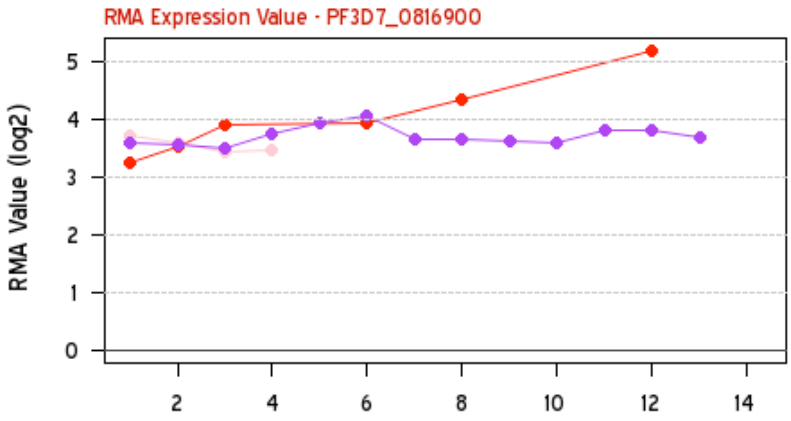

Figure A- 3 Gametocyte stages (I–V) transcriptomes of PF3D7_0816900 (*Pf* AK2)

The expression profile of PF3D7_0816900 is based on a oligonucleotide microarray analysis (Young et al., 2005). In red: 3D7 parasites; in pink: MACS purified 3D7 parasites; in purple: isolate NF54. Different gametocyte stages (stage I–V) were analyzed (x-axis): days of gametocytogenesis. Y-axis: (rma) Affymetrix RMAExpress expression value (normalized by experiment).

7.4 Potential proteins of the *P. falciparum* genome as candidate proteins of an alternative secretory pathway

	N-Myristoy-lation	Palmitoy-lation	Basic residues	Acidic residues	Blood stage	Sexual stage
***Pf* adenylate kinase 2** (PF3D7_0816900)	✓	✓	17	7	----	✓
***Pf* calpain** (PF3D7_0502300)	✓	✓	15	11	----	✓
***Pf* protein phosphatase, putative** (PF3D7_0810300)	✓	✓	14	11	✓	✓
***Pf* CDPK1** (PF3D7_0217500)	✓	✓	13	5	✓	✓
***Pf* cAMP dependent protein kinase** (PF3D7_1223100)	✓	✓	12	13	✓	✓
***Pf* ABC transporter (MDR family)** (PF3D7_1339900)	✓	---	12	6	----	✓
***Pf* protein phosphatase 2c-like** (PF3D7_1309200)	✓	✓	12	9	----	✓
***Pf* glideosome associated protein** (PF3D7_1222700)	✓	✓	11	20	✓	✓
***Pf* Conserved Plasmodium membrane protein, unknown function** (PF3D7_0930800)	✓	✓	10	12	----	✓
***Pf* conserved plasmodium protein** (PF3D7_0913800)	✓	✓	9	12	--	✓
***Pf* secretory complex protein 61 alpha** (PF3D7_1310600)	✓	✓	8	3	✓	✓
***Pf* armadillo-domain containing rhoptry protein (ARO)** (PF3D7_0414900)	✓	✓	8	9	✓	✓
***Pf* inner membrane complex protein, putative** (PF3D7_1011000)	✓	-	7	8	✓	✓

Acknowledgement

First, I would like to thank Prof. Dr. Klaus Lingelbach for giving me the opportunity to work in his group, to work independently on my project and his guidance.

I would also like to thank Prof. Dr. Jude Przyborski for giving me an introduction into molecular biology, for his supervision and motivation on this project and his thoughtful ideas and advice.

I also wish to thank my second supervisor Prof. Dr. Anthony Holder from the MRC (London, UK) for the many helpful discussions around my project and your support especially towards the last months of my PhD.

I would like to thank Prof. Dr. Uwe G. Maier and Prof. Dr. Gerhard Bremer for agreeing to be part of my thesis commitee.

Thanks also to my Graduate School of Malaria Research for the generous funding and for giving me the opportunity to visit great international conferences and workshops. Thanks to Alessia Valdarno and Elisa Kless for helping me out in different situations.

Many thanks to Dr. Sabrina Heiny for the helpful discussions around my project and for proof-reading parts of my thesis.

Many, many thanks to all my former and present colleagues, especially: Dr. Luis Barniol, Dr. Sabrina Heiny, Preetish Gangopadhyay, Qi Zhang and the best colleague and friend in the world Jyotsna Sharma. Also a big thank you to all the students I met during my PhD time as well as Mareike Lorenz, Nadja Braun, Gabi Köllisch and my 'little sunshine' Kathrin Dippel for the nice time we shared.

Thanks also to my Marburg friends for the great time we had, which helped me forget lab work on the 'Lahnmountain' for awhile– thanks especially to Jo, Netti, Kiki, Raj and Katrin.

I would like to express my deepest gratitude to my family, who supported me my entire life. I would especially like to thank my dearest mother, for always motivating and supporting me and having confidence in whatever I do.

Curriculum vitae

Personal data

Name:	Thuvaraka Thavayogarajah
Date of birth:	06.12.1985
Place of birth:	Detmold

University education

2010 – 2014	Philipps-University Marburg Faculty of Biology PhD in the group of Professor Lingelbach Topic 'An alternative secretory pathway in the malaria parasite *Plasmodium falciparum*'
2008 – 2010	Westfälische-Wilhelms University Münster Faculty of Medicine Master thesis at the Institute of Pharmacology and Toxicology
2005 – 2008	Westfälische-Wilhelms University Münster Faculty of Biology Bachelor thesis at the Institute of Animal Physiology

School education

1996 – 2005	Stadtgymnasium Detmold, Allgemeine Hochschulreife

Publications

04/2010	Jessica M. Vanslambrouck, Angelika Bröer, Thuvaraka Thavayogarajah, Jeff Holst, Charles G. Bailey, Stefan Bröer and John E. J. Rasko (2010) Renal imino acid and glycine transport system ontogeny and involvement in developmental iminoglycinuria. *Biochemical Journal* 428 (397-407)

Eigenständigkeitserklärung

Ich versichere hiermit, dass ich meine dem Fachbereich Biologie der Universität Marburg vorgelegte Dissertation, mit dem Titel

'An alternative secretory pathway in the malaria parasite *Plasmodium falciparum*'

selbstständig, ohne unerlaubte Hilfe angefertigt und mich dabei keiner anderen als der von mir ausdrücklich bezeichneten Quellen und Hilfen bedient habe.

Die Dissertation wurde in der jetztigen oder einer ähnlichen Form noch bei keiner anderen Hochschule eingereicht und hat noch keinen sonstigen Prüfungszwecken gedient.

_____ _____

(Ort/Datum) (Unterschrift mit Vor- und Zuname)